Andean Geology 41 (3): 447-506. September, 2014
doi: 10.5027/andgeoV41n3-a01

Andean Geology
formerly Revista Geológica de Chile
www.andeangeology.cl

Timing of the magmatism of the paleo-Pacific border of Gondwana: U-Pb geochronology of Late Paleozoic to Early Mesozoic igneous rocks of the north Chilean Andes between 20° and 31°S

Víctor Maksaev[1], Francisco Munizaga[1, 2], Colombo Tassinari[3]

[1] *Departamento de Geología, Universidad de Chile, Plaza Ercilla 803, Santiago, Chile.*
vmaksaev@ing.uchile.cl; fmunizag@ing.uchile.cl

[2] *Geología, Facultad de Ingeniería, Universidad Andrés Bello, Salvador Sanfuentes 2375, Santiago, Chile.*

[3] *Instituto de Geociencias, Universidade de Sao Paulo, Rua do Lago, 562-Cidade Universitária CEP 05508-080, Sao Paulo, Brasil.*
ccgtassi@usp.br

ABSTRACT. U-Pb zircon geochronological data provide record of about 130 Ma of igneous activity in the Andes of northern Chile, which extended episodically from the latest Early Carboniferous to Early Jurassic (328-194 Ma). The overall U-Pb data show that volcanism and plutonism were essentially synchronous and major episodes of igneous activity developed during the Late Carboniferous to Mid-Permian (310 to 260 Ma) and from Late Permian to Late Triassic (255-205 Ma), with less prominent episodes in the mid-Carboniferous (330 to 320 Ma), and Early Jurassic (200-190 Ma). Thus, from the Carboniferous to the Early Triassic dominantly silicic magmatism developed along the Chilean segment of the southwestern border of Gondwana supercontinent. Further magmatism developed during the Mid-Late Triassic (250-194 Ma) was bimodal and synchronous with rift-related, continental and/or marine sedimentary strata related to the early stages of break-up of Gondwana. Most of the silicic volcanic rocks of the Precordillera and Domeyko Cordillera of northern Chile (21°30' to 25°30'S) are older than the silicic rocks assigned to the Choiyoi succession in Argentina, being instead equivalent in age to Carboniferous to Early Permian marine sedimentary sequences present in the eastern Argentinean foreland. On the other hand, silicic volcanic successions exposed in the easternmost part of northern Chile are equivalent in age to the Choiyoi succession of the San Rafael Block of Argentina. An eastward expansion or migration of the volcanism during the Mid-Permian to Early Triassic is inferred, interpretation that is consistent with expansion of the volcanism at that time in Argentina. The timing of the Late Paleozoic to Early Jurassic magmatism is coincident with that of the Andes of Perú and of western Argentina according to the available U-Pb data, revealing a rather consistent evolution in time of the magmatism along the southwestern, paleo-Pacific border of Gondwana.

Keywords: Geochronology, U-Pb, Andes, Gondwana, Choiyoi, Paleozoic, Carboniferous, Triassic.

RESUMEN. Temporalidad del magmatismo del borde paleo-Pacífico de Gondwana: geocronología U-Pb de rocas ígneas del Paleozoico tardío a Mesozoico temprano de los Andes del norte de Chile entre los 20° y 31°S. Los datos de U-Pb en circón registran aproximadamente 130 Ma de actividad ígnea en los Andes del norte de Chile, la que se extendió episódicamente desde el Carbonífero temprano hasta el Jurásico temprano (328-194 Ma). Los datos globales de U-Pb indican que el volcanismo y plutonismo fueron esencialmente sincrónicos con episodios mayores desde el Carbonífero tardío al Pérmico Medio (310-260 Ma) y durante el Pérmico Tardío a Triásico Tardío (255-205 Ma) y episodios menos prominentes durante el Carbonífero medio (330-320 Ma) y el Jurásico Temprano (200-190 Ma). Desde el Carbonífero hasta el Triásico Temprano se desarrolló magmatismo predominantemente félsico a lo largo del borde suroccidental del supercontinente de Gondwana, mientras que durante el Triásico medio a tardío (250-194 Ma) se desarrolló magmatismo bimodal sincrónico con estratos sedimentarios continentales y/o marinos relacionados con extensión (rift), durante las etapas tempranas de la desintegración de Gondwana. La mayor parte de las rocas volcánicas silíceas de la precordillera y la cordillera de Domeyko en el norte de Chile (21°30' a 25°30'S) son más antiguas que las rocas silíceas asignadas a la sucesión Choiyoi en Argentina, y son, en cambio, equivalentes en edad con las secuencias sedimentarias marinas del Carbonífero al Pérmico temprano presentes en el antepaís argentino al oriente. Por otra parte, las sucesiones volcánicas félsicas expuestas en la parte más oriental del norte de Chile, de la cordillera de Domeyko y de la cordillera Frontal al sur de 25°S son equivalentes en edad a la sucesión Choiyoi de Argentina. Se infiere una migración o expansión del volcanismo hacia el este durante el Pérmico Medio a Triásico Temprano, interpretación que es consistente con la expansión del volcanismo en Argentina durante ese período. La temporalidad del magmatismo del Paleozoico tardío a Mesozoico temprano es coincidente con la de los Andes de Perú y del oeste de Argentina, de acuerdo a los datos U-Pb disponibles, lo que revela una evolución temporal del magmatismo concordante a lo largo del borde suroeste del Gondwana.

Palabras clave: Geocronología, U-Pb, Andes, Gondwana, Choiyoi, Paleozoico, Carbonífero, Triásico.

1. Introduction

The Late Paleozoic-Early Mesozoic magmatism is a significant, but not completely understood geological event, which has been recognized along much of the length of western South America (*e.g.*, Vaughan and Pankhurst, 2008). It is characterized by a high proportion of felsic volcanic rocks and granitic plutons over intermediate and mafic igneous rocks, and represents magmatism that developed along the southwestern paleo-Pacific border of Gondwana supercontinent (Llambías and Sato, 1990; Sato and Llambías, 1993; Mpodozis and Kay, 1992; Strazzere *et al*., 2006; Munizaga *et al*., 2008; Vaughan and Pankhurst, 2008; Rocha-Campos *et al*., 2011). The previous K-Ar dating of this extensive volcano-plutonic complex in northern Chile has yielded an overall range from 332 to 197 Ma for this magmatic activity (*e.g.*, Huete *et al*., 1977; Nasi *et al*., 1985; Mpodozis *et al*., 1993; Lucassen *et al*., 1999; Tomlinson *et al*., 2001; Tomlinson and Blanco, 2008). The K-Ar ages have mostly been obtained for intrusive rocks, since volcanic rocks commonly are altered or show low-grade metamorphism, which have prevented the application of the K-Ar dating method or produced inaccurate dates. More recent studies have provided a more accurate geochronological database of U-Pb dates for the Late Paleozoic-Early Mesozoic igneous rocks of northern Chile (north of 31°S latitude), which we have compiled in Tables 1 and 2 (references therein), but also in Argentina (*i.e.*, Pankhurst *et al*., 2006; Gulbranson *et al*., 2010; Rocha-Campos *et al*., 2011). In this contribution we present 41 new SHRIMP U-Pb dates for volcanic and plutonic rocks of northern Chile, which together with the compilation of U-Pb dates from previous studies, provide a more accurate timing for the Late Paleozoic to Early Jurassic magmatism of the north-Chilean segment of the southwestern border of Gondwana. The numerical ages are assigned to the International Stratigraphic Chart of the International Commission on Stratigraphy 2013 (Cohen *et al*., 2013).

2. Geological background

The Late Paleozoic to Triassic igneous units along the Andes of northern Chile and the Argentinean Frontal Cordillera are commonly known by a variety of names, but Stipanicic *et al*. (1968) employed the name Choiyoi Group for volcanic rocks attributed to the Permian to Triassic outcropping in the Argentinean Cordillera, and this name has been widely used to refer to 'Permo-Triassic' magmatism in both countries, even though the actual timing of the igneous rocks was quite inaccurate and only limited and inaccurate geochronological data was available.

TABLE 1. COMPILED U-Pb ZIRCON AGES FOR VOLCANIC ROCKS OF NORTHERN CHILE.

Sample	Location (Geodetic WGS 84)			U-Pb age			
	Latitude S	Longitude W	Lithology	Ma±2σ	Method	Formation or Unit	Reference
VAM-137	25°11'05.24"	69°18'12.33"	Rhyolitic tuff	309.9±2.2	LA-ICP-MS	La Tabla	Venegas *et al.* (2013)
CHT-59	22°26'50.38"	68°57'18.24"	Rhyolite	303.9±0.2	CA-TIMS	Collahuasi	Tomlinson and Blanco (2008)
D-9	28°46'30.58"	70°26'20.45"	Rhyolite	300.8±4.6	LA-ICP-MS	Cerro Bayo	Salazar *et al.* (2009)
CHT-201	22°25'33.45"	68°58'25.42"	Rhyolitic tuff	300.3±1.8	SHRIMP	Collahuasi	Tomlinson and Blanco (2008)
LVN-317	22°35'22.00"	68°55'50.78"	Rhyolite	299.3±1.7	ID-TIMS	Collahuasi	Mpodozis *et al*. (1993)
CLL-76	21°02'09.83"	68°51'00.67"	Dacite	298.8±2.2	SHRIMP	Collahuasi	Munizaga *et al.* (2008)
Unidentified	24°12'53"	69°03'40"	Rhyolite	298.2±5.5	LA-ICP-MS	La Tabla	Jara *et al*. (2009)
78012	23°53'07.49"	69°00'45.45"	Rhyolite	296.8±0.2	ID-TIMS	La Tabla	Cornejo *et al*. (2006)
VAM-070	25°17'53.27"	69°16'17.15"	Rhyolitic tuff	294.6±2.1	LA-ICP-MS	La Tabla	Venegas *et al*. (2013)
Unidentified	24°12'53"	69°03'40"	Andesite	294.4±4.6	LA-ICP-MS	La Tabla	Jara *et al*. (2009)
ESC-50	24°20'20.45"	69°01'04.46"	Dacite	293±4	LA-ICP-MS	La Tabla	Urzúa (2009)
R990259	20°58'25.81"	68°41'59.07"	Rhyolite	293±14	LA-ICP-MS	Collahuasi	Masterman (2003)
MF-650	23°41'19.97"	69°05'17.73"	Rhyolite	292±5	ID-TIMS	Sierra del Jardín	Marinovic (2007)
MF-653	23°52'03.50"	69°09'27.15"	Rhyolite	292±5	ID-TIMS	Sierra del Jardín	Marinovic (2007)
Unidentified	24°14'37"	69°02'57"	Andesite	288.8±2.4	Uncertain	La Tabla	Hervé *et al*. (2012)
Unidentified	24°14'37.03"	69°02'57.31"	Andesite	288.0±2.4	Uncertain	La Tabla	Hervé *et al*. (2012)
Unidentified	24°13'04.72"	69°03'46.42"	Rhyolite	287.1±4.4	LA-ICP-MS	La Tabla	Jara *et al*. (2009)
ESC-45	24°16'20.86"	69°03'13.07"	Andesite tuff	287±3	LA-ICP-MS	La Tabla	Urzúa (2009)
ESC-36	24°16'20.86"	69°03'13.07"	Andesite tuff	286±2	LA-ICP-MS	La Tabla	Urzúa (2009)
ESC-47	24°13'04.73"	69°00'42.13"	Andesite tuff	284±4	LA-ICP-MS	La Tabla	Urzúa (2009)
ESC-37	24°16'15.37"	69°02'43.88"	Andesite tuff	282±2	LA-ICP-MS	La Tabla	Urzúa (2009)
Unidentified	22°25'13"	68°56'58"	Dacite tuff	279±9	LA-ICP-MS	Collahuasi	Tomlinson and Blanco (2008)
Unidentified	22°24'50"	68°57'18"	Dacite tuff	273.5±11.0	LA-ICP-MS	Collahuasi	Tomlinson and Blanco (2008)
IJ-108.2	29°19'27.08"	70°01'58.13"	Rhyolite tuff	265.0±5.6	ID-TIMS	Guanaco Sonso	Martin *et al*. (1999)

table 1 continued.

Sample	Location (Geodetic WGS 84)			U-Pb age			
	Latitude S	Longitude W	Lithology	Ma±2σ	Method	Formation or Unit	Reference
DCC-130	25°34'42.40"	69°05'34.66"	Rhyolite	262.9±2.0	ID-TIMS	La Tabla	Cornejo *et al*. (2009)
CV-130321-02	25°01'53.27"	69°13'45.52"	Altered tuff	259.0±3.4	LA-ICP-MS	La Tabla	Venegas *et al*. (2013)
CC-44-130-138-168	23°40'06"	68°00'50"	Ignimbrite	248±3	ID-TIMS	Peine Group	Breitkreuz and Van Schmus (1996)
Unidentified	23°09'	68°36'	Tuff	240.8±0.3	ID-TIMS	El Bordo	Basso and Marinovic (2003)
Unidentified	23°09'	68°36'	Tuff	238.7±0.4	ID-TIMS	El Bordo	Basso and Marinovic (2003)
CHT-192	22°25'36.5"	68°59'17.5"	Andesitic breccias	235.4±1.6	SHRIMP	Quetena	Tomlinson and Blanco (2008)
CHT-193	22°25'34"	68°59'24.3"	Volcanoclastic sandstone	234.5±3.2	SHRIMP	Quetena	Tomlinson and Blanco (2008)
BF-225	23°00'16.35"	69°59'21.41"	Rhyolitic tuff	233±12	ID-TIMS	Sierra Miranda	Basso (2004)
DCC-124	25°59'30.40"	69°19'13.96"	Rhyolite	232.9±0.2	ID-TIMS	Quebrada del Salitre	Cornejo *et al*. (2009)
Unidentified	22°12'51"	68°51'25"	Dacite	231.6±0.5	ID-TIMS	Cerros de Chuquicamata	Tomlinson and Blanco (2008)
St-62d	28°42'35.34"	70°24'00.99"	Rhyolitic tuff	222.8±2.1	LA-ICP-MS	San Félix	Padel *et al*. (2012)
BF-2	23°04'11.18"	69°47'38.55"	Rhyolite	220±19	ID-TIMS	Sierra de Miranda	Basso (2004)
FO 06 95	29°49'54.3"	70°30'38.7"	Dacitic ignimbrite	219.5±1.7	SHRIMP	Las Breas	Hervé *et al*. (2014)
ST-93Ad	28°39'32.42"	70°09'50.23"	Rhyolitic tuff	217.9±1.4	LA-ICP-MS	La Totora	Salazar *et al*. (2012, 2013)
ST196d	28°34'03.42"	70°08'22.65"	Rhyolitic tuff	216.2±1.6	LA-ICP-MS	La Totora	Salazar *et al*. (2013)
CV-111212-02	25°17'58.75"	69°09'14.64"	Andesite	214.2±2.0	LA-ICP-MS	Quebrada del Salitre	Venegas *et al*. (2013)
VAM-167	25°07'06.16"	69°11'22.20"	Dacite	212.8±2.0	LA-ICP-MS	Quebrada del Salitre	Venegas *et al*. (2013)
ST-175d	28°47'44.23"	70°24'48.83	Rhyolitic tuff	212.4±2.6	LA-ICP-MS	San Félix	Salazar *et al*. (2013)
ST-65d	28°41'09.64"	70°23'16.60"	Basaltic andesite	210.4±2.9	LA-ICP-MS	La Totora	Salazar *et al*. (2013)
MF-646	23°37'51.6"	69°04'35.0"	Tuff	194.0±9.2	ID-TIMS	Cerro La Ballena	Marinovic (2007)

TABLE 2 COMPILED U-Pb ZIRCON AGES FOR INTRUSIVE ROCKS OF NORTHERN CHILE.

Sample	Location (Geodetic WGS84)			U-Pb age		
	Latitude S	Longitude W	Lithology	Ma±2σ	Method	Reference
GP-2089	30°44'19.54"	70°30'17.56"	Foliated muscovite-biotite granite	328.1±2.8	SHRIMP	Pineda and Calderón (2008)
VAM-053	25°15'29.74"	69°17'04.78"	Rhyolitic porphyry	328.3±3.4	LA-ICP-MS	Venegas *et al*. (2013)
VAV	25°23'00.03"	69°05'02.91"	Monzogranite	323.9±2.6	LA-ICP-MS	Venegas *et al*. (2013)
Unidentified	23°40'30.56"	69°31'46.70"	Monzogranite	310.1±4.8	ID-TIMS	Cortés (2000)
CLL-238	20°58'04.34"	68°42'24.01"	Rhyolitic porphyry	308.5±2.2	SHRIMP	Munizaga *et al*. (2008)
CLL-75	21°02'09.81"	68°50'39.71"	Rhyolitic porphyry	307.9±2.8	SHRIMP	Munizaga *et al*. (2008)
CLL-114	20°58'04.34"	68°42'24.01"	Rhyolitic porphyry	304.6±3.2	SHRIMP	Munizaga *et al*. (2008)
CLL-237	20°57'54.34"	68°42'28.01"	Rhyolitic porphyry	303.9±3.0	SHRIMP	Munizaga *et al*. (2008)
Unidentified	21°59'49"	68°52'47"	Rhyolitic porphyry	303.8±0.7	ID-TIMS	Tomlinson and Blanco (2008)
CLL-44	20°59'59.33"	68°49'01.01"	Granitic porphyry	303.2±2.0	SHRIMP	Munizaga *et al*. (2008)
LVN-291	22°39'58.46"	68°57´11.24"	Foliated diorite	303±5	ID-TIMS	Mpodozis *et al*. (1993)
Unidentified	21°40'06"	68°49'59"	Rhyolitic porphyry	302.4±0.8	ID-TIMS	Tomlinson and Blanco (2008)
Unidentified	24°17'03"	69°03'08"	Tonalite	300.1±3.5	Uncertain	Hervé *et al*. (2012)
CV-120118-05	25°02'08.20"	69°01'17.56"	Rhyolitic porphyry	299.4±2.5	LA-ICP-MS	Venegas *et al*. (2013)
ZERD356	24°12´50.10"	69°03'19.82"	Quartz Porphyry	298.9±2.6	SHRIMP	Urzúa (2009)
CLL-223	20°58'08.70"	68°42'17.56"	Rhyolitic porphyry	298.3±2.1	SHRIMP	Munizaga *et al*. (2008)
84-22-12	22°40'15"	68°55'00"	Granite	298.0±1.5	ID-TIMS	Damm *et al*. (1990)
CLL-85	21°09'54.54"	68°39'42.14"	Rhyolitic porphyry	297.6±2.4	SHRIMP	Munizaga *et al*. (2008)
CLL-221	20°59'21.05"	68°38'09.68"	Dacitic porphyry	296.9±4.3	SHRIMP	Munizaga *et al*. (2008)
Unidentified	22°16'30"	68°51'20"	Granite	296.9±2.1	ID-TIMS	Tomlinson and Blanco (2008)
Unidentified	24°17'03"	69°03'43"	Monzodiorite porphyry	296.8±3.2	Uncertain	Hervé *et al*. (2012)
Unidentified	24°17'03"	69°03'08"	Monzogranite porphyry	296.6±4.4	Uncertain	Hervé *et al*. (2012)
VAV-006	25°18'35.21"	69°09'04.60"	Dacitic porphyry	296.3±2.9	LA-ICP-MS	Venegas *et al*. (2013)
ST-9d	28°50'15.97"	70°25'51.27"	Muscovite-biotite Granodiorite	296.1±4.8	LA-ICP-MS	Coloma *et al*. (2012)

table 2 continued.

Sample	Location (Geodetic WGS84)			U-Pb age		
	Latitude S	Longitude W	Lithology	Ma±2σ	Method	Reference
VAM-031	25°05”30.67”	69°14’03.20”	Syenogranite	295.6±2.6	LA-ICP-MS	Venegas *et al*. (2013)
ST-72d	28°42’56.55”	70°17’50.35”	Muscovite-biotite Granodiorite	295.4±3.3	LA-ICP-MS	Coloma *et al*. (2012)
QFP1	24°11’59.70”	69°03’12.71”	Rhyolitic Porphyry	294.2±2.4	SHRIMP	Urzúa (2009)
CAB-267A	24°35’36”	69°10’48”	Foliated biotite-muscovite tonalite	294±3	ID-TIMS	Marinovic *et al*. (1995)
AM-25	30°56’53.40”	70°30’35.30”	Foliated tonalite	293.7±2.4	SHRIMP	Pineda and Calderón (2008)
ZERD958	24°12’56”	69°02’57”	Monzogranite porphyry	293.0±6.0	LA-ICP-MS	Urzúa (2009)
CLL-73	21°01’53.71”	68°50’39.72”	Granitic porphyry	292.7±1.9	SHRIMP	Munizaga *et al*. (2008)
CAB-301A	24°36’46”	69°12’19”	Foliated hornblende-biotite tonalite	292±5	ID-TIMS	Marinovic *et al*. (1995)
ST-4d	28°41’39.54”	70°17’26.99”	Biotite tonalite	291.5±3.4	LA-ICP-MS	Coloma *et al*. (2012)
7	25°54’38”	70°37’00”	Syenogranite	291.8±14.3	ID-TIMS	Berg *et al*. (1983)
FO 06 96	29°51’42”	70°30’21”	Hornblende-biotite granodiorite	291.2±2.7	SHRIMP	Hervé *et al*.(2014)
ZAL3	24°13’13”	69°04’25”	Rhyolitic porphyry	290±4	LA-ICP-MS	Richards *et al*. (1999)
ESC-49	24°18’45.22”	69°59’18.25”	Monzonite	290±2	Uncertain	Urzúa (2009)
FO 06 98	30°08’08”	70°24’39”	Biotite-muscovite granite	289.7±1.8	SHRIMP	Hervé *et al*. (2014)
LVN-293	22°39’38.95”	68°57’46.29”	Biotite granite	288.3±1.4	ID-TIMS	Mpodozis *et al*. (1993)
FO 06 94	29°50’46.0”	70°22’59.9”	Foliated hornblende-biotite tonalite	288.2±1.5	SHRIMP	Hervé *et al*. (2014)
CAB-252A	24°38’45”	69°12’22”	Foliated biotite tonalite	288±5	ID-TIMS	Marinovic *et al*. (1995)
Unidentified	24°14’37.03”	69°02’57.31”	Quartz Monzodiorite porphyry	287.6±3.3	Uncertain	Hervé *et al*. (2012)
CON-90-1	28°51’57.58”	70°17’14.28”	Hornblende-biotite granodiorite	285.7±0.6	ID-TIMS	Pankhurst *et al*. (1996)
78009	23°51’55.95”	69°01’29.79”	Diorite	283.6±2.8	ID-TIMS	Cornejo *et al*. (2006)
MF-651	23°51’38.64”	69°03’38.12”	Granite	279.0±2.4	ID-TIMS	Marinovic (2007)
CAB-292A	24°59’45”	69°10’12”	Muscovite-biotite granodiorite	277±4	ID-TIMS	Marinovic *et al*. (1995)
78001	23°53’29.88”	69°00’40.85”	Diorite	273±4	ID-TIMS	Cornejo *et al*. (2006)
CT-160d	28°45’34.06”	70°04’37.73”	Tonalite	270.8±4.0	LA-ICP-MS	Salazar *et al*. (2013)

table 2 continued.

Sample	Location (Geodetic WGS84)			U-Pb age		
	Latitude S	Longitude W	Lithology	Ma±2σ	Method	Reference
84-19-01	23°40'44.23"	68°23'49.96"	Granodiorite	268±5	ID-TIMS	Damm *et al*. (1990)
CL2-HN11/07	23°45'30.52"	68°21'07.38"	Monzodiorite	267.3±2.5	LA-ICP-MS	Niemeyer (2013)
JA01	28°45'53.92"	70°10'11.99"	Foliated biotite granodiorite	266.1±3.5	LA-ICP-MS	Álvarez *et al.* (2013)
CL4-HN09	23°41'10.18"	68°22'35.49"	Monzodiorite	266.1±3.5	LA-ICP-MS	Niemeyer (2013)
CT-358d	28°58'29.89"	70°14'30.39"	Tonalite	257.0±1.9	LA-ICP-MS	Salazar *et al*. (2013)
Di01-HN09	23°43'15.47"	68°26'10.46"	Diorite	256.0±2.0	LA-ICP-MS	Niemeyer (2013)
CT-358Bd	28°58'29.89"	70°14'30.39"	Felsic band of mylonite	255.3±4.0	LA-ICP-MS	Salazar *et al*. (2013)
FO 06 87	30°05'37.2"	70°04'31.9"	Clinopyroxene gabbro	255.2±1.8	SHRIMP	Hervé *et al*. (2014)
CL15-HN04	23°46'41.20"	68°24'19.23"	Feldspar porpyhry	254.2±2.3	LA-ICP-MS	Niemeyer (2013)
D-1	20°49'25"	68°42'00"	Granite	252.5±2.8	ID-TIMS	Vergara and Thomas (1984)
CHIN01-HN9	23°41'56.42"	68°23'09.91"	Monzogranite	252.0±2.8	LA-ICP-MS	Niemeyer (2013)
IM83-4	30°05'22.63"	70°00'26.90"	Granitic porphyry	249.7±3.2	ID-TIMS	Martin *et al*. (1999)
CLL-297	20°50'49.68"	68°45'05.31"	Granitic porphyry	248.7±3.3	SHRIMP	Munizaga *et al*. (2008)
Ja-02	28°58'39.93"	70°10'12.87"	Biotite granite	247.7±3.4	LA-ICP-MS	Álvarez *et al*. (2013)
ST-16d	28°59'06.54"	70°12'49.77"	Muscovite-biotite granodiorite	247.0±3.1	LA-ICP-MS	Coloma *et al*. (2012)
FO10104B	28°57'46.4"	70°14'51.7"	Biotite leucogranite	245.0±2.3	SHRIMP	Hervé *et al*. (2014)
R200085	20°58'38.69"	68°41'55.38"	Granodiorite porphyry	245±12	LA-ICP-MS	Masterman (2003)
CLL-30	21°00'04.34"	68°36'54.02"	Dacitic porphyry	244.8±2.5	SHRIMP	Munizaga *et al*. (2008)
CLL-32	20°50'22.34"	68°45'10.00"	Granitic porphyry	243.2±2.1	SHRIMP	Munizaga *et al*. 2008
FO10100	28°58'27.5"	70°10'05.8"	Leucogranite	242.6±2.2	SHRIMP	Hervé *et al*. (2014)
IM-108.1	29°19'20.66"	70°01'46.95"	Quartz Porphyry	242.5±1.5	ID-TIMS	Martin *et al*. (1999)
IM-113.1	29°19'09.17"	70°02'03.51"	Dacite porphyry	242.0±1.5	ID-TIMS	Martin *et al*. (1999)
Ja-94	28°59'26.23"	70°13'01.01"	Biotite-hornblende tonalite	241.7±3.0	LA-ICP-MS	Álvarez *et al*. (2013)
ST-102d	28°51'48.20"	70°08'25.83"	Monzogranite	240.3±1.7	LA-ICP-MS	Coloma *et al*. (2012)

table 2 continued.

Sample	Location (Geodetic WGS84)			U-Pb age		
	Latitude S	Longitude W	Lithology	Ma±2σ	Method	Method
Unidentified	22°22'40"	68°54'50"	Dacite dike	237.6±1.4	LA-ICP-MS	Tomlinson and Blanco (2008)
Unidentified	22°22'40"	68°54'50"	Granodiorite	233.6±1.5	LA-ICP-MS	Tomlinson and Blanco (2008)
Unidentified	22°16'02"	68°53'07"	Granodiorite	233.1±2.2	SHRIMP	Tomlinson and Blanco (2008)
Unidentified	22°16'02"	68°53'07"	Granodiorite	231.4±2.0	SHRIMP	Tomlinson and Blanco (2008)
I-21	26°13'05"	70°35'36"	Monzogranite	230±8	ID-TIMS	Berg and Baumann (1985)
QT-460	22°15'20"	68°52'10"	Granodiorite	229.0±2.0	ID-TIMS	Tomlinson *et al*. (2001)
QT-459	22°17'13"	68°53'14"	Granodiorite	227.2±2.0	ID-TIMS	Tomlinson *et al*. (2001)
ESC-51	24°11'27.64"	69°01'35.05"	Feldspar porphyry	227±3	LA-ICP-MS	Urzúa (2009)
FO 06 89	29°58'05.8"	70°06'37.7"	Porphyritic granite	225.9±1.8	SHRIMP	Hervé *et al*. (2014)
Unidentified	22°22'40"	68°54'50"	Granodiorite	224±5	LA-ICP-MS	Tomlinson and Blanco (2008)
ESC-52	24°16'20.88"	68°58'20.28"	Feldspar porphyry	223±4	LA-ICP-MS	Urzúa (2009)
Unidentified	22°22'40"	68°54'50"	Dacitic dike	222.0±4.9	LA-ICP-MS	Tomlinson and Blanco (2008)
II-15	26°20'28"	70°28'58"	Monzogranite	217±12	ID-TIMS	Berg and Baumann (1985)
FO 06 97	30°07'01.7"	70°26'11.4"	Biotite granite	215.8±1.2	SHRIMP	Hervé *et al*. (2014)
FO 06 93	29°52'39.5"	70°20'22.2"	Cordierite-muscovite granodiorite	215.6±1.9	SHRIMP	Hervé *et al*. (2014)
MEJ-18024	23°05'46.1"	70°30'54.5"	Hornblende-biotite tonalite	208±2	SHRIMP	Casquet *et al*. (2013)
Unidentified	23°24'09"	69°02'52"	Dacitic porphyry	206.1±1.0	ID-TIMS	Marinovic and García (1999)
Unidentified	23°09'41"	69°05'50"	Dacitic porphyry	205.9±0.5	ID-TIMS	Marinovic and García (1999)

The Choiyoi igneous province consists of volcano-plutonic complexes (Kay *et al*., 1989; Llambías *et al*., 1993; Llambías and Sato, 1995) that cover an estimated area of ~500,000 km^2, which extends for about 2,500 km, from the Collahuasi area in northern Chile (20°30'S) to Neuquén and the northern Patagonian Andes of southern Argentina (44°S; Jordan *et al*., 1983; Mpodozis and Ramos, 1989; Ramos and Folguera, 2009; Ramos, 2009). Besides, it is also correlated with the Mitu Group (Carlier *et al*., 1982) and the Yura Group of southern Perú (Sempere *et al*., 2002; Boekhout *et al*., 2013), and geological and geochronological data from magmatic and migmatitic rocks of the Northern Andes have shown that the Late Paleozoic to Triassic magmatism was also extensively recorded from northern Perú to the Central Cordillera of the Colombian Andes (Restrepo *et al*., 1991; Noble *et al*., 1997; Ordóñez and Pimentel, 2002; Vinasco *et al*., 2006; Chew *et al*., 2007; Ibáñez-Mejía *et al*., 2008; Cardona *et al*., 2008, 2009).

The main outcrops of Late Paleozoic to Early Jurassic igneous rocks in northern Chile are exposed in a semi-continuous belt from about 21°S to 31°S latitudes. These rocks are prominent along the Domeyko Cordillera (24° to 27°S) and its northern extension, the so called Chilean Precordillera (20° to 24°S), but also along the High Andes from 27° to 31°S, which are commonly referred as Chilean Frontal Cordillera. Late Carboniferous and Triassic granitic plutons are also scattered from 21°S latitude southwards along the Coastal Cordillera and then forming an almost continuous intrusive belt between 33° to 38°S (*e.g.*, Deckart *et al*., 2014).

The isolation of outcrops, fault-bounded blocks, volcanic deposits of similar petrographic compositions, lack of accurate geochronological data, and the absence of guide horizons, have made difficult to know the exact stratigraphic-structural relationships between separate exposures. Thus, a number of lithostratigraphic units were assigned by different authors to specific time-spans and correlated with other exposures, which at times proved to be incorrect as geochronological data become available. This is reflected by a profuse stratigraphic nomenclature used in previous studies to refer to Late Paleozoic to Early Mesozoic successions of the Andes of northern Chile (*e.g.*, Charrier *et al*., 2007); for unambiguousness figures 1 and 2 illustrate preliminary stratigraphic schemes for two segments of the Andes of northern Chile, modified according to the new geochronological data.

The exposed Late Paleozoic to Mid-Triassic volcanic succession along the Andes in northern Chile has uneven thickness, visible successions typically range between 750 and 2,600 m, but exceeding 3,200 m in the Collahuasi area of the Precordillera (21°S latitude; Vergara and Thomas, 1984). These successions are mostly formed of felsic volcanic rocks that include extensive rhyolitic and dacitic ash flow tuffs (ignimbrites), and banded rhyolite and dacitic domes and lava-flows. A lesser proportion is composed of basaltic and andesitic lavas, and pyroclastic deposits of the same petrographic composition. Sedimentary intercalations of volcanic sandstones, minor conglomerates, and local limestones (*i.e.*, Collahuasi area; Vergara and Thomas, 1984), are also locally present. The volcanic successions unconformably overlie Devonian to Early Carboniferous shallow-marine, sedimentary successions, but its base is only locally exposed (Mercado, 1982; Niemeyer *et al*., 1985, 1997; Mpodozis and Cornejo, 1988; Nasi *et al*., 1990; Marinovic *et al*., 1995). In addition, calcareous and terrigenous, shallow-marine sedimentary successions, containing Early Permian fossils are exposed in the western foothills of the High Andes and in the Central Depression. These sedimentary units represent Early Permian carbonate sedimentation within a shallow-marine platform, but some of them are either overlying or interstratified with rhyolitic rocks (Sepúlveda and Naranjo, 1982; Marinovic *et al*., 1995; Iriarte *et al*., 1996; Cortés, 2000; Díaz-Martínez *et al*., 2000).

Middle to Late Triassic successions are sedimentary-volcanic in nature and are separated from older rocks by unconformities. A bimodal suite composed of basalts and rhyolites, locally with pillow lavas, and associated rhyolitic and dacitic sills, domes and ash-flow deposits occur within the Mid-Late Triassic to Early Jurassic successions (Naranjo and Puig, 1984; Suárez and Bell, 1992; Tomlinson *et al*., 1999; Cornejo and Mpodozis, 1996, 1997; Cornejo *et al*., 2009). The Late Triassic to Early Jurassic magmatism is fairly common, but it has been poorly investigated (*e.g.*, Franz *et al*., 2006), and has not always been recognized as a distinct unit from older Carboniferous-Triassic rocks.

Carboniferous to Triassic granitic, granodioritic, and tonalitic batholiths and lesser dioritic or gabbroic

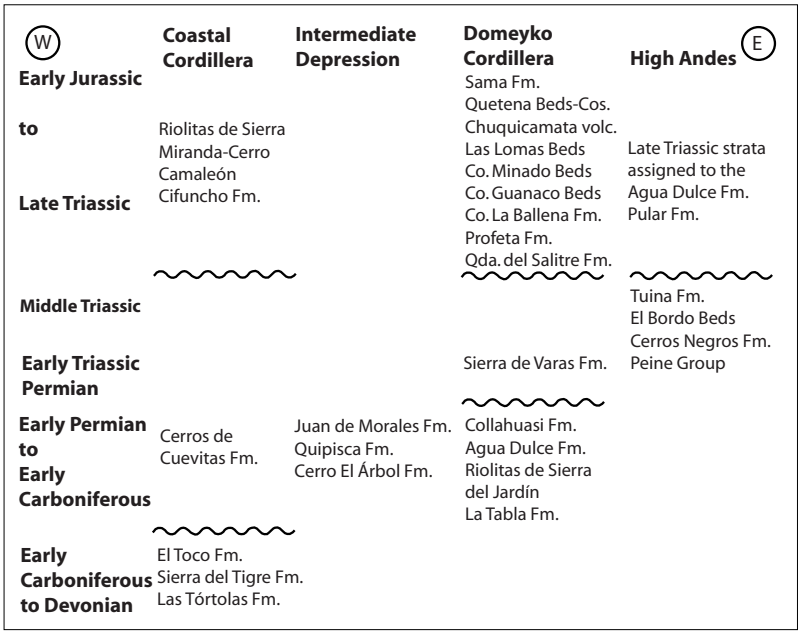

FIG. 1. Late Paleozoic to Early Jurassic stratigraphic units of northern Chile from 20° to 26°S, ordered according to the new geochronological data. The different units are ordered geographically from western (left) to eastern exposures (right) and face each other according to their approximate latitude of occurrence. The reader is referred to the work of Charrier *et al.* (2007 and references therein) for the units that are not mentioned in text.

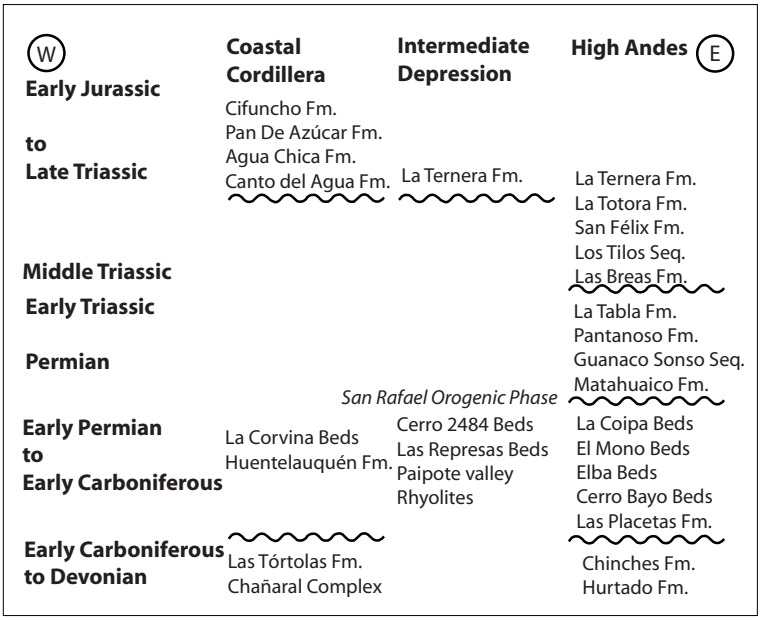

FIG. 2. Late Paleozoic to Early Jurassic stratigraphic units of northern Chile from 26° to 31°S, ordered according to the new geochronological data. The different units are ordered geographically from western (left) to eastern exposures (right) and face each other according to their approximate latitude of occurrence. The reader is referred to the work of Charrier *et al.* (2007 and references therein) for the units that are not mentioned in text.

plutons were emplaced in different segments along the Precordillera (21°-24°S), Domeyko Cordillera (24°-27°S) and an extensive sector of the Chilean Frontal Cordillera between 28° and 31°S (Figs. 3 and 4) is formed of granitic rocks of Late Paleozoic to Triassic age (Parada *et al*., 1981, 2007; Nasi *et al*., 1985; Mpodozis and Kay, 1990, 1992; Mpodozis *et al*., 1993; Cornejo *et al*., 1998; Tomlinson *et al*., 1999; Tomlinson *et al*., 2001; Tomlinson and Blanco, 2008; Hervé *et al*., 2014). Scattered Late Carboniferous and Triassic granitic plutons also extend from 21°S latitude southwards along the Coastal Cordillera, and then forming an almost continuous intrusive belt between 33° to 38°S (Berg *et al*., 1983; Shibata *et al*., 1984; Maksaev and Marinovic, 1980; Skarmeta and Marinovic, 1981; Berg and Baumann, 1985; Mpodozis and Kay, 1992; Parada *et al*., 2007; Deckart *et al*., 2014). Some of the Carboniferous and Early Permian plutons show foliation with preferred orientation of their tabular minerals, and local bands of mylonites with high-temperature, ductile, shearing deformation (Nasi *et al*., 1985; Ribba *et al*., 1988; Marinovic *et al*., 1995; Murillo *et al*., 2012; Hervé *et al*., 2014). Close associations of granitic plutons and ignimbrites in the Andes have been interpreted as large relict calderas (Davidson *et al*., 1985; Breitkreuz, 1995; Tomlinson *et al*., 2001). In addition, a belt of porphyry copper prospects and hydrothermal alteration zones are associated with the Permian and Triassic intrusions in Chile and Argentina (Sillitoe, 1977; Camus, 2003; Cornejo *et al*., 2006; Tomlinson and Blanco, 2008).

The Carboniferous to Mid-Triassic igneous rocks constitute a calc-alkaline to potassium-rich calc-alkaline suite, are metaluminous to peraluminous in composition, and have overall geochemical characteristics consistent with subduction-related, magmatic arc origin, but with evolution into extensional magmatism and significant involvement of crustal melts, evidencing significant crustal recycling (Nasi *et al*., 1985; Kay *et al*., 1989; Breitkreuz *et al*., 1989; Mpodozis and Kay, 1990, 1992; Mpodozis *et al*., 1993; Breitkreuz and Zeil, 1994; Marinovic *et al*., 1995; Lucassen *et al*., 1999; Llambías *et al*., 2003; Parada *et al*., 2007; Urzúa, 2009; Vásquez *et al*., 2011; Parada, 2013). Brown (1990) compared the major and trace elements geochemistry of the Permian to Middle Triassic Coastal granitic plutons at latitude 26°S with those exposed some 120 km to the east in the High Andes, showing their similar compositions with subduction-related affinity, and concluded that they were part of the same magmatic arc split during Mesozoic extension.

The Middle to Late Triassic igneous rocks show a distinct bimodal composition with a within plate tendency, consistent with an origin in an extensional, rift-related setting (Vergara *et al*., 1991; Parada *et al*., 1991; Morata *et al*., 2000; Vásquez *et al*., 2011; Parada, 2013).

3. Previous U-Pb geochronological data

U-Pb geochronological data for Late Paleozoic to Early Mesozoic rocks compiled from previous studies are presented in Tables 1 and 2 and figures 3 and 4.

The oldest zircon U-Pb ages compiled for volcanic rocks range from 309.9±2.2 to 273.5±11.0 Ma (Table 1; Fig. 3); these rocks are exposed from 20°30' to 25°30'S in a ~50 km wide, longitudinal belt along ~69°W longitude along the Precordillera and the Domeyko Cordillera (Fig. 3), and according to the U-Pb data represent a Late Carboniferous to Early Permian, felsic volcanism and subordinate intermediate and basic volcanic rocks, and minor sedimentary intercalations (Collahuasi, Agua Dulce and La Tabla Formations, and the Sierra del Jardín Rhyolites; Vergara and Thomas, 1984; Mpodozis *et al*., 1993; Marinovic and García, 1999; Masterman, 2003; Cornejo *et al*., 2006; Marinovic, 2007; Munizaga *et al*., 2008; Tomlinson and Blanco, 2008; Urzúa, 2009; Jara *et al*., 2009; Hervé *et al*., 2012). The Late Carboniferous to Early Permian volcanism is less known southward of 25°30'S, but a U-Pb zircon age of 300.8±4.6 Ma has been reported by Salazar *et al*. (2013) for rhyolites outcropping in the El Tránsito river valley in the High Andes, 65 km west of the divide (28°46'S; Fig. 4).

Rhyolitic volcanic rocks exposed along the Domeyko Cordillera and Frontal Cordillera south of 25°30'S latitude have yielded U-Pb ages of 262.9±2.0 and 265.0±5.6 Ma (Table 1; Fig. 4), thus essentially representing a Mid-Permian felsic volcanism, which has been previously ascribed to the to the Permian-Triassic (Martin *et al*., 1999) or to the Carboniferous-Permian (Cornejo *et al*., 2009).

A U-Pb zircon U-Pb age of 248±3 Ma, resulting from combining analyses of four separate samples, was reported by Breitkreuz and van Schmus (1996) for felsic volcanic rocks of the Peine Group, exposed in on the eastern border of the Salar de Atacama salt

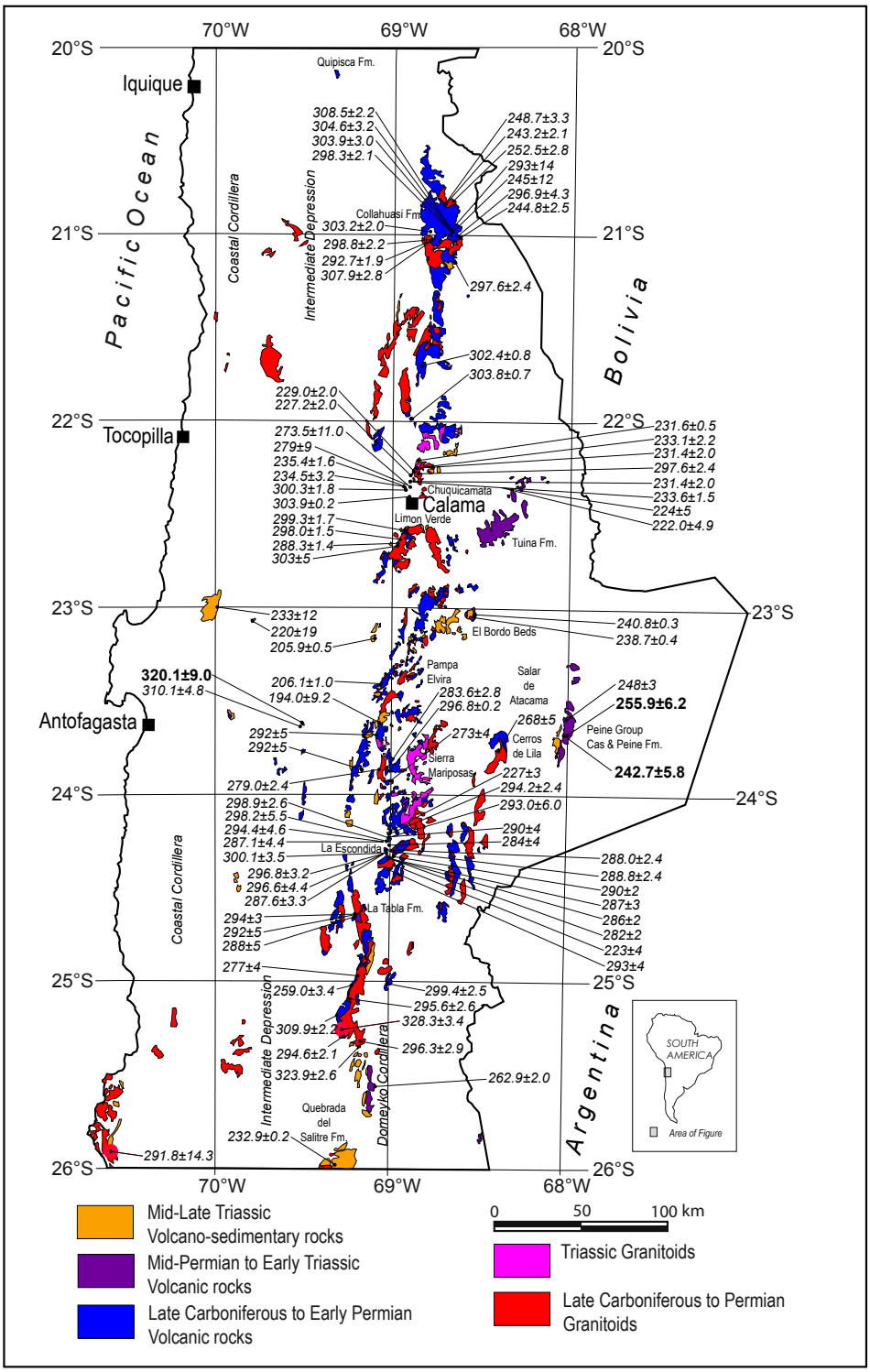

FIG. 3. Map showing the distribution of the Late Paleozoic to Late Triassic rocks of northern Chile between latitudes 20° and 26°S and location of U-Pb zircon ages (Ma±2σ). New SHRIMP U-Pb ages in bold; previous U-Pb dates compiled from previous works in italics (references in Tables 1 and 2).

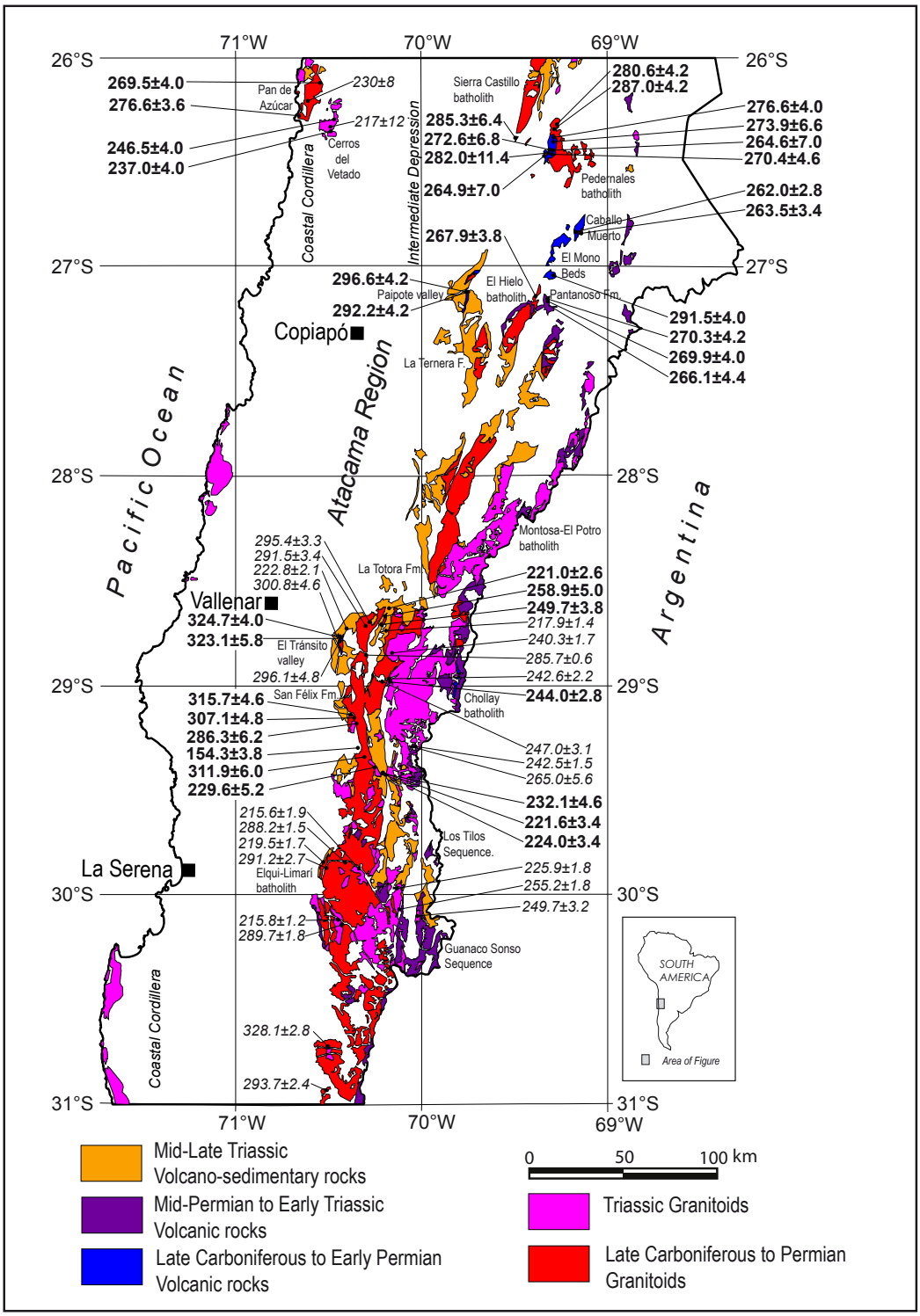

FIG. 4. Map showing the distribution of the Late Paleozoic to Late Triassic rocks of northern Chile between latitudes 26° and 31°S and location of U-Pb zircon ages (Ma±2σ). New SHRIMP U-Pb ages in bold; previous U-Pb dates compiled from previous works in italics (references in Tables 1 and 2).

flat at about 23°30'S (Fig. 3). Thus, these eastern-most outcrops of northern Chile represent an Early to Middle Triassic volcanism, which originally was assigned to the Late Permian by Breitkreuz and van Schmus (1996), as befitted to the geologic time scale in that year.

Middle Triassic to Early Jurassic volcanism has yielded U-Pb dates from 249.7±3.8 to 194.0±9.2 Ma (Table 1). During this time span andesitic to basaltic volcanism coexisted with rhyolitic volcanism (bimodal volcanism), and was synchronous with rift-related, continental and/or marine sedimentary deposits widely distributed in northern Chile (Naranjo and Puig, 1984; Charrier, 1979; Suaárez and Bell, 1992; Martin *et al*., 1999; Tomlinson *et al*., 1999; Cornejo and Mpodozis, 1996, 1997; Cornejo *et al*., 2009).

The zircon U-Pb ages for intrusive rocks exposed along the High Andes and Domeyko Cordillera range from 328.1±2.8 to 205.9±0.5 Ma (Table 2), overlapping with the corresponding interval of U-Pb dates of volcanic rocks (*ca*. 310 to 194 Ma; Table 1). The intrusions include coarse-grained granitoids and porphyritic felsic plutons; the late are closely related to the volcanic rocks. Foliated plutons (ductile deformation) show U-Pb ages in the range 328 to 288 Ma (Table 2).

There are scarce and inaccurate previous U-Pb dates for granitic plutons scattered along the Coastal Cordillera of northern Chile from 21° to 31°S, which range from 291.8±14.3 to 217±12 Ma (Berg *et al*., 1983; Berg and Baumann, 1985). Yet, a number of whole rock Rb-Sr dates that range from 296±5.4 to 222±3 Ma have been published (Berg *et al*., 1983; Shibata *et al*., 1984; Berg and Baumann, 1985), and biotite K-Ar dates of 318±6 and 322±5 Ma (Maksaev and Marinovic, 1980; Skarmeta and Marinovic, 1981). Besides, eight U-Pb ages ranging from 319.6±2.4 to 308.9±2.4 Ma have been recently obtained for the granitoids that are exposed from 33° to 38°S along the Coastal Cordillera of central-southern Chile (Deckart *et al*., 2014).

4. Analytical methods

SHRIMP II U-Pb analyses of zircon grains were carried out at the Geochronological Research Center (Centro de Pesquisas Geocronológicas) of the Sao Paulo University, Brazil. Zircon grains were obtained from rock samples following normal mineral separation procedures in Universidad de Chile, which included crushing, washing, and heavy liquid and magnetic separation. Hand-picked zircon grains were mounted in epoxy, together with chips of the Temora reference zircons, sectioned approximately in one half, and polished in Brazil. Cathodoluminescence (CL) Scanning Electron Microscope (SEM) images were prepared for all zircons. The CL images were used to decipher the internal structures of the sectioned grains and to ensure that the ~20 μm SHRIMP spot was wholly within a single age component within the sectioned grains. Uranium-Th-Pb analyses were made using a sensitive high resolution ion microprobe (SHRIMP II) for determining the respective zircon Concordia U-Pb ages following procedures given in Williams (1998, and references therein). Each analysis consisted of six scans through the mass range, with a Temora U-Pb reference grain analyzed for every three unknown analyses. The data have been reduced using the SQUID Excel Macro of Ludwig (2001); U-Pb ratios have been normalized relative to a value of 0.0668 for the Temora reference zircon, equivalent to an age of 417 Ma (Black *et al*., 2003). Uncertainties given for individual analyses (ratios and ages) are at the one-sigma level (Appendix 2). Tera and Wasserburg (1972) concordia plots, and mean U-Pb age calculations were carried out using ISOPLOT/EX (Ludwig, 2003). The data tabulations for all 43 samples are presented in Appendix 1 and 2.

5. Results

The new SHRIMP U-Pb zircon concordia ages are summarized in Tables 3 and 4 for volcanic and intrusive rocks, respectively and sample locations are shown in figures 3 and 4; Tera-Wasserburg concordia plots and SHRIMP zircon U-Pb analytical data are included in the Appendix 1 and 2, respectively.

5.1. Volcanic rocks

The new zircon U-Pb ages for volcanic rocks range from 324.7±4.0 to 221.0±2.6 Ma (Table 3), which is consistent with the *ca*. 310 to 194 Ma interval showed by the compiled U-Pb dates (Table 1). Nevertheless, we obtained some of the oldest age determinations for Late Paleozoic volcanic rocks in Chile to date, particularly for volcanic deposits exposed in the current Intermediate Depression and the western foothills of the High Andes. These include U-Pb ages of 324.7±4.0 and 323.1±5.8 for rhyolites outcropping

TABLE 3. SUMMARY OF NEW SHRIMP ZIRCON U-Pb CONCORDIA AGES FOR VOLCANIC ROCKS.

Sample	Location (Geodetic-WGS 84)		Lithology	U-Pb age	Unit
	Latitude S	Longitude W		Ma±2σ	
CHY-50	28°46'19.39"	70°26'15.80"	Rhyolite	324.7±4.0	Cerro Bayo Beds
CHY-11	28°46'38.77"	70°25'49.51"	Rhyolite	323.1±5.8	Cerro Bayo Beds
FO-11-35	23°38'04.96"	69°30'27.27"	Rhyolitic ignimbrite	320.1±9.0	Cerro del Árbol Fm.
CHY-29	27°06'58.71"	69°44'28.75"	Rhyolite	296.6±4.2	Paipote valley
CHY-31	27°06'50.51"	69°43'59.49"	Rhyolite	292.2±4.2	Paipote valley
CHY-33	27°03'15.21"	69°17'42.15"	Andesitic tuff	291.5±4.0	El Mono Beds
CHY-14	26°28'49.60"	69°19'04.29"	Rhyolitic tuff	282.0±11.4 *311.3±8.2	La Tabla Formation
CHY-18	26°25'11.76"	69°16'56.65"	Rhyolitic tuff	276.6±4.0	La Tabla Formation
CHY-17	26°26'05.81"	69°16'58.77"	Rhyolitic tuff	273.9±6.6	La Tabla Formation
CHY-15	26°28'42.56"	69°19'12.39"	Rhyolitic tuff	272.6±6.8	La Tabla Formation
CHY-22	26°28'41.13"	69°18'13.19"	Banded rhyolite	270.4±4.6	La Tabla Formation
CHY-25	27°09'37.98"	69°18'42.56"	Dacite	270.3±4.2	Pantanoso Formation
CHY-27	27°10'24.48"	69°18'31.21"	Dacitic tuff	269.9±4.0	Pantanoso Formation
CHY-26	27°09'49.87"	69°18'30.97"	Rhyolitic ignimbrite	266.1±4.4	Pantanoso Formation
CHY-36	26°49'46.33"	69°10'06.58"	Fluidal rhyolite	262.0±2.8	La Tabla Formation
FO-11-27	23°40'23.32"	68°01'07.42"	Rhyolitic ignimbrite	255.9±6.2	Cas Formation
CHY-56	28°42'30.38"	70°12'34.79"	Basaltic tuff	249.7±3.8 *323.6±5.8	La Totora Formation
FO-11-26	23°39'59.19"	67°59'50.29"	Rhyolite	242.7±5.8	Cas Formation
CHY-10	29°24'57.58"	70°13'13.05"	Banded Rhyolite	232.1±4.6	Los Tilos Sequence
CHY-01	29°25'00.02"	70°13"01.99"	Banded rhyolite	224.0±3.4	Los Tilos Sequence
CHY-02	29°24'50.60"	70°13'01.87"	Rhyolitic tuff	221.6±3.4	Los Tilos Sequence
CHY-57	28°39'14.52"	70°10'37.43"	Basalt	221.0±2.6	La Totora Formation
CHY-08	29°17'38.46"	70°21'41.86"	Andesite	154.3±3.8	Lagunillas Formation

* Samples CHY-14 and CHY-56 are tuffs that returned bimodal age distributions; the older population of U-Pb ages correspond to inherited older zircon cores as seen in the cathode luminescence images.

in the El Tránsito river valley (at 28°46'S; Fig. 4), which were previously mapped as the Permian to Triassic Pastos Blancos Formation (Moscoso *et al*., 2010), but were recognized as an older separate unit named Cerro Bayo Formation by Salazar *et al*. (2013). Besides, a U-Pb age of 320.1±9.0 Ma was obtained for an ignimbrite outcropping in the Intermediate Depression of the Antofagasta Region, which is part of a rhyolitic volcanic succession that underlies and is partly interfingered with carbonate strata that contains Early Permian marine fossils in its upper section (Cerro del Árbol Formation; Marinovic *et al*., 1995; Marinovic, 2007). In addition, U-Pb ages of 296.6±4.2 and 292.2±4.2 Ma were obtained for rhyolites that are part of a succession exposed in the Paipote valley which was assigned to the Pantanoso

TABLE 4. SUMMARY OF NEW SHRIMP ZIRCON U-Pb CONCORDIA AGES FOR INTRUSIVE ROCKS.

Sample	Location (Geodetic-WGS 84)		Lithology	U-Pb age	Unit
	Latitude S	Longitude W		Ma±2σ	
CHY-05	29°08'19.52"	70°22'41.82"	Biotite monzogranite	315.7±4.6	Guachicay pluton
CHY-09	29°20'25.47"	70°19'14.69"	Biotite syenogranite	311.9±6.0	Guanta pluton
CHY-06	29°09'16.19"	70°21'31.11"	Biotite-hornblende tonalite	307.1±4.8	Guanta pluton
CHY-24	26°22'07.72"	69°16'37.94"	Hornblende-biotite quartz monzodiorite	287.0±4.2	Pedernales batholith
CHY-07	29°10'10.89"	70°20'59.70"	Muscovite-biotite monzogranite	286.3±6.2	Burro Muerto pluton
CHY-19a	26°23'34.30"	69°29'24.72"	Foliated biotite-hornblende tonalite	285.3±6.4	Sierra Castillo batholith
CHY-23	26°20'58.88"	69°15'42.50"	Biotite monzogranite	280.6±4.2	Pedernales batholith
CHY-48	26°16'27.71"	70°39'22.80"	Muscovite-biotite monzogranite	276.6±3.6	Pan de Azúcar pluton
CHY-47	26°07'21.74"	70°31'53.93"	Muscovite leucogranite	269.5±4.0	Pan de Azúcar pluton
CHY-35	27°08'21.17"	69°22'05.53"	Biotite monzogranite	267.9±3.8	El Hielo batholith
CHY-12	26°28'53.10"	69°19'25.75"	Biotite-hornblende monzogranite	264.9±7.0	Pedernales batholith
CHY-16	26°28'19.36"	69°17'50.67"	Andesitic dike	264.6±7.0	Dike in La Tabla Fm.
CHY-38	26°50'46.18"	69°08'50.32"	Biotite monzogranite	263.5±3.4	Caballo Muerto Pluton
CHY-58	28°39'59.13"	70°10'55.94"	Biotite-bearing mylonitized tonalite	258.9±5.0	Quebrada Pintado tonalite
CHY-46	26°18'22.54"	70°27'05.87"	Biotite-muscovite leucogranite	246.5±4.0	Cerros del Vetado Pluton
CHY-60	28°58'18.69"	70°09'44.14"	Biotite monzogranite	244.0±2.8	Chollay batholith
CHY-45	26°22'41.05"	70°27'36.16"	Biotite monzogranite	237.0±4.0	Cerros del Vetado pluton
CHY-03	29°24'29.70"	70°14'24.51"	Syenogranite	229.6±5.2	La Coneja pluton; Colorado unit

Formation (Sepúlveda and Naranjo, 1982; Iriarte *et al*., 1996) and unconformably underlies Late Triassic conglomerates of La Ternera Formation in the Atacama Region (Fig. 4). The same rhyolitic unit underlies limestone beds with Early Permian marine fossils in the region, though the contact between them has been interpreted as a low-angle, normal fault (Quebrada de Las Represas Beds; Mpodozis and Allmendinger, 1993; Iriarte *et al*., 1996).

In the High Andes a U-Pb age of 291.5±4.0 Ma was obtained for an andesitic tuff intercalated in the upper section of El Mono Beds (*sensu* Mercado, 1982; Mpodozis *et al*., 2012), which is a mostly alluvial and lacustrine sedimentary succession,

ca. 1,000 m thick, formed of sandstone and conglomerate strata that unconformably overlie Devonian to Early Carboniferous sandstones of the Chinches Formation in the High Andes at ~27°S (Fig. 4) and underlies in apparent conformity Jurassic marine strata (Mercado, 1982; Mpodozis *et al*., 2012). This sedimentary-volcanic succession was previously attributed to the Late Triassic based on fossil flora and conchostracans (Davidson *et al*., 1978; Mercado, 1982; Suárez and Bell, 1991; Blanco, 1994; Cornejo *et al*., 1998; Gallego and Covacevich, 1998; Mpodozis *et al*., 2012).

U-Pb dates ranging from 282.0±11.4 to 270.4±4.6 Ma were obtained for 4 samples of banded rhyolites and rhyolitic tuff from the type locality of La Tabla Formation, (*sensu* García, 1967), in the eastern part of the Domeyko Cordillera and southwest of the Pedernales Salar in the Atacama Region (26°30'S; Fig. 4). One sample (CHY-14; Table 3) returned a bimodal age distribution with an older population at 311.3±8.2 Ma and a younger one at 282.0±11.4; the analytic spots on the cathode luminescence images of the zircons indicate that the older age population corresponds to inherited zircon cores, while the younger ages to zircon rims, thus the younger population corresponding to the actual crystallization age of the dated rock. The La Tabla Formation is an 800 m thick succession formed of rhyolites, rhyolitic tuffs, breccias, and basaltic intercalations (without exposed base) which originally was thought to be Early Triassic in age (García, 1967), but later assigned to the Late Paleozoic by Tomlinson *et al*. (1999), based on K-Ar ages of intrusions that crosscut the unit. The volcanic rocks of La Tabla Formation are crosscut by granitoids of the Pedernales Batholith and andesitic dikes that yielded U-Pb ages from 287.0±4.2 to 264.6±7.0 Ma (Table 4). According to the new U-Pb dates it represent Permian volcanism, which is a bit younger but overlapping with the U-Pb ages from 309.9±2.2 to 282±2 Ma published for rocks assigned to the La Tabla Formation along the Domeyko Cordillera north of 25°30'S latitude (Table 1). In addition, a U-Pb age of 262.0±2.8 was obtained for a sample of fluidal rhyolite farther south (26°49'S; Table 3), mapped as La Tabla Formation by Cornejo *et al*. (1998) that is part of a succession crosscut by granite of the Caballo Muerto Pluton, which yielded a U-Pb age of 263.5±3.4 Ma (Table 4).

A U-Pb age of 270.3±4.2 Ma was obtained for a basal dacite horizon and additional U-Pb ages of 269.9±4.0 and 266.1±4.4 Ma were obtained for dacitic tuff and rhyolitic ignimbrite of the Pantanoso Formation (Mercado, 1982; Mpodozis *et al*., 2012), at its type locality (Table 3; Fig. 4). The Pantanoso Formation is crosscut by granite of the El Hielo batholith that yielded a U-Pb age of 267.9±3.8 Ma (Table 4). The Pantanoso Formation is a 1,000 thick succession of rhyolitic and dacitic volcanic rocks and minor conglomerate and volcanic sandstone intercalations exposed in the High Andes at 27°28'S latitude, and according to the new U-Pb data it represent Mid-Permian volcanism. It unconformably overlies mainly Devonian to Early Carboniferous sandstones of the Chinches Formation (Mercado, 1982; Bell, 1985), but also a local lens of folded sandstone and conglomerate beds up to 200 m thick of the Elba Beds, which were ascribed to the Carboniferous-Permian by Mercado (1982).

U-Pb zircon ages of 255.9±6.2 and 242.7±5.8 Ma (Table 3) were obtained for samples of ignimbrite and rhyolite from the Cas Formation (*sensu* Ramírez and Gardeweg, 1982), which is a succession of about 300 m thick (without exposed base), outcropping immediately east of the Peine town, in the eastern part of the Antofagasta Region (Fig. 3). The new U-Pb ages are consistent with the mean weighted U-Pb age of 248±3 based on 4 separate determinations published by Breitkreuz and van Schmus (1996) and indicate that the rhyolitic rocks of the Cas Formation represent a Late Permian to Early Triassic felsic volcanism.

A sample of basaltic tuff from the basal meters of the mostly basaltic-andesitic La Totora Formation in the homonymous creek in the High Andes of the Vallenar region (28º42'; Fig. 4) yielded a U-Pb age of 249.7±3.8 Ma. The dated sample (CHY-56) actually returned a bimodal age distribution with an older population at 323.6±5.8 Ma; the analytic spots on the cathode luminescence images of the zircons indicate that the older age population corresponds to inherited zircon cores, while the younger ages to zircon rims, thus the younger population corresponding to the actual crystallization age of the dated rock. Another sample of basalt of the same succession in the Totora creek yielded an U-Pb age of 221.0±2.6 Ma; these ages are coherent with the U-Pb ages from 217.9±1.4 to 210.4±2.9 Ma published by Salazar *et al*. (2013) for the same formation. This volcanic

unit unconformably overlies a mylonitized tonalite of the Quebrada Pintado intrusive unit (*sensu* Salazar *et al*., 2013) for which we obtained a U-Pb age of 258.9±5.0 Ma (Table 4), and conformably underlies fossiliferous, Mid-Late Jurassic (Sinemurian) marine limestones (Reutter, 1974; Nasi *et al*., 1990; Salazar *et al*., 2013); stratigraphic position that is consistent with the new U-Pb data. In addition, strata of the western belt of La Totora Formation are in part conformably overlying the 4,000 m thick, mostly clastic-sedimentary Mid-Late Triassic San Felix Formation to the southwest (Salazar *et al*., 2013).

U-Pb ages of 232.1±4.6, 224.0±3.4, and 221.6±3.4 were obtained for samples of banded rhyolites and rhyolitic tuffs from the Los Tilos sequence of the Pastos Blancos Group (*sensu* Martin *et al*., 1999), exposed in the Potrerillos river valley in the High Andes, 20 km west of the divide (29°30'S; Fig. 4); this new U-Pb data confirms the Late Triassic age of the Los Tilos volcanic sequence of the Pastos Blancos Group, which unconformably overlies the Permian silicic volcanics of the Guanaco Sonso sequence as defined by Martin *et al*. (1999).

A U-Pb age of 154.3±3.8 Ma was obtained for andesite that is part of a succession outcropping in the west flank of the El Carmen river valley (29°17'S; Fig. 4). This intermediate volcanic unit was originally mapped as part of the Late Paleozoic-Triassic Pastos Blancos Formation (with a question mark) by Nasi *et al*. (1990). Actually, the new U-Pb age shows that these andesitic rocks are Late Jurassic in age, being equivalent in age and lithology to the Picudo Formation (Reutter, 1974; Moscoso *et al*., 2010) exposed in the El Tránsito river valley and to the Lagunillas Formation, which has been recognized farther north between 27°30' and 28°30´S in the High Andes of the Atacama Region and these represent Late Jurassic back-arc volcanism (Iriarte *et al*., 1999; Oliveros *et al*., 2011).

5.2. Intrusive rocks

The new zircon U-Pb ages for Late Paleozoic intrusive rocks range from 315.7±4.6 to 229.6±5.2 Ma (Table 4), well within the 328 to 206 Ma interval of the compiled U-Pb dates (Table 2).

Granitoids exposed along the Domeyko Cordillera and its southern continuation in the Frontal Cordillera yielded U-Pb ages from 287 to 263 Ma (Table 4; Fig. 4), representing Permian granitic plutonism, these include: a U-Pb age of 285.3±6.4 Ma for a foliated tonalite that is part of the Sierra Castillo batholith (*sensu* Tomlinson *et al*., 1999; Fig. 4); a U-Pb age of 287.0±4.2 Ma for a hornblende-biotite monzodiorite and U-Pb ages of 280.6±4.2, and 264.9±7.0 Ma for biotite-hornblende, monzogranite plutons of the Pedernales batholiths (*sensu* Tomlinson *et al*., 1999; Fig. 4); a U-Pb age of 263.5±3.4 Ma for monzogranite of the Caballo Muerto pluton (*sensu* Cornejo *et al*., 1998); and a U-Pb age of 267.9±3.8 Ma for leucocratic, monzogranite of the El Hielo batholith (*sensu* Mercado, 1982; Bell, 1985; Mpodozis *et al*., 2012) in the High Andes of the Atacama Region (Fig. 4).

A U-Pb age of 244.0±2.8 Ma was obtained for a coarse-grained monzogranite of the Chollay Batholith (Fig. 4), which is consistent with U-Pb ages from 247.7±3.4 to 240.3±1.7 Ma that have recently been reported for the same batholith (Coloma *et al*., 2012; Salazar *et al*., 2013; Álvarez *et al*., 2013; Hervé *et al*., 2014). These U-Pb ages confirm the Mid-Triassic age ascribed to the granitic Chollay batholith by Nasi *et al*. (1985) and Martin *et al*. (1999).

The dating of plutons of the northern part of the composite Elqui-Limarí Batholith in the Frontal Cordillera of the Atacama Region (Fig. 4) have yield U-Pb ages from 315.7±4.6 to 229.6±5.2 Ma (Table 4). These are consistent with the 330 to 215 U-Pb interval of recently published U-Pb ages for the same batholith (*e.g.*, Pineda and Calderón, 2008; Salazar *et al*., 2009, 2013; Coloma *et al*., 2012, Álvarez *et al*., 2013; Hervé *et al*., 2014). We have obtained a U-Pb age of 315.7±4.6 Ma for a coarse-grained, biotite monzogranite from the Guachicay pluton (*sensu* Nasi *et al*., 1985) exposed in the Del Carmen river valley and 311.9±6.0 Ma for a coarse-grained, biotite syenogranite exposed in the Potrerillos river valley. The latter was included in the extensive tonalitic Guanta pluton by Nasi *et al*. (1985, 1990). In addition, we obtained a zircon U-Pb age of 307.1±4.8 Ma for a foliated, coarse-grained, biotite-hornblende tonalite of the Guanta pluton (*sensu* Nasi *et al*., 1985, 1990) exposed in the Del Carmen river valley, and a U-Pb zircon age of 286.3±6.2 Ma was obtained for a coarse-grained, muscovite-biotite granite of the Burro Muerto pluton (*sensu* Nasi *et al*., 1985), which is emplaced within the foliated tonalite of the Guanta pluton in the El Carmen river valley, and corresponds to the Cochiguaz intrusive unit of Nasi *et al*. (1985, 1990); and a U-Pb zircon age of 229.6±5.2 Ma was obtained for a brick-red, fine-grained, syenogranite

of the La Coneja pluton (*sensu* Nasi *et al*., 1985) that corresponds to the Colorado intrusive unit of Nasi *et al*. (1985, 1990).

A U-Pb zircon age of 258.9±5.0 Ma (Late Permian) was obtained for mylonitized tonalite of the Quebrada Pintado tonalitic unit of Salazar *et al*. (2013) in the La Totora creek (28°40'S; Fig 4). The mylonites at La Totora creek show a N35°E/75°E foliation and centimetric to decimetric white, felsic bands alternating with dark gray, biotitic bands. This mylonitized intrusion unconformably underlies the Mid-Late Triassic volcanic rocks of La Totora Formation.

Along the Pacific coast north of Chañaral, about 120 km west of the High Andes, U-Pb ages of 276.6±3.6 and 264.6±7.0 Ma were obtained for biotite-muscovite, monzogranite of the Pan de Azúcar pluton (*sensu* Mercado, 1980; Godoy and Lara, 1998), while two U-Pb ages of 246.5±4.0 and 237.0±4.0 were obtained for coarse-grained, muscovite-biotite monzogranite of the Cerros del Vetado pluton of the Coastal Cordillera immediately east of Chañaral (Fig. 4).

6. Discussion

The U-Pb data provide evidence for the onset of volcanism at ~325 Ma (by the end of the Mississippian), which is approximately coeval with the onset of granitic plutonism at ~328 Ma (Tables 2 and 3), confirming a previous conclusion of Hervé *et al*. (2014). This marks reestablishment of magmatism during the Carboniferous after a gap in igneous activity during the Devonian in northern Chile and Perú (*e.g.*, Charrier *et al*., 2007; Boekhout *et al*., 2013).

6.1. Volcanic rocks

The oldest rhyolitic rocks (325 to 292 Ma; Table 1 and 3) are present within the current Intermediate Depression and the western foothills of the High Andes of northern Chile (Figs. 3 and 4). Part of this initial volcanism developed within a shallow marine platform represented by carbonate strata with Late Permian marine fossils that are overlying and partly interfingered with the dated rhyolitic rocks (Juan de Morales Formation in the Tarapacá Region; Galli, 1956, 1968; Díaz-Martínez *et al*., 2000; Cerro del Árbol Formation in Antofagasta Region; Marinovic *et al*., 1995; Marinovic, 2007; and Quebrada de Las Represas Beds in the Atacama Region; Iriarte *et al*., 1996). While, the rhyolitic succession exposed in the El Tránsito river valley includes conglomerates, sandstones and andesites (Cerro Bayo Formation; Salazar, 2012; Salazar *et al*., 2013).

The mainly felsic volcanic rocks widely exposed along the Domeyko Cordillera and Precordillera of northern Chile north of 25°30'S latitude have yielded U-Pb ages from 310 to 282 Ma Tables 1 and 3), thus represent a Late Carboniferous to Early Permian volcanism that is older than the Choiyoi succession of the San Rafael Block in western Argentina for which U-Pb ages from 281 to 251 Ma have been published (Rocha-Campos *et al*., 2011). Actually, the Chilean Carboniferous to Early Permian volcanic rocks are chronologically equivalent to sedimentary successions with submarine volcanic deposits that are present farther east in Argentina (Azcuy *et al*., 1999; López-Gamundí, 2006; Koukharsky *et al*., 2009; Gulbranson *et al*., 2010). Therefore, when the Carboniferous to Early Permian magmatism was active along the current Domeyko Cordillera and Precordillera northwards, in Argentina farther east developed contemporary marine basins; this situation has been interpreted as a magmatic arc and back-arc basins by Gulbranson *et al*. (2010).

The U-Pb age of 291.5±4.0 Ma that we obtained for an andesitic tuff intercalated in the upper part of El Mono Beds at its type locality (Mpodozis *et al*., 2012), in the High Andes at ~27°S, indicates an Early Permian age for the upper part of the succession. Even though it underlies in apparent conformity Jurassic marine strata, implying a hiatus in what was considered a continuous sedimentary sequence (*e.g.*, Blanco, 1994). The mostly clastic, alluvial and lacustrine sedimentary El Mono Beds have previously been assigned to the Late Triassic, based mainly on fossil flora attributed to Dicroidium sp. (Mercado, 1982; Suárez and Bell, 1991; Blanco, 1994; Cornejo *et al*., 1998; Gallego and Covacevich, 1998; Mpodozis *et al*., 2012). We cannot exclude the possibility that Triassic sedimentary rocks exists in the same region, but the new U-Pb age of 291.5±4.0 Ma is consistent with the stratigraphic position of the El Mono Beds unconformably overlying Devonian to Early Carboniferous sandstones of the Chinches Formation (Bell, 1985; Mpodozis *et al*., 2012), and evidences that this unit represents a Late Carboniferous to Early Permian sedimentation and coetaneous pyroclastic volcanism, at least where sampled for

dating. Therefore, El Mono Beds could be equivalent to a sedimentary unit with Late Carboniferous flora and marine fossils exposed near the watershed of the Andes at ~29°S latitude (Las Placetas Formation; Reutter, 1974; Nasi *et al*., 1990); these sedimentary deposits probably represent the westernmost part of sedimentary basins developed mainly farther east in Argentina during the Carboniferous to Early Permian (Azcuy *et al*., 1999; López-Gamundí, 2006; Koukharsky *et al.*, 2009; Gulbranson *et al*., 2010).

Rhyolitic volcanism with andesitic and basaltic intercalations persisted during the Permian along the current Domeyko Cordillera and the Chilean Frontal Cordillera (High Andes) as the volcanic rocks exposed south of 25°30'S latitude have yielded U-Pb ages from 282 to 262 Ma (Figs. 3 and 4). These are represented by the La Tabla, and Pantanoso Formations, and the Guanaco Sonso Sequence of the Pastos Blancos Group (Mercado, 1982; Cornejo *et al*., 1993, 1998, 2009; Martin *et al*., 1999; Tomlinson *et al*., 1999; Mpodozis *et al*., 2012) and their U-Pb ages fall well within the 281 to 251 Ma time span of U-Pb ages published by Rocha-Campos *et al*. (2011) for the Choiyoi Succession of the San Rafael Block in western Argentina.

The U-Pb age of 270.3±4.6 Ma for the basal unit of the Pantanoso Formation (Table 3) indicates the onset of volcanic accumulation in the current High Andes at ~27°S latitude unconformably on top of deformed Devonian to Early Carboniferous sedimentary rocks (Chinches Formation; Mercado, 1982; Bell, 1985), but also over folded sandstone and conglomerate beds ascribed to the Carboniferous-Permian (Elba Beds; Mercado, 1982). Thus, according to the new U-Pb data the accumulation of the volcanic rocks of the Pantanoso Formation at its type locality occurred at least 20 My later than the rhyolitic succession that is exposed 47 km to the west in the Paipote valley, which in previous works has also been assigned to the Pantanoso Formation (Iriarte *et al*., 1996).

Late Permian to Early Triassic rhyolitic volcanism is represented by the Cas Formation that yielded U-Pb ages from 256 to 243 Ma (Fig. 3; Tables 1 and 3) and is exposed in the easternmost part of Chile (68°W), along the eastern side of the Salar de Atacama salt flat in the Antofagasta Region (Ramírez and Gardeweg, 1982; Breitkreuz and van Schmus, 1996). The rhyolitic rocks of the Cas Formation at its type locality are significantly younger than the Early Permian rhyolitic rocks exposed some 90 km to the west along the Domeyko Cordillera (*e.g.*, Sierra del Jardín Rhyolites; Marinovic, 2007), even though the latter were mapped as the same formation by Mpodozis *et al*. (1993).

The occurrence of Mid-Permian to Early Triassic volcanic rocks eastward from the Carboniferous to Early Permian volcanic rocks in Chile is interpreted as a Mid-Permian to Early Triassic expansion and/or eastward migration of the volcanic front, which is consistent with evidences of expansion of the volcanic activity farther east in Argentina at that time (*e.g.*, Ramos and Folguera, 2009; Ramos, 2009).

Middle Triassic to Early Jurassic volcanic rocks yielded zircon U-Pb ages from 249.7±3.8 to 194.0±9.2 Ma, their outcrops are more discontinuous (patchy) and dispersed compared to the older volcanic rocks, and are separated from them by erosional surfaces. During this period andesitic to basaltic volcanism coexisted with felsic volcanism (bimodal volcanism), and was synchronous with rift-related, continental and/or marine sedimentary deposits in northern Chile (*e.g.*, Suárez and Bell, 1992; Bell and Suarez, 1994). Middle to Upper Triassic strata show strong facies changes along the longitudinal axis of the High Andes, for example according to the U-Pb data the mostly basaltic-andesitic La Totora Formation (250-210 Ma) overlaps in age with the upper part of the mainly clastic, sedimentary San Félix Formation (223-212 Ma), but also with rhyolites of Los Tilos Sequence (232-221 Ma), within less than 100 km in the Atacama Region. These striking north-south facies changes probably reflect the main northwest orientation of extensional basins that developed in the Mid-Late Triassic in Chile and Argentina (Charrier, 1979; Chong and Von Hillebrandt, 1985; Uliana *et al*., 1989; Ramos and Kay, 1991; Jenchen and Rosenfeld, 2002; Charrier *et al*., 2007; Barredo *et al*., 2012).

A probability density plot and stacked histogram of all U-Pb ages for volcanic rocks exposed along the segment of the Chilean Andes from 20° to 31°S (Fig. 5) evidences a protracted volcanic activity that extended for about 130 million years, from about 325 to 194 Ma (Late Mississippian to Early Jurassic). The histogram (Fig. 5) shows two largest concentrations of U-Pb dates from 310 to 250 Ma and from 240 to 210 Ma, and other less prominent concentrations of U-Pb ages from 330 to 320 Ma and at about 190 Ma. Even though the histogram probably is biased to zircon-bearing rocks and easily accessible outcrops

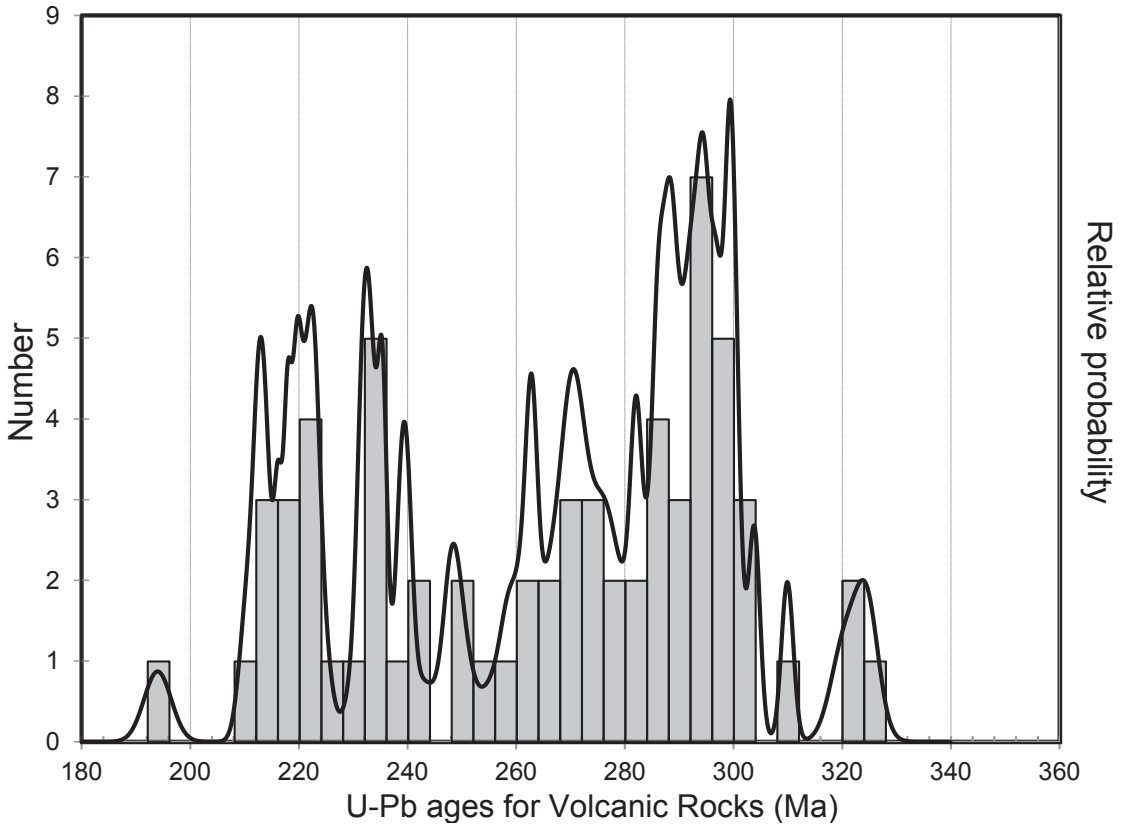

FIG. 5. Probability density plot and stacked histogram of zircon U-Pb ages for volcanic rocks.

for sampling, the statistical analysis of the U-Pb data may signify that major volcanic episodes extended from the Late Carboniferous to Late Permian and then from Mid- to Late Triassic, but were preceded by a mid-Carboniferous volcanic episode and followed by an Early Jurassic one.

6.2 Intrusive rocks

U-Pb data for plutonic rocks show that earliest intrusions crystallized from 328.1±2.8 to 311.9±6.0 Ma, including coarse-grained, biotite-muscovite granite to granodiorite (S-type) and biotite monzogranite and biotite-hornblende granodiorite plutons (I-type). From 308.5±2.2 to 290±2 Ma rhyolitic and granitic porphyries and equigranular monzogranite plutons crystallized and biotite-muscovite granitic and granodioritic plutons, and hornblende-diorite tonalitic to dioritic plutons were emplaced. Furthermore, 33 compiled and 9 new U-Pb zircon ages, which altogether range from 298.9±2.6 to 252.5±1.8 Ma attest that plutonism was active during the whole Permian in northern Chile, when there was a strong predominance of coarse-grained monzogranite plutons, both equigranular and porphyritic, followed by coarse-grained biotite-hornblende tonalites, and only minor monzonite, diorite and gabbro intrusions; two-mica (S-type) granites, granodiorites, and tonalites also intruded during this time span. Most of the Permian plutons are exposed along the High Andes and Domeyko Cordillera, but Permian granites with U-Pb ages of 277-270 Ma are also present some 120 km west in the Pacific coast (Pan de Azúcar pluton, Fig 4).

Triassic plutonism is represented by granitic porphyries, biotite- and two-mica granites, granodiorites, and brick-red syenogranite intrusions with U-Pb ages that range from 247.0±3.1 to 215.6±1.9 Ma. Some of these intrusions are of large volume, as most of the Chollay and Montosa granitic batholiths are formed of Triassic medium to coarse-grained monzogranites for which U-Pb ages of 245.0±3.1

and 240.3±1.7 Ma have been reported (Coloma *et al*., 2012; Hervé *et al*., 2014) and we obtained a U-Pb age of 244.0±2.8 Ma. Triassic granitic plutons are also present in the current Coastal Cordillera as Cerros del Vetado pluton yielded U-Pb ages of 247-237 Ma (Fig. 4).

The U-Pb data now available evidence that muscovite-bearing intrusive, with S-type granite characteristics, were not confined to a single discrete Permian magmatic episode as previously thought, but crystallized within the entire time span from Late Carboniferous to Late Triassic and synchronically with biotite- and hornblende-bearing intrusions with petrographic characteristics of I-type granitoids; this is in agreement with a similar conclusion based on U-Pb data for the Elqui-Limarí Batholith (Hervé *et al*., 2014). Actually, the synchronic emplacement of I- and S-Type granitoids was already noted and sustained by chemical data by Marinovic *et al*. (1995) in the Domeyko Cordillera, though it was attributed to a local phenomenon related to a hypothetical longitudinal segmentation of the Late Paleozoic to Triassic plutonism, rather than to a regional characteristic.

The new U-Pb data from 277 to 237 Ma (Table 4) confirm that Permian and Mid-Triassic granitic magmatism is also exposed in the current coastal area, which combined with previously published geochronological data suggests a protracted plutonism extending from 322 to 217 Ma along the Coastal Cordillera of northern Chile from 21° to 33°S (Maksaev and Marinovic, 1980; Skarmeta and Marinovic, 1981; Berg *et al*., 1983; Shibata *et al*., 1984; Berg and Baumann, 1985). However, there appears to be a difference with the Coastal Batholith exposed to the south between 33° to 38°S, which has yielded eight 320 to 300 Ma (Pennsylvanian) U-Pb zircon ages (Deckart *et al*., 2014), but to date there are no Permian and Early Triassic granitoids intruded in the main body of this Coastal Batholith of central-southern Chile, and only some small Late Triassic-Early Jurassic stocks of calc-alkaline to transitional A-type affinities, with U-Pb zircon ages from 225 to 197 Ma that are emplaced into its metamorphic envelope (Vásquez *et al*., 2011; Hervé *et al*., 2014).

A probability density plot and stacked histogram of all U-Pb ages for intrusive rocks (Fig. 6) shows

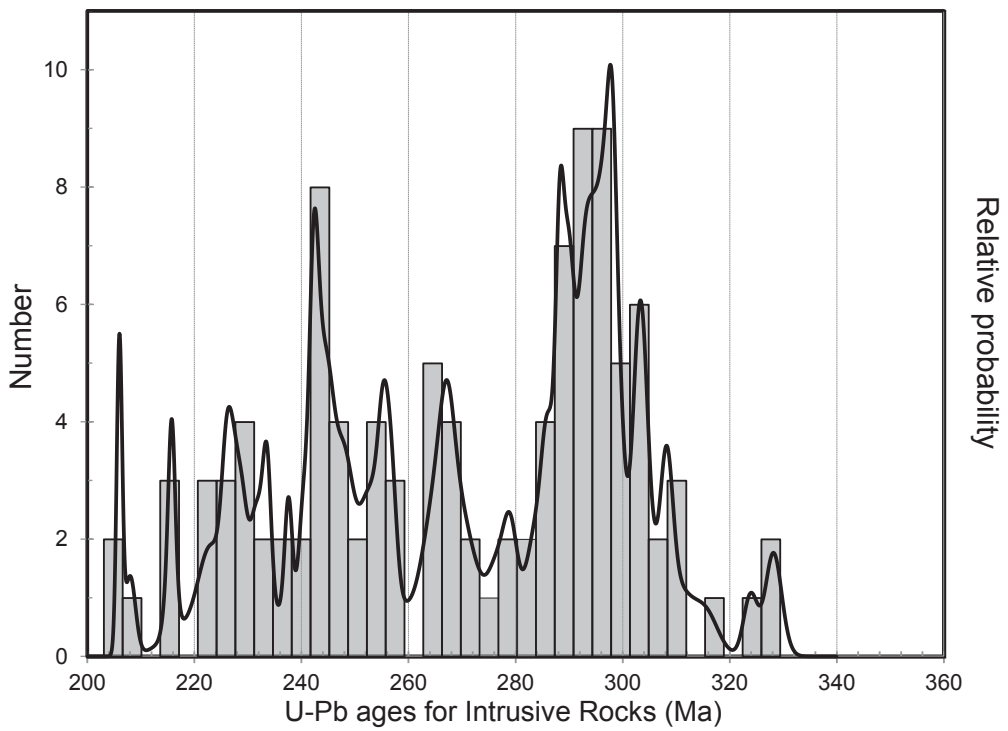

FIG. 6. Probability density plot and stacked histogram of zircon U-Pb ages for intrusive rocks.

that plutonic activity extended for at least 120 My from about 328 to 206 Ma (Late Missisipian to Late Triassic) with a largest concentration of U-Pb dates between 310 and 280 Ma, followed by another significant concentration of U-Pb dates from 255 to 205 Ma, and other less prominent U-Pb age concentrations from 330 to 310 Ma and 280 to 260 Ma. This statistical analysis of the U-Pb data may signify that major intrusive episodes took place from the Late Carboniferous to Early Permian and from the Late Permian to Late Triassic, but also there were mid-Carboniferous and mid-Permian intrusive episodes. The inferred plutonic episodes are fundamentally coincident with the major episodes of volcanism inferred from the statistical analysis of U-Pb data (Figs. 5 and 6). A sequential plot of the U-Pb ages (Fig. 7) shows that there are no apparent periods when the volcanism or plutonism prevailed, but both developed simultaneously from the Carboniferous to the Early Jurassic. A probability density plot and stacked histogram of all U-Pb ages for igneous rocks (Fig. 8) show the largest concentration of dates from 310 to 260 Ma and from 255 to 205 Ma, which are interpreted as the major magmatic episodes developed during from the Late Carboniferous to Mid-Permian and from Late Permian to Late Triassic. Other less prominent U-Pb age concentrations reveal a mid-Carboniferous episode (330 to 320 Ma) and an Early Jurassic episode (200-190 Ma).

The magmatic episodes of the Chilean Andes fall well within the 336 to 230 Ma interval of published U-Pb geochronological data for igneous rocks of Argentina (Pankhurst, 2006; Gulbranson *et al*., 2010; Rocha-Campos *et al*., 2011; Barredo *et al*., 2012; Suárez *et al*., 2012; Gregori and Benedini, 2013), but also with the interval from 342 to 190 of U-Pb data from the Andes of Perú, Ecuador and Colombia (Restrepo *et al*., 1991; Noble *et al*., 1997; Ordoñez and Pimentel, 2002; Vinasco *et al*., 2006; Chew *et al*., 2007; Ibáñez-Mejía *et al*., 2008; Cardona *et al*., 2008, 2009; Mišković *et al*., 2009, Mišković and Shaltegger, 2009; Witt *et al*., 2013; Boekhout *et al*., 2013). Therefore, despite local particularities, there was a rather consistent evolution in time of the magmatism along the southwestern, paleo-Pacific border of Gondwana.

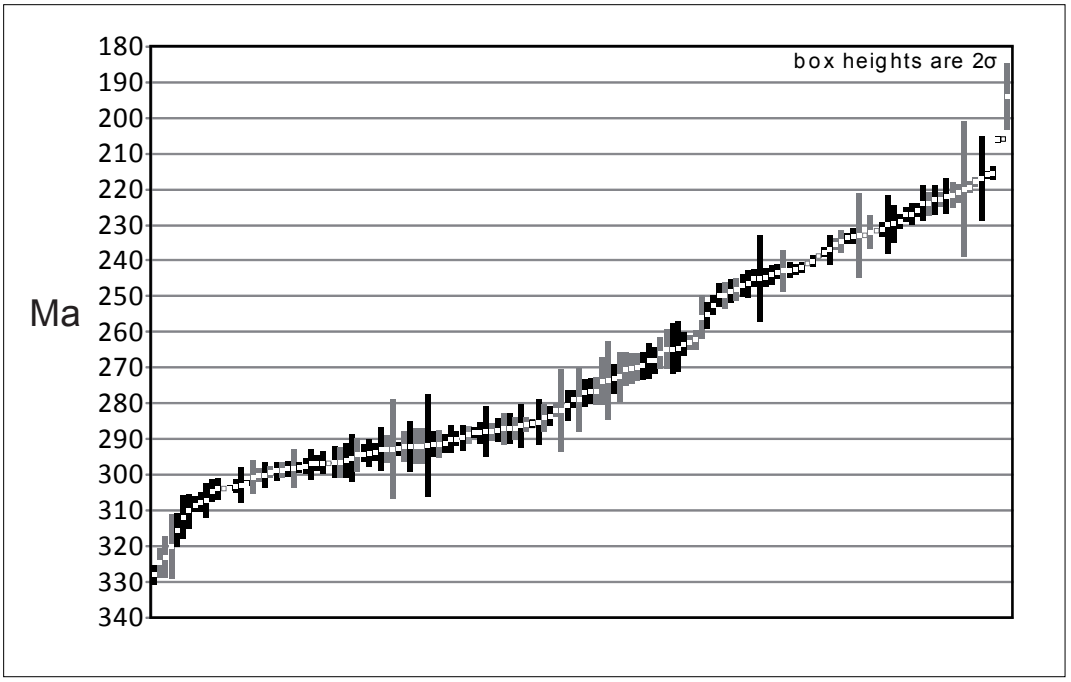

FIG. 7. Plot of all zircon U-Pb ages for Late Paleozoic to Early Jurassic intrusive and volcanic rocks ordered from older to younger with 2σ error bars; black bars=intrusive rocks and gray bars=volcanic rocks.

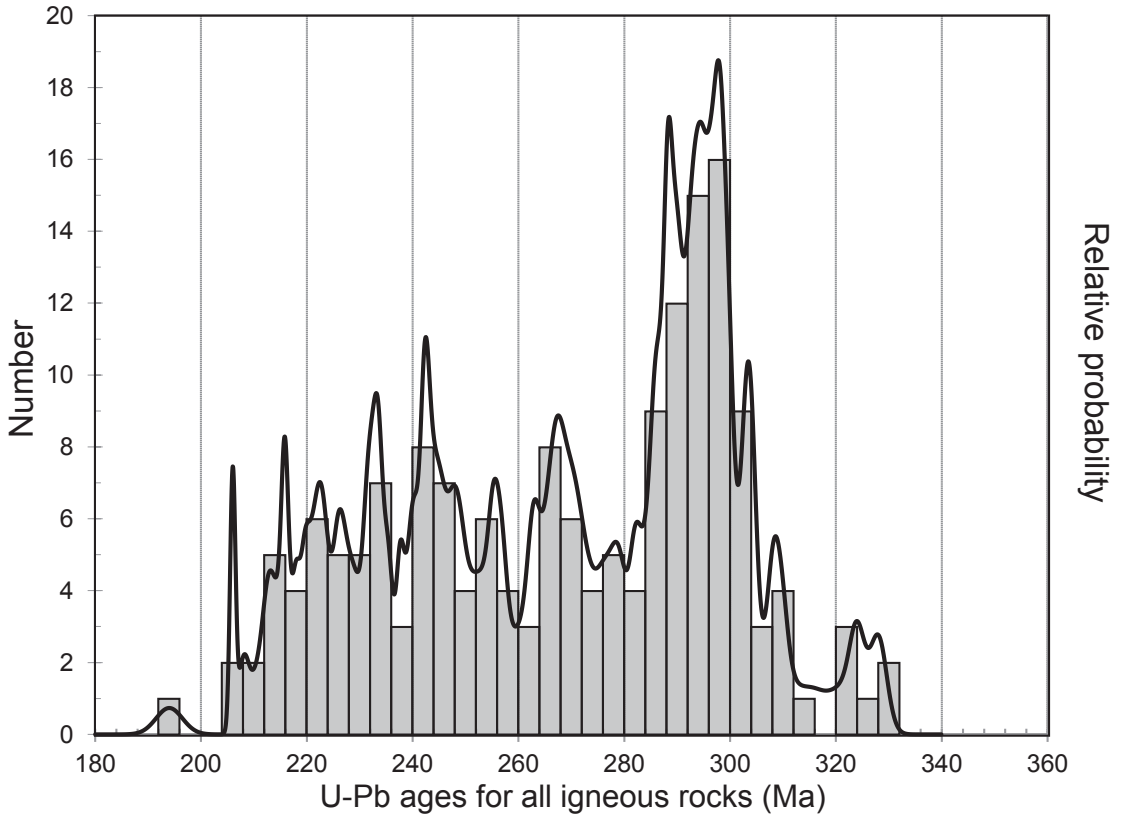

FIG. 8. Probability density plot and stacked histogram of all zircon U-Pb ages for igneous rocks.

7. Conclusions

U-Pb zircon geochronological data provide record of about 130 Ma of igneous activity in the Andes of northern Chile that extended episodically from the latest Early Carboniferous to Early Jurassic (328-194 Ma). The overall U-Pb data show that volcanism and plutonism were essentially synchronous and inferred major episodes of igneous activity developed during the Late Carboniferous to Permian (310 to 260 Ma) and from Late Permian to Late Triassic (255-205 Ma), with less prominent episodes in the mid-Carboniferous (330 to 320 Ma), and Early Jurassic (200-190 Ma). Thus, from the Carboniferous to the Early Triassic dominantly silicic magmatism developed along the Chilean segment of the southwestern border of Gondwana supercontinent. Further magmatism developed during the Mid-Late Triassic (250-194 Ma) was bimodal and synchronous with rift-related, continental and/or marine sedimentary strata related to the early stages of break-up of Gondwana.

Most of the siliceous volcanic rocks of the Precordillera and Domeyko Cordillera of northern Chile (21°30' to 25°30'S) are older than the silicic rocks assigned to the Choiyoi succession in Argentina, being instead equivalent in age to Carboniferous to Early Permian marine sedimentary sequences present in the eastern Argentinean foreland. On the other hand, silicic volcanic successions exposed in the easternmost part of northern Chile are equivalent in age to the Choiyoi succession of the San Rafael Block of Argentina. An eastward expansion or migration during the Mid-Permian to Early Triassic is inferred by the age difference between older western rhyolitic deposits and younger eastern rhyolitic volcanic that originally were supposed to be of the same age; interpretation that is consistent with expansion of the volcanism at that time in Argentina.

The timing of the magmatism is coincident with that of the Andes of Perú and of Argentina according to the available U-Pb data, revealing a rather consistent evolution in time of the magmatism along the southwestern, paleo-Pacific border of Gondwana.

The correct allocation of lithostratigraphic units to the geological time results in changes in the stratigraphy modifying the tectonic interpretation and evolution of the studied volcano-plutonic event. The current U-Pb data allow a better understanding of the temporal evolution of the Late Paleozoic to Early Jurassic volcano-plutonic event in northern Chile, but certainly further work is required to solve particularly stratigraphic problems still remaining and some outcrops that have not been sampled by logistic reasons.

Acknowledgements

This study was supported by CONICYT, Chile, through Fondecyt 1110093 grant to V. Maksaev and F. Munizaga (Universidad de Chile). We are obliged to F. Hervé and his Fondecyt project 1095099 for sharing data from the Elqui-Limarí batholith and provided some samples for dating during this study. We thank K. Sato in charge of the SHRIMP and the staff of the Geochronological Research Center (Centro de Pesquisas Geocronológicas) of the University of Sao Paulo, Brazil, for their cooperation during the U-Pb dating on the SHRIMP. Reviews by V. Oliveros and C. Mpodozis contributed to improve this paper.

References

Álvarez, J.; Mpodozis, C.; Blanco-Quintero, I.; García-Casco, A.; Arriagada, C.; Morata, D. 2013. U-Pb ages and metamorphic evolution of the La Pampa Gneisses: Implications for the evolution of the Chilenia Terrane and Permo-Triassic tectonics of north Central Chile. Journal of South American Earth Sciences 47: 100-115. doi: 10.1016/j.jsames.2013.07.001.

Azcuy, C.L.; Carrizo, H.A.; Caminos, R. 1999. Carbonífero y Pérmico de las Sierras Pampeanas, Famatina, Precordillera, Cordillera Frontal y Bloque de San Rafael. Geología Argentina, Anales del Instituto de Geología y Recursos Minerales 29: 261-318.

Barredo, S.; Chemale, F.; Marsicano, C.; Ávila, J.N.; Ottone, E.G.; Ramos, V. 2012. Tectono-sequence stratigraphy and U-Pb zircon ages of the Rincón Blanco Depocenter, northern Cuyo Rift, Argentina. Gondwana Research 21: 624-536.

Basso, M. 2004. Carta Baquedano, Región de Antofagasta. Servicio Nacional de Geología y Minería, Carta Geológica de Chile, Serie Geología Básica 82: 26 p. 1 mapa escala 1:100.000. Santiago.

Basso, M.; Marinovic, N. 2003. Antecedentes geocronológicos de volcanismo Triásico en la zona de los Estratos El Bordo, Antofagasta, Chile. *In* Congreso Geológico Chileno, No. 10, Sesión Temática 5: CD-ROM. Concepción.

Bell, C.M. 1985. The Chinches Formation: an early Carboniferous lacustrine succession in the Andes of northern Chile. Revista Geológica de Chile 24: 29-48. doi: 10.5027/andgeoV12n1-a03.

Bell, C.M.; Suárez, M. 1994. The sedimentation and tectonics of a marine fan-delta developed on anactive continental margin: the Triassic San Felix Formation in the Andes of northern Chile. Journal of South American Earth Sciences 7 (3-4): 403-413.

Berg, K.; Baumann, A. 1985. Plutonic and metasedimentary rocks from the Coastal Range of northern Chile: Rb-Sr and U-Pb systematic. Earth and Planetary Science Letters 75: 101-115.

Berg, K.; Breitkreuz, C.; Damm, K-W.; Pichowiak, S.; Zeil, W. 1983. The North-Chilean Coast Range-an Example for the Development of an Active Continental Margin. Geologische Rundschau 72 (2): 715-731.

Black, L.P.; Kamo, S.L.; Allen, C.M.; Aleinikoff, J.N.; Davis, D.W.; Korsch, R.J.; Foudoulis, C. 2003. TEMORA1: a new zircon standard for phanerozoic U-Pb geochronology. Chemical Geology 200: 155-170.

Blanco, N. 1994. Sedimentología y ambientes sedimentarios de los estratos El Mono, Triásico de la Región de Atacama, Chile. *In* Congreso Geológico Chileno, No. 7, Actas 1: 409-413. Concepción.

Boekhout, F.; Sempere, T.; Spikings, R.; Schaltegger, U. 2013. Late Paleozoic to Jurassic chronostratigraphy of coastal southern Perú: Temporal evolution of sedimentation along an active margin. Journal of South American Earth Sciences 47: 179-200.

Breitkreuz, C. 1995. The Late Permian Peine and Cas Formations at the Eastern margin of the Salar de Atacama, Northern Chile: stratigraphy, volcanic facies, and tectonics. Revista Geológica de Chile 22 (1): 3-23. doi: 10.5027/andgeoV22n1-a01.

Breitkreuz, C.; Zeil, W. 1994. The Late Carboniferous to Triassic Volcanic Belt in Northern Chile. *In* Tectonics of the Southern Andes (Reutter, K.J.; Scheuber, E.; Wigger, P.J.; editors). Springer: 277-292.

Breitkreuz, C.; Van Schmus, W.R. 1996. U-Pb geochronology and significance of Late Permian ignimbrites

in Northern Chile. Journal of South American Earth Sciences 9: 281-293.

Breitkreuz, C.; Bahlburg, H.; Delakowitz, B.; Pichowiak, S. 1989. Paleozoic volcanic events in the Central Andes. Journal of South American Earth Sciences 2: 171-189.

Brown, M. 1990. Comparative geochemical interpretation of Permian-Triassic plutonic complexes of the Coastal Range and Altiplano (25º30' to 26º30'S), northern Chile. *In* Andean Magmatism and its Tectonic Setting (Harmon, R.S.; Rapela, C.E.; editors). Geological Society of America, Special Paper 265: 157-177.

Camus, F. 2003. Geología de los sistemas porfíricos en los Andes de Chile. Servicio Nacional de Geología y Minería: 267 p. Santiago.

Cardona, A.; Cordani, U.; Nutman, A. 2008. U-Pb SHRIMP zircon, $^{40}Ar/^{39}Ar$ geochronology and Nd isotopes from gneissic and granitoid rocks of the Illescas massif, Perú: a southern extension of a fragmented Late Paleozoic orogen? *In* South American Symposium on Isotope Geology, No. 6. Proceedings, Abstract: p. 78. San Carlos de Bariloche.

Cardona, A.; Cordani, U.G.; Ruiz, J.; Valencia, V.A.; Armstrong, R.; Chew, D.; Nutman, A.; Sanchez, W. 2009. U-Pb Zircon Geochronology and Nd Isotopic Signatures of the Pre-Mesozoic Metamorphic Basement of the Eastern Peruvian Andes: Growth and Provenance of a Late Neoproterozoic to Carboniferous Accretionary Orogen on the Northwest Margin of Gondwana. The Journal of Geology 117 (3): 285-305.

Carlier, G.; Grandin, G.; Laubacher, G.; Marocco, R.; Megard, F. 1982. Present knowledge of the magmatic evolution of the eastern Cordillera of Perú. Earth-Science Reviews 18: 253-283.

Casquet, C.; Hervé, F.; Pankhurst, R.J.; Baldo, E.; Calderón, M.; Fanning, C.M.; Rapela, C.W.; Dahlquist, J. 2014. The Mejillonia suspect terrane (Northern Chile): Late Triassic fast burial and metamorphism of sediments in a magmatic arc environment extending into the Early Jurassic. Gondwana Research 25 (3): 1272-1286. doi: 10.1016/j.gr.2013.05.016.

Charrier, R. 1979. El Triásico en Chile y regiones adyacentes de Argentina: Una reconstrucción paleogeográfica y paleoclimática. Universidad de Chile, Departamento de Geología. Comunicaciones 26: 1-47. Santiago.

Charrier, R.; Pinto, L.; Rodríguez, M.P. 2007. Tectonostratigraphic evolution of the Andean Orogen in Chile. *In* The Geology of Chile (Moreno, T.; Gibbons, W.; editors). The Geological Society: 21-114. London.

Chew, D.M.; Schaltegger, U.; Kosler, J.; Whitehouse, M.J.; Gutjahr, M.; Spikings, R.A.; Miskovíc, A. 2007. U-Pb geochronologic evidence for the evolution of the Gondwanan margin of the north-central Andes. Geological Society of America Bulletin 119 (5-6): 697-711.

Chong, G.; Von Hillebrandt, A. 1985. El Triásico preandino de Chile entre los 23º30' y 26º00' de lat. Sur. *In* Congreso Geológico Chileno, No. 4, Actas 1: 138-154. Antofagasta.

Cohen, K.M.; Finney, S.; Gibbard, P.L. 2013. International Chronostratigraphic Chart, v2013/01. International Commission on Stratigraphy. http//www.stratigraphy.org/ICSchart/ChronostratChart2013-01.pdf: 1 p.

Coloma, F.; Salazar, E.; Creixell, C. 2012. Nuevos antecedentes acerca de la construcción de los plutones Pérmicos y Permo-Triásicos en el valle del río Tránsito, Región de Atacama, Chile. *In* Congreso Geológico Chileno, No. 13, Actas: 330-332. Antofagasta.

Cornejo, P.; Mpodozis, A.C. 1996. Geología de la región de Sierra Exploradora (25°-26ºS). Servicio Nacional de Geología y Minería, Informe Registrado IR-96-09: 330 p. Santiago.

Cornejo, P.; Mpodozis, C. 1997. El rift Triásico-Sinemuriano de Sierra Exploradora, Cordillera de Domeyko (25°-26°): asociaciones de facies y reconstrucción tectónica. *In* Congreso Geológico Chileno, No. 8, Actas 1: 550-554. Antofagasta.

Cornejo, P.; Mpodozis, C.; Ramírez, C.F.; Tomlinson, A. 1993. Estudio geológico de la región de Potrerillos y El Salvador (26°-27° Lat. S). Servicio Nacional de Geología y Minería, Informe Registrado IR-93-01: 258 p. Santiago.

Cornejo, P.; Mpodozis, A.C.; Tomlinson, A.J. 1998. Hoja Salar de Maricunga, Región de Atacama. Servicio Nacional de Geología y Minería, Mapas Geológicos 7, 1 mapa escala 1:100.000. Santiago.

Cornejo, P.; Matthews, S.; Marinovic, N.; Pérez de Arce, C.; Basso, M.; Alfaro, J.; Navarro, M. 2006. Alteración hidrotermal y mineralización recurrente de Cu y Cu-Mo durante el Pérmico y el Triásico en la Cordillera de Domeyko (Zona de Zaldívar-Salar de los Morros): antecedentes geocronológicos U-Pb, $^{40}Ar/^{39}Ar$ y Re-Os. *In* Congreso Geológico Chileno, No. 11, Actas 2: 219-222. Antofagasta.

Cornejo, P.; Mpodozis, C.; Rivera, O.; Matthews, S.J. 2009. Carta Exploradora, Región de Antofagasta y Atacama. Servicio Nacional de Geología y Minería, Carta Geológica de Chile, Serie Geología Básica 119: 100 p. Santiago.

Cortés, J. 2000. Hoja Palestina, Región de Antofagasta. Servicio Nacional de Geología y Minería, Mapas Geológicos 19, 1 mapa escala 1:100.000. Santiago.

Damm, W.; Pichowiak, S.; Harmon, R.S.; Todt, W.; Kelley, S.; Omarini, R.; Niemeyer, H. 1990. Pre-Mesozoic evolution of the Central Andes, the basement revisited. *In* Plutonism from Antarctica to Alaska (Kay, M.S.; Rapela, C.W.; editors). Geological Society of America, Special Papers 241: 101-126.

Davidson, J.; Mpodozis, C.; Bunger, C.; Cornejo, P.; Faunes, A.; Foerster, H.; Fuster, N.; Gardeweg, M.; Godoy, S.; Jannas, R.; Muzzio, G.; Reyes, J.C.; Salinas, P.; Sepúlveda, J.; Solano, A.; Velasco, L. 1978. Geología de la Precordillera de Copiapó: las nacientes de la quebrada Paipote al oeste del Salar de Maricunga (resultados del curso de Geología de Campo II, 1977). Universidad de Chile, Departamento de Geología, Comunicaciones 23: 1-34.

Davidson, J.; Ramírez, C.F.; Gardeweg, M.; Brook, M.; Pankhurst, M. 1985. Calderas del Palaeozoico superior-Triásico Inferior y mineralización asociada. Universidad de Chile, Departamento de Geología, Comunicaciones 35: 53-57. Santiago.

Deckart, K.; Hervé, F.; Fanning, M.; Ramírez, V.; Calderón, M.; Godoy, E. 2014. Geocronología U-Pb e isótopos de Hf-O en circones del batolito de la costa Pensilvaniana, Chile. Andean Geology 41 (1): 49-82. doi: 10.5027/andgeoV41n1-a03.

Díaz-Martínez, E.; Mamet, B.; Isaacson, P.E.; Grader, G.W. 2000. Permian marine sedimentation in northern Chile: new paleontological evidence from Juan de Morales Formation, and regional paleogeographic implications. Journal of South American Earth Sciences 13 (6): 511-525.

Franz, G.; Lucassen, F.; Kramer,W.; Trumbull, R.B.; Romer, R.L.; Wilke, H.-G.; Viramonte, J.G.; Becchio, R.; Siebel, W. 2006. Crustal evolution at the Central Andean continental margin: a geochemical record of crustal growth, recycling and destruction. *In* The Andes-Active Subduction Orogeny (Oncken, O.; Chong, G.; Franz, G.; Giese, P.; Götze, H.-J.; Ramos, V.; Strecker, M.R.; Wigger, P.; editors). Springer: 45-64.

Gallego, O.F.; Covacevic, V. 1998. Conchostracos triásicos de las regiones de Antofagasta, Atacama y Coquimbo, Chile. Revista Geológica de Chile 25 (2): 115-131. doi: 10.5027/andgeoV25n2-a01.

Galli, C. 1956. Nota sobre el hallazgo del Palaeozoico superior en la Provincia de Tarapacá. Revista Minerales 53-54: 30-31.

Galli, C. 1968. Cuadrángulo Juan de Morales, Provincia de Tarapacá. Instituto de Investigaciones Geológicas, Carta Geológica de Chile 18: 53 p. Santiago.

García, F. 1967. Geología del Norte Grande de Chile. *In* Simposio sobre el Geosinclinal Andino. Sociedad Geológica de Chile, Publicación 3: 138 p. Santiago.

Godoy, E.; Lara, L. 1998. Hojas Chañaral y Diego de Almagro, Región de Atacama. Servicio Nacional de Geología y Minería, Mapa Geológico 5-6, 1 mapa escala 1:100:000. Santiago.

Gregori, D.; Benedini, L. 2013. The Cordón del Portillo Permian magmatism, Mendoza, Argentina, plutonic and volcanic sequences at the western margin of Gondwana. Journal of South American Earth Sciences 42: 61-73.

Gulbranson, E.L.; Montañez, I.P.; Schmitz, M.D.; Limarino, C.O.; Isbell, J.L.; Marenssi, S.A.; Crowley, J.L. 2010. High-precision U-Pb calibration of Carboniferous glaciation and climate history, Paganzo Group, NW Argentina. Geological Society of America, Bulletin 122 (9-10): 1480-1498.

Hervé, F.; Fanning, C.M.; Calderón, M.; Mpodozis, C. 2014. Early Permian to Late Triassic batholiths of the Chilean Frontal Cordillera (28°-31°S): SHRIMP U-Pb zircon ages and Lu-Hf and O isotope systematic. Lithos 184-187: 436-446. doi: 10.1016/j.lithos.2013.10.018.

Hervé, M.; Sillitoe, R.H.; Wong, C.; Fernández, P.; Crignola, F.; Ipinza, M.; Urzúa, F. 2012. Geologic Overview of the Escondida Porphyry Copper District, Northern Chile. *In* Geology and Genesis of Major Copper Deposits and Districts of the World: A Tribute to Richard H. Sillitoe (Hedenquist, J.W.; Harris, M.; Camus, F.; editors). Society of Economic Geologists, Special Publication 16: 55-78.

Huete, C.; Maksaev, V.; Moscoso, R.; Ulriksen, C.; Vergara, H. 1977. Antecedentes geocronológicos de rocas intrusivas y volcánicas de la Cordillera de los Andes comprendida entre la Sierra de Moreno y el río Loa y los 21º y 22º de latitud Sur, II Región, Chile. Revista Geológica de Chile 4: 35-41. doi: 10.5027/andgeoV4n1-a03.

Ibáñez-Mejía, M.; Jaramillo-Mejía, J.M.; Valencia, V. 2008. U-Th/Pb zircon geochronology by multicollector LA-ICP-MS of the Samaná Gneiss: a Middle Triassic syn-tectonic body in the Central Andes of Colombia, related to the latter stages of Pangea assembly. *In* South American Symposium on Isotope Geology, No. 6, Extended Abstracts. San Carlos de Bariloche.

Iriarte, S.; Arévalo, C.; Mpodozis, C.; Rivera, O. 1996. Hoja Carrera Pinto, Región de Atacama. Servicio

Nacional de Geología y Minería, Mapas Geológicos 3, 1 mapa escala 1:100.000. Santiago.

Iriarte, S.; Arévalo, C.; Mpodozis, C. 1999. Hoja La Guardia, Región de Atacama. Servicio Nacional de Geología y Minería, Mapas Geológicos 13, 1 mapa escala 1:100.000. Santiago.

Jara, C.; Rabbia, O.; Valencia, V. 2009. Petrología y dataciones U-Pb del depósito tipo pórfido Cu Zaldívar, II Región de Antofagasta, Chile. *In* Congreso Geológico Chileno, No. 12, Actas 4: 4 p. Santiago.

Jenchen, U.; Rosenfeld, U. 2002. Continental Triassic in Argentina: response to tectonic activity. Journal of South American Earth Sciences 15: 461-479.

Jordan, T.E.; Isacks, B.L.; Allmendinger, R.W.; Brewer, J.A.; Ramos, V.A.; Ando, C.J. 1983. Andean tectonics related to geometry of subducted Nazca plate: Geological Society of America Bulletin 94: 341-361.

Kay, S.M.; Ramos, V.A.; Mpodozis, C.; Sruoga, P. 1989. Late Palaeozoic to Jurassic silicic magmatism at the Gondwana margin: Analogy to the middle Proterozoic in North America? Geology 17: 324-328.

Koukharsky, M.; Kleiman, L.; Etcheverría, M.; Quenardelle, S.; Bercowski, F. 2009. Upper Carboniferous retroarc volcanism with submarine and subaerial facies at the western Gondwana margin of Argentina. Journal of South American Earth Sciences 27: 299-308.

Llambías, E.J.; Sato, A.M. 1990. El Batolito de Colangüil, cordillera frontal de Argentina: Estructura y marco tectónico. Revista Geológica de Chile 17 (1): 89-108. doi: 10.5027/andgeoV17n1-a04.

Llambías, E.J.; Sato, A.M. 1995. El Batolito de Colangüil: transición entre orogénesis y anorogénesis. Revista de la Asociación Geológica Argentina 50 (1-4): 111-131. Buenos Aires.

Llambías, E.J.; Kleiman, L.E.; Salvarredi, J.A. 1993. El Magmatismo Gondwánico. *In* Geología y Recursos Naturales de Mendoza (Ramos, V.; editor). Congreso Geológico Argentino, No. 12 y Congreso de Exploración de Hidrocarburos, No. 2. Relatorio: 53-64. Mendoza.

Llambías, E.J.; Quenardelle, S.; Montenegro, T. 2003. The Choiyoi Group from central Argentina: a subalkaline transitional to alkaline association in the craton adjacent to the active margin of the Gondwana continent. Journal of South American Earth Sciences 16: 243-257.

López-Gamundí, O. 2006. Permian plate margin volcanism and tuffs in adjacent basins of west Gondwana: Age constraints and common characteristics. Journal of South American Earth Sciences 22: 227-238.

Lucassen, F.; Franz, G.; Thirlwall, M.F.; Mezger, K. 1999. Crustal recycling of metamorphic basement, Late Paleozoic granitoids of northern Chile (~22°S): implications for the composition of the Andean crust. Journal of Petrology 40: 1527-1551.

Ludwig, K.R. 2001. SQUID 1.02, A User's Manual. Berkeley Geochronology Center, Special Publication 2, 2455 Ridge Road, Berkeley, CA 94709, USA.

Ludwig, K.R. 2003. User's Manual for Isoplot/Ex, Version 3.0, A Geochronological Toolkit for Microsoft Excel. Berkeley Geochronology Center, Special Publication 4, 2455 Ridge Road, Berkeley CA 94709, USA.

Maksaev, V.; Marinovic, N. 1980. Cuadrángulos Cerro de la Mica, Quillagua, Cerro Posada y Oficina Prosperidad, Región de Antofagasta. Instituto de Investigaciones Geológicas, Carta Geológica de Chile 45-48: 63 p.

Marinovic, N. 2007. Carta Oficina Domeyko, Región de Antofagasta. Servicio Nacional de Geología y Minería, Carta Geológica de Chile, Serie Geología Básica 105: 41 p., 1 mapa escala 1:100.000. Santiago.

Marinovic, N.; Smoje, I.; Maksaev, V.; Hervé, M.; Mpodozis, C. 1995. Hoja Aguas Blancas, Región de Antofagasta. Servicio Nacional de Geología y Minería, Carta Geológica de Chile 70: 142 p. 1 mapa escala 1:250.000. Santiago.

Marinovic, N.; García, M. 1999. Hoja Pampa Unión, Región de Antofagasta. Servicio Nacional de Geología y Minería, Mapas Geológicos 9, 1 mapa escala 1:100.000. Santiago.

Martin, M.W.; Clavero, J.; Mpodozis, C. 1999. Late Palaeozoic to Early Jurassic tectonic development of the high Andean Principal Cordillera, El Indio region, Chile (29º-30ºS). Journal of South American Earth Sciences 12: 33-49.

Masterman, G.L. 2003. Structural and geochemical evolution of the Rosario Copper-molybdenum porphyry deposit and related copper veins, Collahuasi District, Northern Chile. Doctorate Thesis (Unpublished), University of Tasmania: 253 p. Australia.

Mercado, M. 1980. Geología del área Pan de Azúcar, Región de Atacama. Servicio Nacional de Geología y Minería, Carta Geológica de Chile 37: 30 p., 1 mapa escala 1:100.000. Santiago.

Mercado, M. 1982. Geología de la Hoja Laguna del Negro Francisco, Región de Atacama. Servicio Nacional de Geología y Minería, Carta Geológica de Chile 56: 73 p., 1 mapa escala 1:100.000. Santiago.

Miskovic, A.; Schaltegger, U. 2009. Crustal growth along a non-collisional cratonic margin: A Lu-Hf isotopic survey of the Eastern Cordilleran granitoids of Perú. Earth and Planetary Science Letters 279 (3-4): 303-315.

Miskovic, A.; Spikings, R.A.; Chew, D.M.; Kosler, J.; Ulianov, A.; Schaltegger, U. 2009. Tectonomagmatic evolution of Western Amazonia: Geochemical characterization and zircon U-Pb geochronologic constraints from the Peruvian Eastern Cordilleran granitoids. Geological Society of America Bulletin 121 (9-10): 1298-1324.

Morata, D.; Aguirre, L.; Oyarzún, M.; Vergara, M. 2000. Crustal contribution in the genesis of the bimodal Triassic volcanism from the Coastal Range, central Chile. Revista Geológica de Chile 27 (1): 83-98. doi: 10.5027/andgeoV27n1-a06.

Moscoso, R.; Mpodozis, C.; Nasi, C.; Ribba, L.; Arévalo, C. 2010. Geología de la Hoja El Tránsito, Región de Atacama. Servicio Nacional de Geología y Minería, Carta Geológica de Chile, Serie Preliminar 7: 17 p., 1 mapa escala 1:250.000. Santiago.

Mpodozis, C.; Cornejo, P. 1988. Hoja Pisco Elqui, IV Región de Coquimbo. Servicio Nacional de Geología y Minería, Carta Geológica de Chile 68: 164 p., 1 mapa escala 1:250.000. Santiago.

Mpodozis, C.; Ramos, V. 1989. The Andes of Argentina and Chile. *In* Geology of the Andes and its relation to hydrocarbon and mineral resources (Ericksen, G.E.; Cañas Pinochet, M.T.; Reinemund, J.A.; editors). Circumpacific Council for Energy and Mineral Resources, Earth Science Series 11: 59-90.

Mpodozis, C.; Kay, S. 1990. Provincias magmáticas ácidas y evolución tectónica de Gondwana: Andes chilenos (28-31°S). Revista Geológica de Chile 17 (2): 153-180. doi: 10.5027/andgeoV17n2-a03.

Mpodozis, C.; Kay, S. 1992. Late Paleozoic to Triassic evolution of the pacific Gondwana margin: evidence from Chilean frontal Cordilleran batholiths. Geological Society of America Bulletin 104: 999-1014.

Mpodozis, C.; Allmendinger, R.W. 1993. Extensional tectonics, Cretaceous Andes, northern Chile (27°S). Geological Society of America Bulletin 105: 1462-1477.

Mpodozis, C.; Marinovic, N.; Smoje, I.; Cuitiño, L. 1993. Estudio Geológico-Estructural de la Cordillera de Domeyko entre Sierra Limón Verde y Sierra Mariposas, Región de Antofagasta. Servicio Nacional de Geología y Minería, Informe Registrado IR-93-04: 282 p. Santiago.

Mpodozis, C.; Iriarte, S.; Gardeweg, M.; Valenzuela, M. 2012. Carta Laguna del Negro Francisco, Región de Atacama. Servicio Nacional de Geología y Minería, Carta Geológica de Chile, Serie Geología Básica 145: 30 p. 1 mapa escala 1:100.000. Santiago.

Munizaga, F.; Maksaev, V.; Fanning, C.M.; Giglio, S.; Yaxley, G.; Tassinari, C.C.G. 2008 Late Paleozoic-Early Triassic magmatism on the western margin of Gondwana: Collahuasi area, Northern Chile. Gondwana Research 13: 407-427.

Murillo, I.; Álvarez, J.; Arriagada, C.; Calderón, M.; Charrier, R. 2012. Geología estructural del Valle de El Tránsito con énfasis en las Milonitas El Portillo, III Región, Chile. *In* Congreso Geológico Chileno, No. 13, T2: 314-316. Antofagasta.

Naranjo, J.A.; Puig, A. 1984. Hojas Taltal y Chañaral, Regiones de Antofagasta y Atacama. Servicio Nacional de Geología y Minería, Carta Geológica de Chile 62-63: 140 p., 1 mapa escala 1:250.000. Santiago.

Nasi, C.; Mpodozis, C.; Cornejo, P.; Moscoso, R.; Maksaev, V. 1985. El Batolito Elqui-Limarí (Paleozoico Superior-Triásico): características petrográficas, geoquímicas y significado tectónico. Revista Geológica de Chile 25-26: 77-11. doi: 10.5027/andgeoV12n2-3-a06.

Nasi, C.; Moscoso, R.; Maksaev, V. 1990. Hoja Guanta, Regiones de Atacama y Coquimbo. Servicio Nacional de Geología y Minería, Carta Geológica de Chile 67: 140 p., 1 mapa escala 1:250.000. Santiago.

Niemeyer, H. 2013. Geología del Cerro Lila-Peine, Región de Antofagasta. Servicio Nacional de Geología y Minería, Carta Geológica de Chile, Serie Geología Básica 147.

Niemeyer, H.; Venegas, R.; Baeza, L.; Soto, H. 1985. Reconocimiento geológico del sector sur-occidental del Cuadrángulo Cerro Yocas, ubicado en la zona de falla Quebrada Blanca-Chuquicamata, Región de Antofagasta. *In* Congreso Geológico Chileno, No. 4, Actas 1: 629-653. Antofagasta.

Niemeyer, H.; Urzúa, F.; Rubinstein, C. 1997. Nuevos antecedentes estratigráficos y sedimentológicos de la Formación Zorritas, Devónico-Carbonífero de Sierra de Almeida, Región de Antofagasta, Chile. Revista Geológica de Chile 24 (1): 25-43. doi: 10.5027/andgeoV24n1-a02.

Noble, S.R.; Aspden, J.A.; Jemelita, R. 1997. Northern Andean crustal evolution: New U-Pb geochronological constraints from Ecuador. Geological Society of America Bulletin, 109: 789-798.

Oliveros, V.; Labbé, M.; Rossel, P.; Charrier, R.; Encinas, A. 2011. Late Jurassic paleogeographic evolution of the Andean back-arc basin: New constrains from the Lagunillas Formation, northern Chile (27°30'-

28°30'S). Journal of South American Earth Sciences 37: 25-40.

Ordóñez, O.; Pimentel, M. 2002. Rb-Sr and Sm-Nd isotopic study of the Puqui complex, Colombian Andes. Journal of South American Earth Sciences 15: 173-182.

Padel, M.; Salazar, E.; Coloma, F. 2012. Arquitectura y evolución tectonoestratigráfica del Depocentro de San Félix, Triásico Medio a Superior: Resultados preliminares. *In* Congreso Geológico Chileno, No. 13, T5: 715-717. Antofagasta.

Pankhurst, R.; Millar, I.; Hervé, F. 1996. A Permo-Carboniferous U-Pb age for part of the Guanta unit of the Elqui-Limarí Batholith at Río del Tránsito, Northern Chile. Revista Geológica de Chile 23 (1): 35-42. doi: 10.5027/andgeoV23n1-a03.

Pankhurst, R.J.; Rapela, C.W.; Fanning, C.M.; Márquez, M. 2006. Gondwanide continental collision and the origin of Patagonia. Earth-Science Reviews 76: 235-257.

Parada, F. 2013. Geoquímica de las rocas ígneas del Carbonífero-Triásico de la Alta Cordillera, Región de Atacama, Chile. Memoria de Título (Inédito), Universidad de Chile, Departamento de Geología: 93 p. Santiago.

Parada, M.A.; Munizaga, F.; Kawashita, K. 1981. Edades Rb-Sr roca total del Batolito compuesto de los ríos Elqui-Limarí a la latitud 30°S. Revista Geológica de Chile 13-14: 87-93. doi: 10.5027/andgeoV8n2-3-a07.

Parada, M.A.; Levi, B.; Nystrom, J.O. 1991. Geochemistry of the Triassic to Jurassic plutonism of Central Chile (30 to 33°S); petrogenetic implications and a tectonic discussion. *In* Andean Magmatism and its Tectonic Setting (Harmon, R.S.; Rapela, C.W.; editors). Geological Society of America, Special Papers 265: 99-112. Boulder.

Parada, M.A.; López-Escobar, L.; Oliveros, V.; Fuentes, F.; Morata, D.; Calderón, M.; Aguirre, L.; Féraud, G.; Espinoza, F.; Moreno, H.; Figueroa, O.; Muñoz, J.; Troncoso, R.; Stern, C.R. 2007. Andean Magmatism. *In* The Geology of Chile (Moreno, T.; Gibbons, W.; editors). The Geological Society, Special Publication 4: 115-146. London.

Pineda, G.; Calderón, M. 2008. Geología del área Monte Patria-El Maqui, Región de Coquimbo. Servicio Nacional de Geología y Minería, Carta Geológica de Chile, Serie Geología Básica 116: 44 p., 1 mapa escala 1:100.000. Santiago.

Ramírez, C.F.; Gardeweg, M. 1982. Geología de la Hoja Toconao, Región de Antofagasta. Servicio Nacional de Geología y Minería, Carta Geológica de Chile 54: 117 p., 1 mapa escala 1:250.000. Santiago.

Ramos, V. 2009. Anatomy and global context of the Andes: Main geologic features and the Andean orogenic cycle. The Geological Society of America, Memoir 204: 31-65.

Ramos, V.A.; Kay, S.M. 1991. Triassic rifting and associated basalts in the Cuyo basin, central Argentina. *In* Andean magmatism and its tectonic setting (Harmon, R.S.; Rapela, C.W.; editors). Geological Society of America, Special Papers 265: 79-91. Boulder.

Ramos, V.; Folguera, A. 2009. Andean flat-slab subduction through time. Geological Society Special Publication 327: 31-54. London.

Restrepo, J.J.; Toussaint, J.F.; González, H.; Cordani, U.; Kawashita, K.; Linares, E.; Patricia, C. 1991. Precisiones geocronológicas sobre el occidente Colombiano. *In* Simposio sobre magmatismo andino y su marco tectónico, Manizales 1: 1-21.

Reutter, K.J. 1974. Entwicklung und Bauplan der chilenischen Hochkordillere im Bereich 29º südlicher Breite. Neues Jahrbuch für Geologie und Paläontologie 146: 153-178.

Ribba, L.; Mpodozis, C.; Hervé, F.; Nasi, C.; Moscoso, R. 1988. El basamento del valle del Tránsito, Cordillera de Vallenar: Eventos magmáticos y metamórficos y su relación con la evolución paleozoica de los Andes Chileno-Argentinos. Revista Geológica de Chile 15 (2): 129-149. doi: 10.5027/andgeoV15n2-a03.

Richards, J.P.; Noble, S.R.; Pringle, M.S. 1999. A revised late Eocene age for porphyry Cu magmatism in the Escondida area, northern Chile. Economic Geology 94: 1231-1247.

Rocha-Campos, A.C.; Basei, M.A.; Nutman, A.P.; Kleiman, L.; Varela, R.; Llambías, E.; Canile, F.M.; da Rosa, O. de C.R. 2011. 30 million years of Permian volcanism recorded in the Choiyoi igneous province (W Argentina) and their source for younger ash fall deposits in the Paraná Basin: SHRIMP U-Pb zircon geochronology evidence. Gondwana Research 19 (2): 509-523.

Salazar, E. 2012. Evolución tectonoestratigráfica post-Paleozoica de la Cordillera de Vallenar. Tesis de Magister en Ciencias, Mención Geología (Inédito), Universidad de Chile, Departamento de Geología: 126 p. Santiago.

Salazar, E.; Arriagada, C.; Mpodozis, M.; Martínez, F.; Peña, M.; Álvarez, J. 2009. Análisis estructural del Oroclino de Vallenar. Resultados preliminares. *In* Congreso Geológico Chileno, No. 12, Abstract: S9-026. Santiago.

Salazar, E.; Mpodozis, C.; Arriagada, C.; Coloma, F. 2012. Evolución tectonoestratigráfica post-paleozoica

de la Cordillera de Vallenar. *In* Congreso Geológico Chileno, No. 13, T2: 259-261. Antofagasta.

Salazar, E.; Coloma, F.; Creixell, C. 2013. Geología del área El Tránsito-Lagunillas, Región de Atacama. Servicio Nacional de Geología y Minería, Carta Geológica de Chile, Serie Geología Básica 149.

Sato, A.M.; Llambías, E.J. 1993. El Grupo Choiyoi, provincia de San Juan: equivalente del Batolito de Colangüil. *In* Congreso Geológico Argentino, No. 12, Actas 4: 156-165. Mendoza.

Sempere, T.; Carlier, G.; Soler, P.; Fornari, M.; Carlotto, V.; Jacay, J. 2002. Late Permian-Middle Jurassic lithospheric thinning in Perú and Bolivia, and its bearing on Andean-age tectonics. Tectonophysics 345 (1-4): 153-181.

Sepúlveda, P.; Naranjo, J.A. 1982. Geología de la Hoja Carrera Pinto, Región de Atacama. Servicio Nacional de Geología y Minería, Carta Geológica de Chile 53: 60 p. 1 mapa escala 1:100.000. Santiago.

Shibata, K.; Ishihara, S.; Ulriksen, C. 1984. Rb-Sr Ages and Initial $^{87}Sr/^{86}Sr$ ratios of Late Paleozoic Granitic Rocks from Northern Chile. Bulletin of the Geological Survey of Japan 35 (11): 537-545.

Sillitoe, R.H. 1977. Permo-Carboniferous, Upper Cretaceous, and Miocene porphyry copper-type mineralization in the Argentinean Andes. Economic Geology 72: 99-109.

Skarmeta, J.; Marinovic, N. 1981. Geología de la Hoja Quillagua, Región de Antofagasta. Instituto de Investigaciones Geológicas, Carta Geológica de Chile 51: 63 p. 1 mapa escala 1:250.000. Santiago.

Stipanicic, P.; Rodrigo, F.; Baulier, O.; Martínez, C. 1968. Las Formaciones Presenonianas en el denominado Macizo Norpatagónico y regiones adyacentes. Revista de la Asociación Geológica Argentina 23: 67-98.

Strazzere, D.A.; Gregori, D.A.; Dristas, J.A. 2006. Genetic evolution of Permo-Triassic volcaniclastic sequences at Uspallata, Mendoza Precordillera, Argentina. Gondwana Research 9: 485-499.

Suárez, M.; Bell, M. 1991. Sedimentos lacustres de probable edad triásica en el área de La Coipa, Región de Atacama, Chile. *In* Congreso Geológico Chileno, No. 6, Actas 1: 660-663. Viña del Mar.

Suárez, M.; Bell, M. 1992. Triassic rift-related sedimentary basins in northern Chile (24º-29ºS). Journal of South American Earth Sciences 6: 109-121.

Suárez, M.; Fanning, C.M.; Etchart, H.; De La Cruz, R. 2012. New Carboniferous to Toarcian U-Pb SHRIMP ages from Cordillera del Viento, Neuquén, Argentina. *In* Congreso Geologico Chileno, No. 13, Proceedings, CD-ROM. Antofagasta.

Tera, F.; Wasserburg, G. 1972. U-Th-Pb systematics in three Apollo 14 basalts and the problem of initial Pb in lunar rocks. Earth and Planetary Science Letters 14: 281-304.

Tomlinson, A.J.; Blanco, N. 2008. Geología de la franja El Abra-Chuquicamata, II Región (21°45'-22°30'S). Servicio Nacional de Geología y Minería, Informe Registrado IR-08-35: 196 p. Santiago.

Tomlinson, A.; Cornejo, P.; Mpodozis, C. 1999. Hoja Potrerillos, Región de Atacama. Servicio Nacional de Geología y Minería, Mapas Geológicos 14, 1 mapa escala 1:100.000. Santiago.

Tomlinson, A.J.; Blanco, N.; Maksaev, V.; Dilles, J.H.; Grunder, A.L.; Ladino, M. 2001. Geología de la Precordillera Andina de Quebrada Blanca-Chuquicamata, Regiones I y II (20°30'-22°30'S). Servicio Nacional de Geología y Minería, Informe Registrado IR-01-20: 444 p. Santiago.

Uliana, M.A.; Biddle, K.T.; Cerdan, J. 1989. Mesozoic extension and the formation of Argentine sedimentary basins. *In* Extensional Tectonics and Stratigraphy of the North Atlantic Margins (Tankard, A.J.; Balkwill, H.R.; editors). American Association of Petroleum Geologists, Memoir 46: 599-614.

Urzúa, F. 2009. Geology, geochronology and structural evolution of La Escondida copper district, northern Chile. Ph.D. Thesis (Unpublished), University of Tasmania: 486 p. Hobart, Australia.

Vásquez, P.; Glodny, J.; Franz, G.; Frei, D.; Romer, R.L. 2011. Early Mesozoic Plutonism of the Cordillera de la Costa (34°-37°S), Chile: Constraints on the Onset of the Andean Orogeny. The Journal of Geology 119 (2): 159-184.

Vaughan, A.P.M.; Pankhurst, R.J. 2008. Tectonic overview of the West Gondwana margin. Gondwana Research 13: 150-162.

Venegas, C.; Cervetto, M.; Astudillo, N.; Espinoza, F. 2013. Carta Sierra Vaquillas Altas, Regiones de Antofagasta y Atacama. Servicio Nacional de Geología y Minería, Carta Geológica de Chile, Serie Geología Básica 159.

Vergara, H.; Thomas, A. 1984. Hoja Collacagua, Región de Tarapacá, Servicio Nacional de Geología y Minería, Carta Geológica de Chile 59: 79 p., 1 mapa escala 1:250.000. Santiago.

Vergara, M.; López-Escobar, L.; Cancino, A.; Levi, B. 1991. The Pichidangui Formation; some geochemical characteristics and tectonic implications of the Triassic

marine volcanism in central Chile (31º55' to 32º20'S). *In* Andean Magmatism and its Tectonic Setting (Harmon, R.S.; Rapela, C.W.; editors). Geological Society of America, Special Paper 265: 93-98.

Vinasco, C.J.; Cordani, U.; González, G.; Weber, M.; Peláez, C. 2006. Geochronological, isotopic, and geochemical data from Permo-Triassic granitic gneisses and granitoids of the Colombian Central Andes. Journal of South American Earth Sciences 21: 355-371.

Williams, I.S. 1998. U-Th-Pb geochronology by ion microprobe. *In* Applications of Microanalytical Techniques to Understanding Mineralizing Processes (McKibben, M.A.; Shanks III, W.C.; Ridley, W.I.; editors). Reviews in Economic Geology 7: 1-35.

Witt, W.K.; Hagemann, S.G.; Villanes, C.; Zeng, Q. 2013. New geochronological results and structural evolution of the Pataz gold mining district: Implications for the timing and origin of the batholith-hosted veins. Ore Geology Reviews 50: 143-170.

Manuscript received: November 26, 2013; revised/accepted: May 12, 2014; available online: May 14, 2014.

APPENDIX 1

Tera-Wasserburg concordia plots of SHRIMP U-Pb zircon ages for samples dated during this study (ordered according Tables 3 and 4). Ellipses and error in ages in the inset are at 1σ; decay constant errors included.

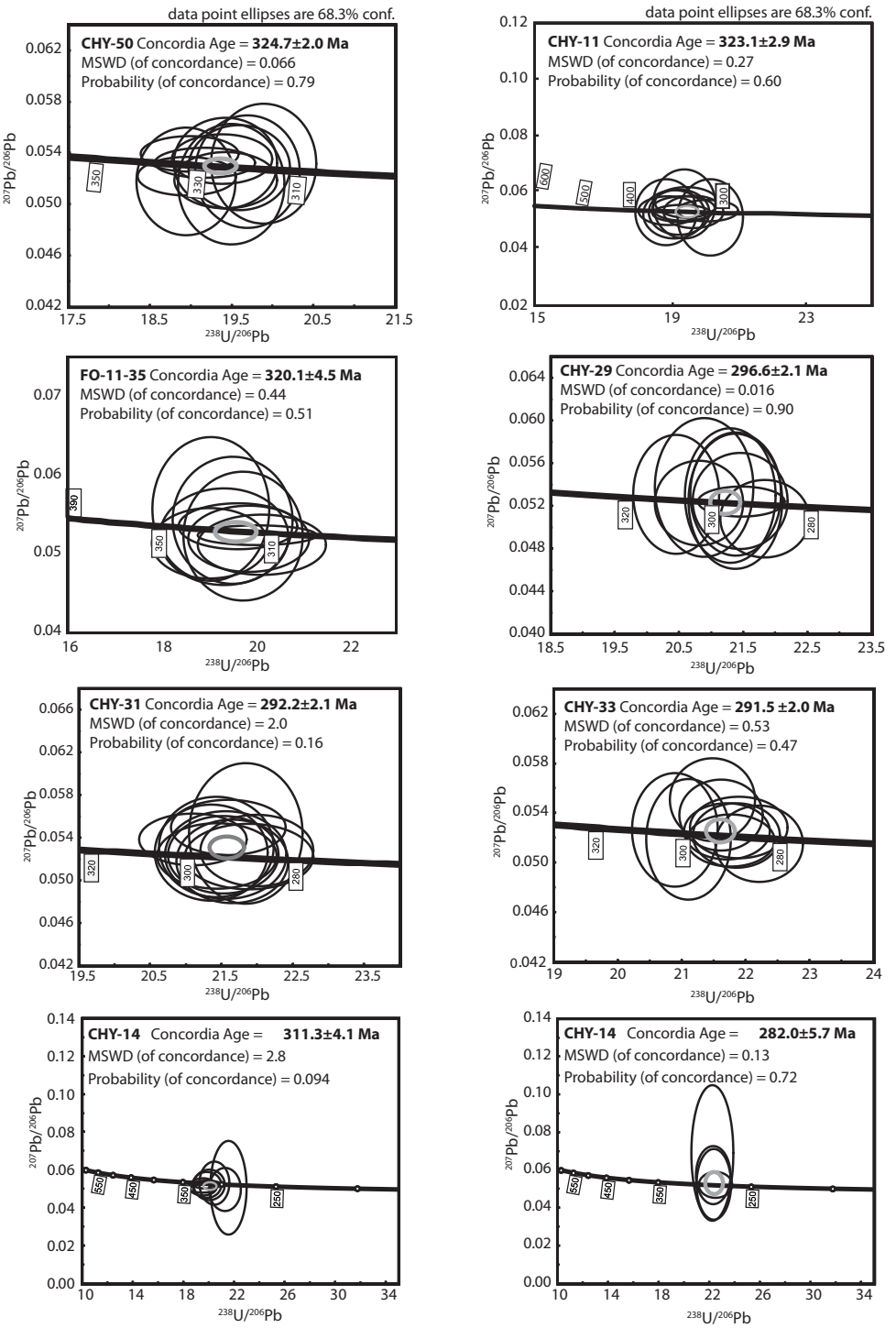

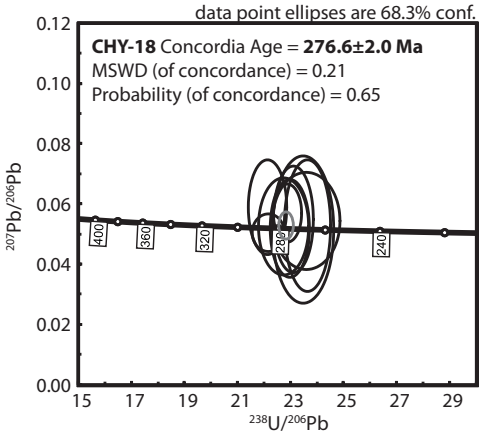
data point ellipses are 68.3% conf.
CHY-18 Concordia Age = 276.6±2.0 Ma
MSWD (of concordance) = 0.21
Probability (of concordance) = 0.65
207Pb/206Pb
238U/206Pb

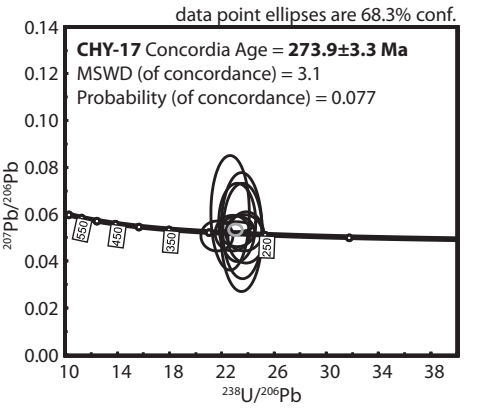
data point ellipses are 68.3% conf.
CHY-17 Concordia Age = 273.9±3.3 Ma
MSWD (of concordance) = 3.1
Probability (of concordance) = 0.077
207Pb/206Pb
238U/206Pb

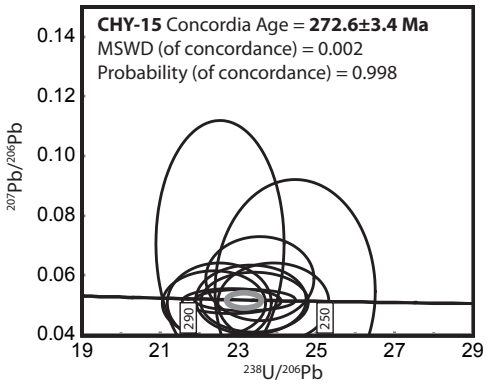
CHY-15 Concordia Age = 272.6±3.4 Ma
MSWD (of concordance) = 0.002
Probability (of concordance) = 0.998
207Pb/206Pb
238U/206Pb

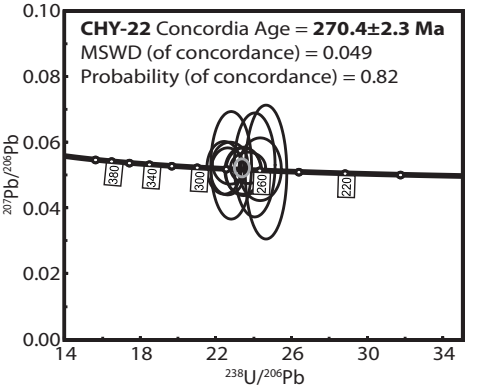
CHY-22 Concordia Age = 270.4±2.3 Ma
MSWD (of concordance) = 0.049
Probability (of concordance) = 0.82
207Pb/206Pb
238U/206Pb

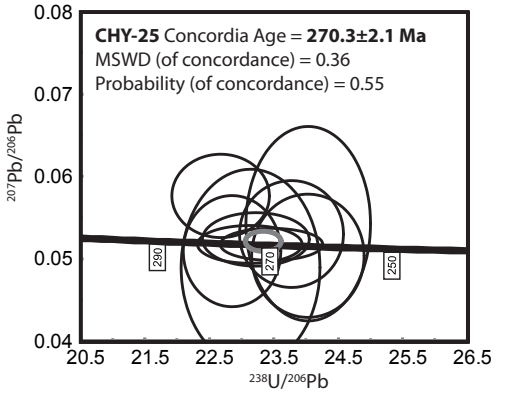
CHY-25 Concordia Age = 270.3±2.1 Ma
MSWD (of concordance) = 0.36
Probability (of concordance) = 0.55
207Pb/206Pb
238U/206Pb

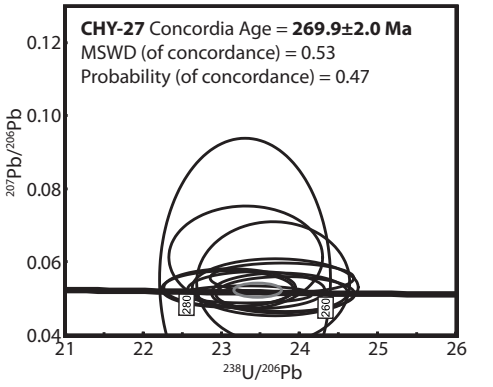
CHY-27 Concordia Age = 269.9±2.0 Ma
MSWD (of concordance) = 0.53
Probability (of concordance) = 0.47
207Pb/206Pb
238U/206Pb

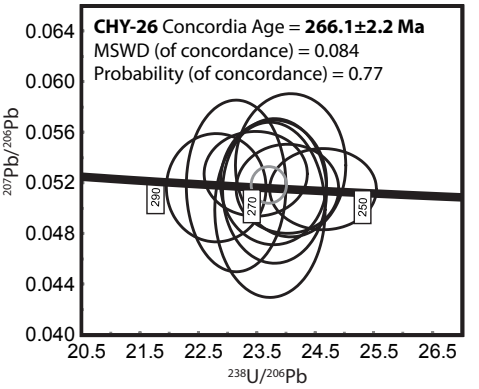
CHY-26 Concordia Age = 266.1±2.2 Ma
MSWD (of concordance) = 0.084
Probability (of concordance) = 0.77
207Pb/206Pb
238U/206Pb

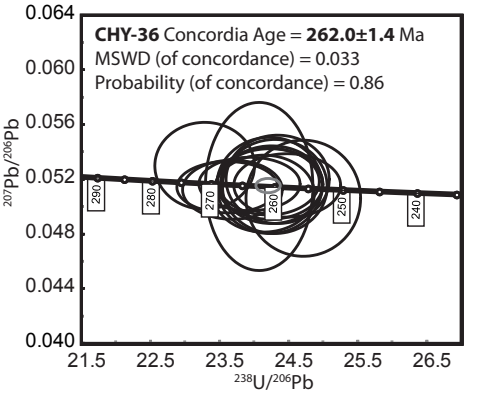
CHY-36 Concordia Age = 262.0±1.4 Ma
MSWD (of concordance) = 0.033
Probability (of concordance) = 0.86
207Pb/206Pb
238U/206Pb

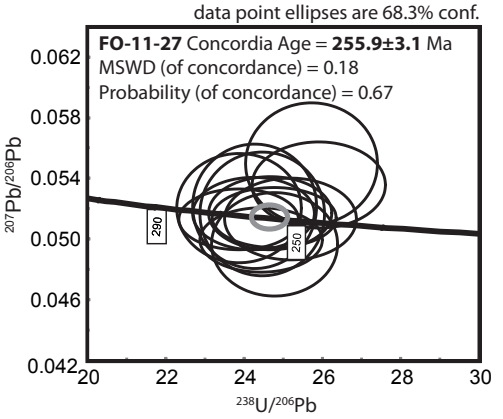
data point ellipses are 68.3% conf.
FO-11-27 Concordia Age = 255.9±3.1 Ma
MSWD (of concordance) = 0.18
Probability (of concordance) = 0.67
207Pb/206Pb
238U/206Pb

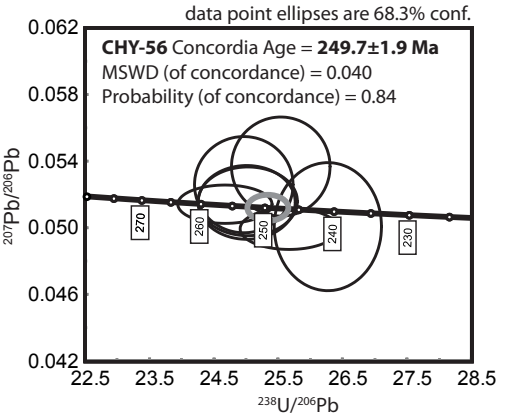
data point ellipses are 68.3% conf.
CHY-56 Concordia Age = 249.7±1.9 Ma
MSWD (of concordance) = 0.040
Probability (of concordance) = 0.84
207Pb/206Pb
238U/206Pb

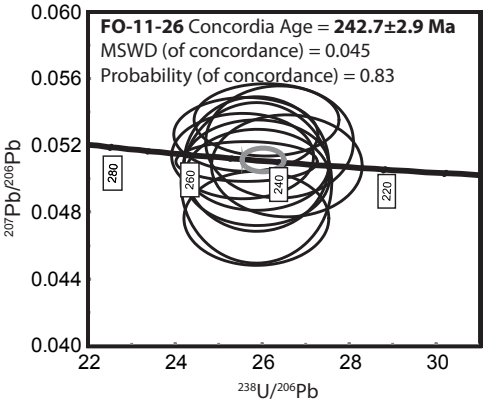
FO-11-26 Concordia Age = 242.7±2.9 Ma
MSWD (of concordance) = 0.045
Probability (of concordance) = 0.83
207Pb/206Pb
238U/206Pb

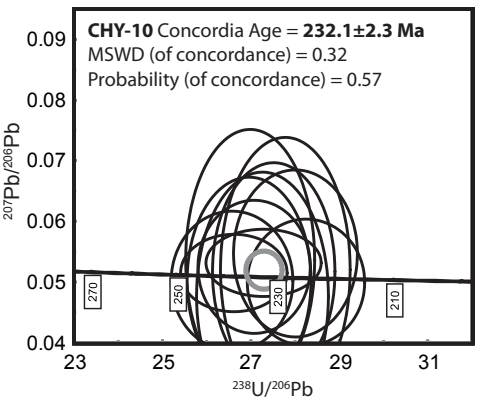
CHY-10 Concordia Age = 232.1±2.3 Ma
MSWD (of concordance) = 0.32
Probability (of concordance) = 0.57
207Pb/206Pb
238U/206Pb

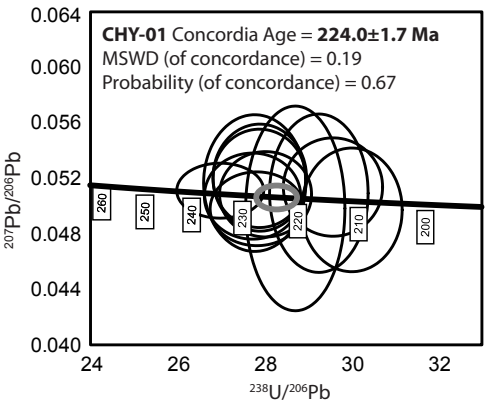
CHY-01 Concordia Age = 224.0±1.7 Ma
MSWD (of concordance) = 0.19
Probability (of concordance) = 0.67
207Pb/206Pb
238U/206Pb

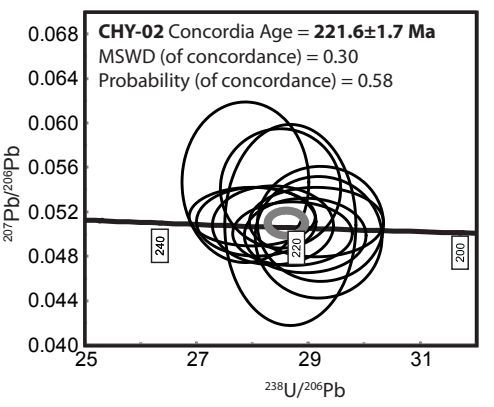
CHY-02 Concordia Age = 221.6±1.7 Ma
MSWD (of concordance) = 0.30
Probability (of concordance) = 0.58
207Pb/206Pb
238U/206Pb

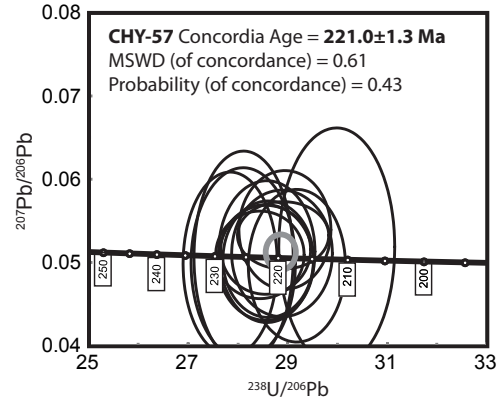
CHY-57 Concordia Age = 221.0±1.3 Ma
MSWD (of concordance) = 0.61
Probability (of concordance) = 0.43
207Pb/206Pb
238U/206Pb

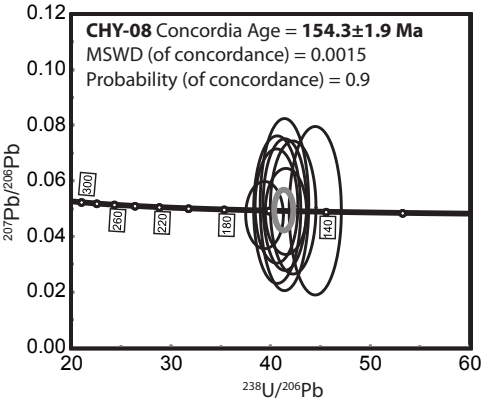
CHY-08 Concordia Age = 154.3±1.9 Ma
MSWD (of concordance) = 0.0015
Probability (of concordance) = 0.9
207Pb/206Pb
238U/206Pb

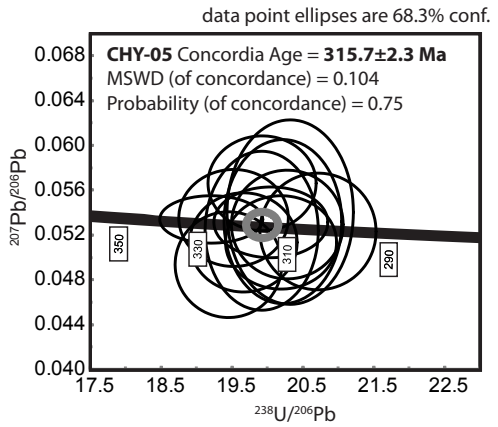
data point ellipses are 68.3% conf.
CHY-05 Concordia Age = 315.7±2.3 Ma
MSWD (of concordance) = 0.104
Probability (of concordance) = 0.75
207Pb/206Pb
238U/206Pb

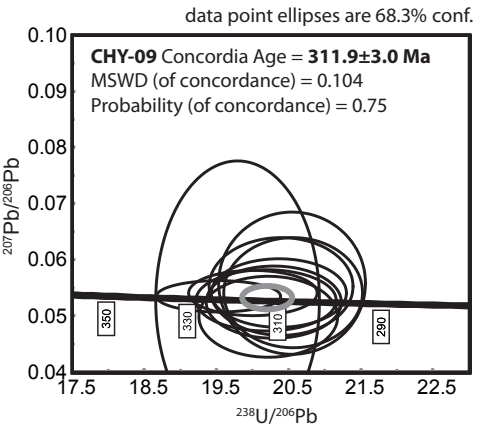
data point ellipses are 68.3% conf.
CHY-09 Concordia Age = 311.9±3.0 Ma
MSWD (of concordance) = 0.104
Probability (of concordance) = 0.75
207Pb/206Pb
238U/206Pb

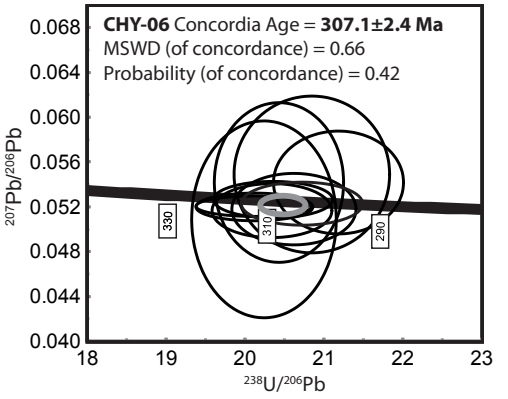
CHY-06 Concordia Age = 307.1±2.4 Ma
MSWD (of concordance) = 0.66
Probability (of concordance) = 0.42
207Pb/206Pb
238U/206Pb

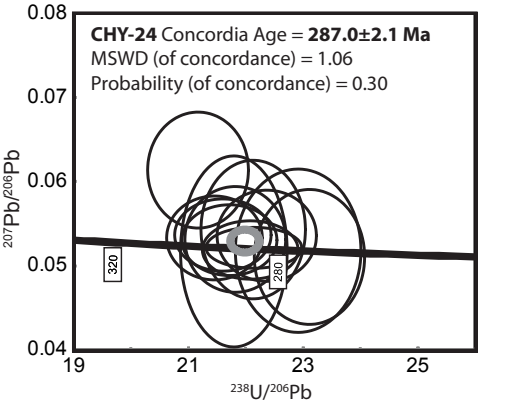
CHY-24 Concordia Age = 287.0±2.1 Ma
MSWD (of concordance) = 1.06
Probability (of concordance) = 0.30
207Pb/206Pb
238U/206Pb

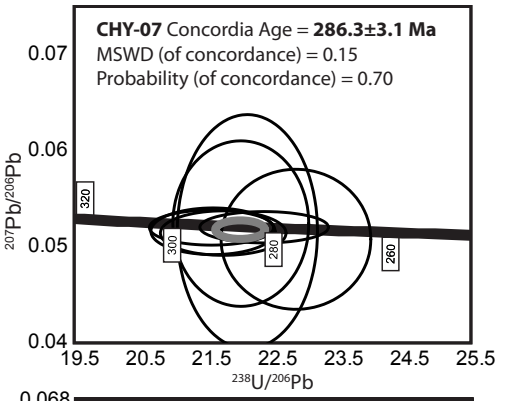
CHY-07 Concordia Age = 286.3±3.1 Ma
MSWD (of concordance) = 0.15
Probability (of concordance) = 0.70
207Pb/206Pb
238U/206Pb

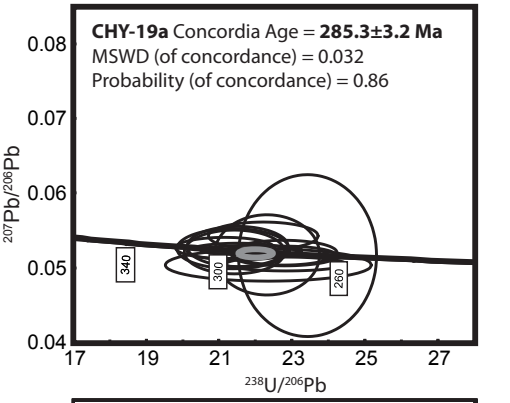
CHY-19a Concordia Age = 285.3±3.2 Ma
MSWD (of concordance) = 0.032
Probability (of concordance) = 0.86
207Pb/206Pb
238U/206Pb

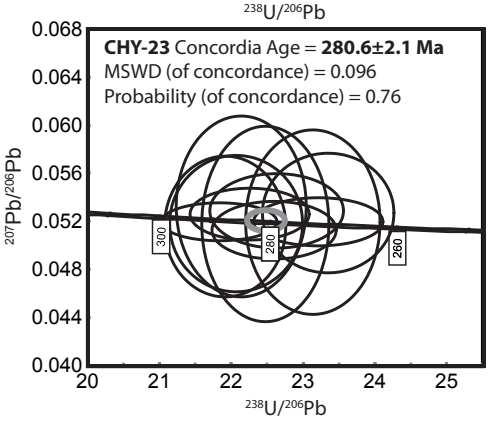
CHY-23 Concordia Age = 280.6±2.1 Ma
MSWD (of concordance) = 0.096
Probability (of concordance) = 0.76
207Pb/206Pb
238U/206Pb

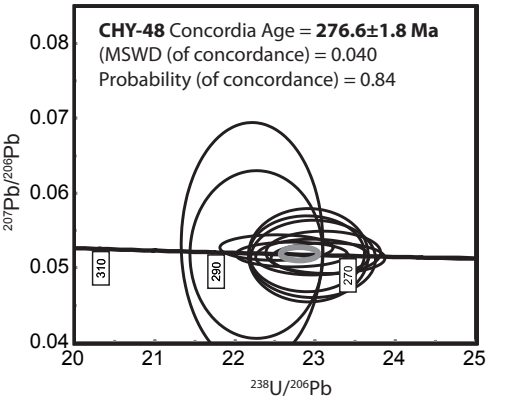
CHY-48 Concordia Age = 276.6±1.8 Ma
(MSWD (of concordance) = 0.040
Probability (of concordance) = 0.84
207Pb/206Pb
238U/206Pb

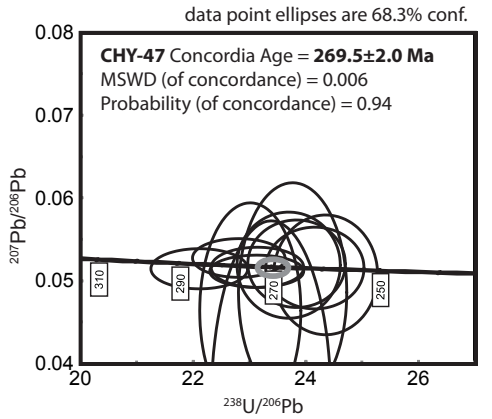
data point ellipses are 68.3% conf.
CHY-47 Concordia Age = 269.5±2.0 Ma
MSWD (of concordance) = 0.006
Probability (of concordance) = 0.94
207Pb/206Pb
238U/206Pb

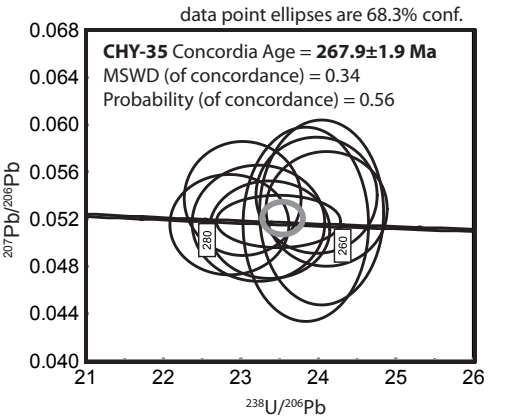
data point ellipses are 68.3% conf.
CHY-35 Concordia Age = 267.9±1.9 Ma
MSWD (of concordance) = 0.34
Probability (of concordance) = 0.56
207Pb/206Pb
238U/206Pb

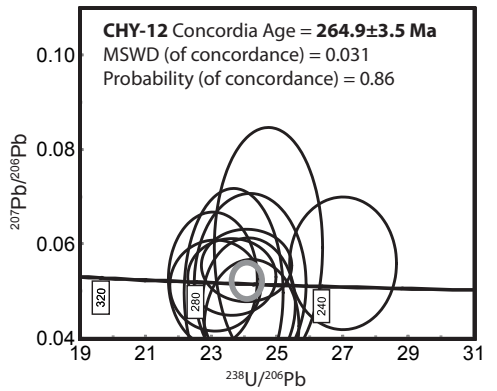
CHY-12 Concordia Age = 264.9±3.5 Ma
MSWD (of concordance) = 0.031
Probability (of concordance) = 0.86
207Pb/206Pb
238U/206Pb

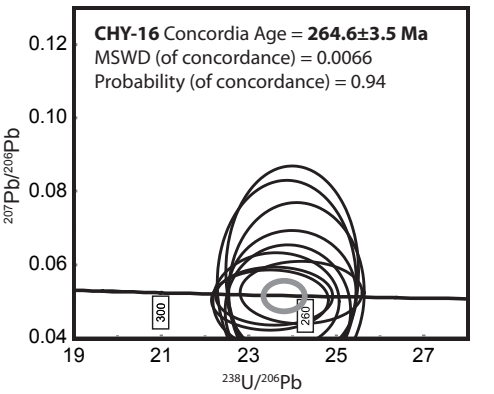
CHY-16 Concordia Age = 264.6±3.5 Ma
MSWD (of concordance) = 0.0066
Probability (of concordance) = 0.94
207Pb/206Pb
238U/206Pb

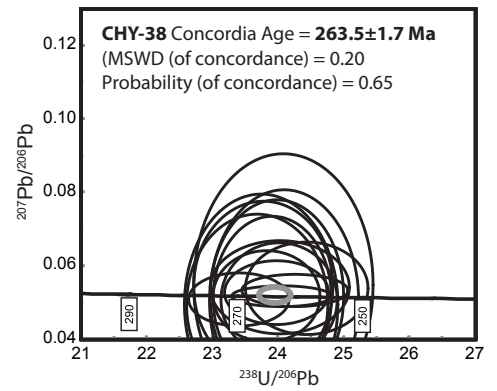
CHY-38 Concordia Age = 263.5±1.7 Ma
(MSWD (of concordance) = 0.20
Probability (of concordance) = 0.65
207Pb/206Pb
238U/206Pb

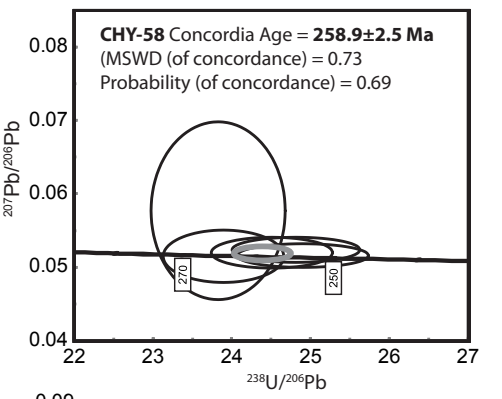
CHY-58 Concordia Age = 258.9±2.5 Ma
(MSWD (of concordance) = 0.73
Probability (of concordance) = 0.69
207Pb/206Pb
238U/206Pb

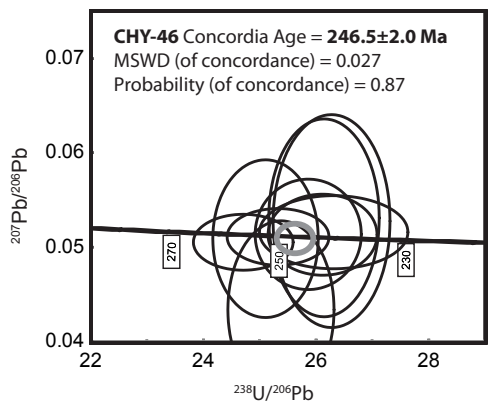
CHY-46 Concordia Age = 246.5±2.0 Ma
MSWD (of concordance) = 0.027
Probability (of concordance) = 0.87
207Pb/206Pb
238U/206Pb

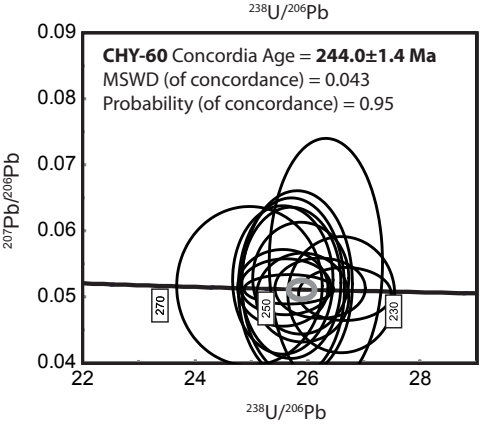
CHY-60 Concordia Age = 244.0±1.4 Ma
MSWD (of concordance) = 0.043
Probability (of concordance) = 0.95
207Pb/206Pb
238U/206Pb

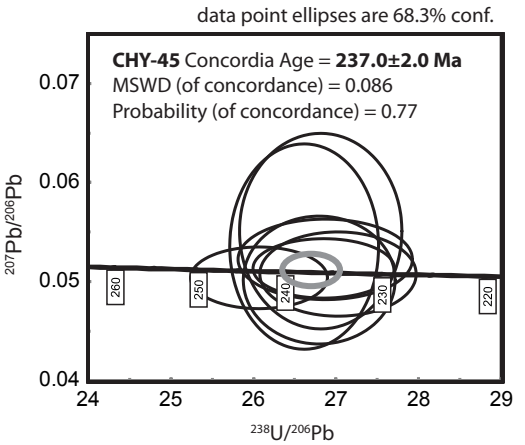
data point ellipses are 68.3% conf.
CHY-45 Concordia Age = 237.0±2.0 Ma
MSWD (of concordance) = 0.086
Probability (of concordance) = 0.77
0.07
0.06
0.05
0.04
24
25
26
27
28
29
260
250
240
230
220
207Pb/206Pb
238U/206Pb

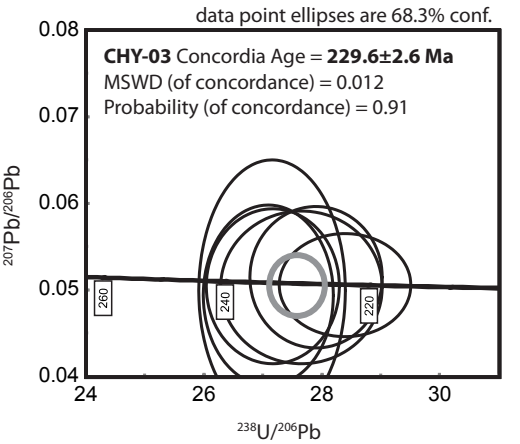
data point ellipses are 68.3% conf.
CHY-03 Concordia Age = 229.6±2.6 Ma
MSWD (of concordance) = 0.012
Probability (of concordance) = 0.91
0.08
0.07
0.06
0.05
0.04
24
26
28
30
260
240
220
207Pb/206Pb
238U/206Pb

APPENDIX 2. SHIMP ZIRCON U-Pb ANALYTICAL DATA.

Grain Spot	Common ^{206}Pb %	U ppm	Th ppm	$^{232}Th/^{238}U$	Radiogenic ^{206}Pb ppm	$^{204}Pb/^{206}Pb$	Total $^{238}U/^{206}Pb$	error %	Total $^{207}Pb/^{206}Pb$	error %	Radiogenic $^{238}U/^{206}Pb$	error %	Radiogenic $^{207}Pb/^{206}Pb$	error %	^{204}Pb corrected $^{206}Pb/^{238}U$ Age Ma	error ±1σ
Sample CHY-50																
CHY50-1.1	0.12	665.79	385.62	0.60	29.87	0.000068	19.15	2.11	0.054223	1.22	19.17	2.11	0.0532	1.44	327.8	6.8
CHY50-2.1	0.69	326.52	110.20	0.35	14.91	0.000377	18.81	2.10	0.057306	3.07	18.94	2.11	0.0518	5.31	331.6	6.8
CHY50-3.1	0.57	215.24	85.94	0.41	9.58	0.000311	19.31	2.14	0.057757	2.25	19.42	2.15	0.0532	4.37	323.6	6.8
CHY50-4.1	0.15	503.78	275.23	0.56	22.87	0.000083	18.92	2.10	0.053387	1.44	18.95	2.10	0.0522	1.90	331.4	6.8
CHY50-5.1	0.37	434.45	135.98	0.32	19.33	0.000204	19.31	2.09	0.056494	1.55	19.38	2.09	0.0535	2.36	324.3	6.6
CHY50-6.1	0.43	522.45	141.96	0.28	23.21	0.000238	19.34	2.13	0.055371	1.43	19.43	2.13	0.0519	2.79	323.5	6.7
CHY50-7.1	0.50	563.87	133.46	0.24	24.85	0.000275	19.49	2.08	0.056876	2.15	19.59	2.09	0.0529	4.13	320.9	6.5
CHY50-8.1	1.08	314.83	132.15	0.43	13.89	0.000594	19.47	2.13	0.061257	1.90	19.69	2.15	0.0526	5.50	319.3	6.7
CHY50-9.1	0.36	513.88	118.07	0.24	23.34	0.000196	18.92	2.08	0.056802	1.41	18.98	2.08	0.0539	1.70	330.9	6.7
CHY50-10.1	0.87	299.20	178.11	0.62	13.30	0.000475	19.32	2.18	0.058539	1.90	19.49	2.20	0.0516	5.97	322.5	6.9
CHY50-11.1	0.42	367.37	157.89	0.44	17.31	0.000229	18.23	2.09	0.057580	1.67	18.31	2.10	0.0542	2.67	342.7*	7.0*
CHY50-12.1	0.01	828.74	225.72	0.28	38.83	0.000005	18.34	2.07	0.055084	1.16	18.34	2.07	0.0550	1.34	342.3*	6.9*
CHY50-13.1	0.98	296.52	181.76	0.63	12.94	0.000537	19.69	2.12	0.061030	2.32	19.89	2.14	0.0532	5.80	316.2	6.6
CHY-50 Greenish rhyolite, Cerro Bayo Formation; Concordia U-Pb age = 324.7±2.0 Ma																
Sample CHY-11																
CHY11-1.1	0.42	615.42	579.43	0.97	27.43	0.000283	19.28	2.96	0.056601	1.99	19.38	2.97	0.0525	3.85	324.4	9.4
CHY11-2.1	0.52	403.98	443.00	1.13	18.04	0.000747	19.24	3.16	0.067239	2.25	19.51	3.18	0.0563	6.34	322.2	10.0
CHY11-3.1	1.65	274.43	158.88	0.60	12.76	0.001205	18.48	3.06	0.070556	5.19	18.89	3.16	0.0529	14.62	332.3	10.3
CHY11-4.1	1.34	312.31	261.46	0.87	14.17	0.000983	18.93	3.03	0.067292	3.92	19.28	3.08	0.0529	10.08	325.9	9.8
CHY11-5.1	0.68	499.46	382.10	0.79	22.26	0.000439	19.27	3.13	0.060639	1.94	19.43	3.14	0.0542	5.17	323.5	9.9
CHY11-6.1	0.98	492.39	368.26	0.77	22.56	0.000599	18.75	3.04	0.062202	2.00	18.96	3.06	0.0534	6.30	331.3	9.9
CHY11-7.1	0.21	964.64	1002.59	1.07	41.47	0.000439	19.98	2.92	0.059814	1.81	20.14	2.93	0.0534	4.62	312.2	8.9
CHY11-8.1	0.18	490.36	404.42	0.85	21.66	0.000753	19.45	2.97	0.064071	3.37	19.72	2.99	0.0530	7.17	318.8	9.3
CHY11-9.1	2.84	272.25	271.05	1.03	12.38	0.001502	18.90	3.08	0.077737	6.70	19.43	3.15	0.0558	14.42	323.3	9.9
CHY11-10.1	1.72	252.09	252.76	1.04	11.04	0.001603	19.62	3.05	0.074676	5.03	20.21	3.18	0.0512	17.41	311.1	9.7
CHY11-11.1	1.71	244.45	230.79	0.98	11.23	0.001266	18.70	3.10	0.070625	2.61	19.14	3.15	0.0521	10.78	328.1	10.1
CHY-11 Pink rhyolite, Cerro Bayo Formation; Concordia U-Pb age = 323.1±2.9 Ma																

appendix 2 continued.

Grain Spot	Common ^{206}Pb %	U ppm	Th ppm	$^{232}Th/^{238}U$	Radiogenic ^{206}Pb ppm	$^{204}Pb/^{206}Pb$	Total $^{238}U/^{206}Pb$	error %	Total $^{207}Pb/^{206}Pb$	error %	Radiogenic $^{238}U/^{206}Pb$	error %	Radiogenic $^{207}Pb/^{206}Pb$	error %	^{204}Pb corrected $^{206}Pb/^{238}U$ Age Ma	error ±1σ
Sample FO-11-35																
FO11-35-1.1	0.85	159.54	92.32	0.60	7.15	0.000466	19.18	4.66	0.058986	3.53	19.34	4.68	0.05216	7.74	324.9	14.8
FO11-35-2.1	0.58	397.46	226.33	0.59	17.05	0.000317	20.03	4.48	0.055744	2.36	20.15	4.49	0.05110	4.92	312.2	13.7
FO11-35-3.1	0.58	288.28	126.88	0.45	12.54	0.000317	19.75	4.27	0.056543	2.77	19.87	4.27	0.05190	5.33	316.5	13.2
FO11-35-4.1	0.97	392.57	261.75	0.69	17.90	0.000535	18.84	4.27	0.059167	2.66	19.03	4.28	0.05132	5.76	330.1	13.8
FO11-35-5.1	1.10	227.66	153.81	0.70	10.13	0.000606	19.31	4.28	0.063071	5.18	19.52	4.31	0.05422	9.84	321.9	13.6
FO11-35-6.1	1.53	345.81	127.20	0.38	23.99	0.000851	12.39	4.25	0.066508	3.35	12.58	4.27	0.05407	8.34	492.8*	20.3*
FO11-35-7.1	2.20	470.13	467.96	1.03	21.68	0.001210	18.63	4.26	0.073316	2.17	19.05	4.31	0.05567	10.76	329.6	13.8
FO11-35-8.1	0.16	1,784.84	1,625.62	0.94	76.61	0.000086	20.02	4.17	0.053605	1.11	20.05	4.17	0.05234	1.59	313.8	12.8
FO11-35-9.1	0.58	301.23	187.74	0.64	13.25	0.000321	19.53	4.26	0.058135	2.63	19.64	4.26	0.05344	3.59	320.0	13.3
FO11-35-10.1	0.23	290.18	92.24	0.33	42.24	0.000136	5.90	4.63	0.078951	1.28	5.92	4.63	0.07703	1.76	1006.5*	43.2*
FO11-35-11.1	0.36	677.99	259.40	0.40	46.60	0.000203	12.50	4.18	0.059864	1.37	12.54	4.18	0.05690	1.63	494.4*	19.9*
FO11-35-10.2	2.10	293.14	224.43	0.79	13.85	0.001154	18.18	4.36	0.081399	2.98	18.57	4.41	0.06475	9.71	337.9	14.5
FO11-35-12.1	2.49	434.85	262.44	0.62	19.41	0.001370	19.25	4.22	0.072296	2.20	19.74	4.26	0.05223	10.28	318.4	13.2
FO-11-35 Rhyolitic ignimbrite, underlies Cerro del Árbol Formation; Concordia U-Pb age = 320.1±4.5 Ma																
Sample CHY-29																
CHY29-1.1	1.32	158.38	81.05	0.53	6.45	0.000721	21.09	2.21	0.062980	3.62	21.37	2.25	0.05242	7.97	294.7	6.5
CHY29-2.1	0.91	182.86	97.17	0.55	7.59	0.000497	20.70	2.38	0.060991	2.73	20.89	2.43	0.05372	7.96	301.4	7.1
CHY29-3.1	0.90	465.47	296.24	0.66	19.40	0.000491	20.62	2.17	0.059465	2.40	20.80	2.18	0.05227	4.99	302.6	6.5
CHY29-4.1	0.53	339.83	178.15	0.54	14.35	0.000292	20.34	2.10	0.057358	2.42	20.45	2.15	0.05308	6.93	307.7	6.4
CHY29-5.1	0.75	480.03	782.97	1.69	19.03	0.000411	21.67	2.09	0.056842	2.43	21.83	2.10	0.05080	4.70	288.7	5.9
CHY29-6.1	0.04	731.55	539.89	0.76	29.29	0.000023	21.46	2.07	0.052742	1.50	21.47	2.08	0.05240	1.76	293.5	6.0
CHY29-7.1	0.67	411.12	282.32	0.71	19.20	0.000368	18.40	2.11	0.058716	1.78	18.52	2.12	0.05333	4.57	338.9*	7.0*
CHY29-8.1	0.98	299.28	157.05	0.54	12.11	0.000539	21.24	2.25	0.060345	2.45	21.45	2.27	0.05246	5.65	293.7	6.5
CHY29-9.1	1.41	203.91	97.53	0.49	8.31	0.000773	21.08	2.16	0.064405	3.56	21.38	2.18	0.05309	7.16	294.6	6.3
CHY29-10.1	1.55	234.69	146.72	0.65	9.62	0.000850	20.96	2.14	0.065397	2.54	21.29	2.18	0.05295	7.84	295.8	6.3
CHY-29 Pinkish rhyolite, Paipote Valley; Concordia U-Pb age = 296.6±2.1 Ma																

appendix 2 continued.

Grain Spot	Common ^{206}Pb %	U ppm	Th ppm	$^{232}Th/^{238}U$	Radiogenic ^{206}Pb ppm	$^{204}Pb/^{206}Pb$	Total $^{238}U/^{206}Pb$	error %	Total $^{207}Pb/^{206}Pb$	error %	Radiogenic $^{238}U/^{206}Pb$	error %	Radiogenic $^{207}Pb/^{206}Pb$	error %	^{204}Pb corrected $^{206}Pb/^{238}U$ Age Ma	error ±1σ
Sample CHY-31																
CHY31-1.1	0.53	610.30	367.77	0.62	24.09	0.000292	21.77	2.70	0.056511	1.44	21.88	2.71	0.05224	3.86	288.0	7.6
CHY31-2.1	0.57	908.38	673.34	0.77	36.41	0.000312	21.44	2.60	0.056968	3.47	21.56	2.61	0.05240	5.17	292.3	7.5
CHY31-3.1	0.65	581.32	322.37	0.57	23.22	0.000357	21.51	2.38	0.057001	2.48	21.65	2.39	0.05177	4.99	291.0	6.8
CHY31-4.1	0.77	750.62	376.92	0.52	29.55	0.000424	21.82	2.36	0.058984	2.17	21.99	2.37	0.05277	4.18	286.6	6.7
CHY31-5.1	3.03	443.30	229.42	0.53	17.48	0.001658	21.78	2.65	0.075182	7.92	22.47	2.71	0.05085	16.34	280.5	7.5
CHY31-6.1	0.57	821.93	410.70	0.52	33.13	0.000313	21.31	2.57	0.056873	1.22	21.43	2.58	0.05229	3.84	293.9	7.4
CHY31-7.1	0.67	715.94	548.74	0.79	28.77	0.000369	21.38	2.37	0.057818	3.36	21.52	2.37	0.05241	4.59	292.7	6.8
CHY31-8.1	1.17	368.60	173.97	0.49	14.67	0.000640	21.58	2.38	0.063773	4.70	21.84	2.41	0.05442	7.98	288.6	6.8
CHY31-9.1	0.68	523.39	340.35	0.67	21.13	0.000373	21.28	2.47	0.058587	3.71	21.43	2.48	0.05313	5.86	294.0	7.1
CHY31-10.1	0.47	598.41	424.21	0.73	23.92	0.000256	21.49	2.47	0.058686	2.74	21.60	2.47	0.05495	3.10	291.8	7.0
CHY31-11.1	0.66	508.16	380.47	0.77	20.58	0.000360	21.21	2.44	0.057886	3.17	21.35	2.45	0.05262	5.64	295.0	7.1
CHY31-12.1	0.38	619.81	390.53	0.65	25.34	0.000206	21.02	2.35	0.056871	1.40	21.10	2.36	0.05385	2.97	298.5	6.9
															CHY-31 Purple rhyolite, Paipote Valley; Concordia U-Pb age = 292.2±2.1 Ma	
Sample CHY-33																
CHY33-1.1	0.48	297.35	93.99	0.33	12.16	0.000262	21.00	2.04	0.055709	3.45	21.10	2.06	0.05187	6.16	298.4	6.0
CHY33-2.1	0.34	3,860.99	684.28	0.18	75.04	0.000185	44.20	2.00	0.051838	1.05	44.36	2.00	0.04912	1.94	143.7*	2.8*
CHY33-3.1	0.39	386.75	318.87	0.85	15.24	0.000213	21.80	2.29	0.055963	1.93	21.89	2.29	0.05284	3.08	287.9	6.5
CHY33-4.1	0.63	685.03	338.48	0.51	27.40	0.000345	21.48	1.98	0.058869	1.37	21.61	1.99	0.05383	3.51	291.5	5.7
CHY33-5.1	0.42	283.74	232.58	0.85	11.40	0.000230	21.39	2.03	0.058440	3.44	21.48	2.04	0.05508	4.00	293.3	5.8
CHY33-6.1	0.53	555.16	236.69	0.44	22.03	0.000291	21.65	2.08	0.056040	1.67	21.77	2.08	0.05177	2.65	289.5	5.9
CHY33-7.1	0.52	374.99	66.51	0.18	15.50	0.000286	20.78	2.08	0.056823	1.88	20.89	2.10	0.05264	5.72	301.4	6.2
CHY33-8.1	0.70	372.87	186.79	0.52	14.86	0.000385	21.56	2.03	0.058143	1.90	21.71	2.03	0.05250	2.84	290.3	5.8
CHY33-9.1	0.65	548.57	326.12	0.61	21.36	0.000355	22.07	2.02	0.056724	1.59	22.21	2.03	0.05152	3.92	283.9	5.6
CHY33-10.1	0.50	629.12	343.26	0.56	24.86	0.000273	21.74	2.04	0.056190	1.57	21.85	2.05	0.05219	3.26	288.4	5.8
															CHY-33 Light-gray, andesitic tuff, El Mono Beds; Concordia U-Pb age = 291.5±2.0 Ma	

appendix 2 continued.

Grain Spot	Common ^{206}Pb %	U ppm	Th ppm	$^{232}Th/^{238}U$	Radiogenic ^{206}Pb ppm	$^{204}Pb/^{206}Pb$	Total $^{238}U/^{206}Pb$	error %	Total $^{207}Pb/^{206}Pb$	error %	Radiogenic $^{238}U/^{206}Pb$	error %	Radiogenic $^{207}Pb/^{206}Pb$	error %	^{204}Pb corrected $^{206}Pb/^{238}U$ Age Ma	error ±1σ
Sample CHY-14																
CHY14-1.1	2.64	203.31	187.15	0.95	8.43	0.001446	20.71	3.78	0.070758	3.02	21.27	3.87	0.04950	15.10	296.0	11.2
CHY14-2.1	3.83	136.39	159.65	1.21	5.45	0.002095	21.51	3.87	0.083100	9.18	22.37	4.02	0.05242	23.45	281.7	11.1
CHY14-3.1	8.54	54.20	40.15	0.77	2.29	0.004677	20.34	4.27	0.136134	6.60	22.24	4.93	0.06904	34.30	282.9	13.7
CHY14-4.1	1.35	511.04	497.27	1.01	22.79	0.000743	19.27	3.67	0.061796	1.79	19.53	3.68	0.05089	5.84	321.7	11.6
CHY14-5.1	2.83	209.54	181.43	0.89	9.07	0.001552	19.84	3.79	0.075690	5.60	20.42	3.85	0.05297	14.19	308.0	11.6
CHY14-6.1	1.55	281.62	204.69	0.75	12.38	0.000852	19.55	3.71	0.064427	4.22	19.85	3.73	0.05194	8.63	316.6	11.5
CHY14-7.1	0.45	1,077.47	1,368.89	1.31	46.81	0.000248	19.78	3.61	0.055752	1.26	19.86	3.62	0.05212	2.69	316.6	11.2
CHY14-8.1	1.94	209.42	169.37	0.84	9.16	0.001066	19.64	4.06	0.067687	4.10	20.03	4.09	0.05207	10.27	313.9	12.5
CHY14-9.1	1.55	316.22	212.82	0.70	12.27	0.000851	22.14	3.83	0.064521	2.32	22.49	3.87	0.05205	8.73	280.4	10.6
CHY14-10.1	2.55	121.19	128.50	1.10	4.79	0.001398	21.74	3.90	0.077632	6.40	22.31	4.03	0.05728	17.52	282.5	11.1
CHY14-11.1	0.55	1,219.29	1,354.19	1.15	54.00	0.000303	19.40	3.61	0.054500	1.20	19.51	3.61	0.05005	2.74	322.2	11.4
CHY14-12.1	6.42	86.09	107.61	1.29	3.67	0.003520	20.13	4.02	0.102148	6.13	21.52	4.34	0.05046	32.10	292.4	12.4
															CHY-14 Dark purple, rhyolitic tuff, La Tabla Formation; Concordia U-Pb ages = 311.3±4.1 and 282.0±5.7 Ma	
Sample CHY-18																
CHY18-1.1	4.45	94.36	57.22	0.63	3.62	0.002436	22.42	2.71	0.087245	6.69	23.46	3.23	0.05152	31.23	268.8	8.5
CHY18-2.1	4.61	78.74	43.20	0.57	3.00	0.002519	22.52	1.96	0.089644	7.78	23.61	2.42	0.05276	27.22	267.1	6.3
CHY18-3.1	2.52	143.35	81.57	0.59	5.70	0.001381	21.59	1.76	0.070675	4.05	22.15	1.77	0.05039	8.16	284.5	4.9
CHY18-4.1	3.51	96.37	83.88	0.90	3.64	0.001922	22.75	3.37	0.082335	3.93	23.58	3.57	0.05425	19.51	267.5	9.4
CHY18-5.1	2.75	143.04	94.65	0.68	5.16	0.001504	23.82	1.49	0.073984	3.38	24.50	1.71	0.05194	14.80	257.8*	4.3*
CHY18-6.1	2.27	149.78	156.21	1.08	6.21	0.001243	20.72	1.46	0.070820	3.44	21.20	1.66	0.05261	13.61	296.9*	4.8*
CHY18-7.1	2.47	108.75	66.69	0.63	4.21	0.001354	22.17	2.46	0.072312	4.91	22.73	2.74	0.05248	20.24	277.4	7.4
CHY18-8.1	2.63	115.56	88.42	0.79	4.44	0.001436	22.36	1.69	0.072952	4.92	22.96	2.07	0.05190	20.51	274.6	5.6
CHY18-9.1	1.74	168.71	97.30	0.60	6.45	0.000951	22.47	1.36	0.070838	3.19	22.87	1.53	0.05699	11.06	275.8	4.1
CHY18-10.1	1.25	304.74	214.44	0.73	12.51	0.000686	20.93	1.07	0.062205	2.71	21.19	1.15	0.05216	7.75	297.2*	3.3*
CHY18-11.1	2.63	95.34	54.91	0.60	3.80	0.001441	21.55	1.79	0.079908	4.02	22.13	2.14	0.05897	17.56	284.7	6.0
CHY18-12.1	2.55	110.80	66.63	0.62	4.23	0.001395	22.50	1.64	0.075274	3.77	23.08	2.14	0.05490	21.22	273.2	5.7
															CHY-18 Dark green, rhyolitic tuff, La Tabla Formation; Concordia U-Pb age = 276.6±2.0 Ma	

appendix 2 continued.

Grain Spot	Common ^{206}Pb %	U ppm	Th ppm	$^{232}Th/^{238}U$	Radiogenic ^{206}Pb ppm	$^{204}Pb/^{206}Pb$	Total $^{238}U/^{206}Pb$	error %	Total $^{207}Pb/^{206}Pb$	error %	Radiogenic $^{238}U/^{206}Pb$	error %	Radiogenic $^{207}Pb/^{206}Pb$	error %	^{204}Pb corrected $^{206}Pb/^{238}U$ Age Ma	error ±1σ
Sample CHY-17																
CHY17-1.1	1.40	288.98	440.78	1.58	10.86	0.000768	22.85	3.70	0.064015	2.32	23.18	3.73	0.05277	8.16	272.2	10.0
CHY17-2.1	0.31	532.98	900.96	1.75	19.93	0.000171	22.97	3.65	0.057090	1.82	23.05	3.65	0.05460	2.58	273.8	9.8
CHY17-3.1	0.99	258.08	181.51	0.73	11.40	0.000545	19.45	3.71	0.059613	3.23	19.65	3.74	0.05162	8.07	319.9*	11.7*
CHY17-4.1	5.56	100.55	76.28	0.78	3.88	0.003040	22.27	3.92	0.097361	3.31	23.58	4.17	0.05285	25.16	267.4	10.9
CHY17-5.1	5.89	70.42	80.46	1.18	2.74	0.003222	22.09	4.05	0.099556	5.68	23.48	4.42	0.05236	31.79	268.5	11.6
CHY17-6.1	4.24	69.60	61.04	0.91	2.76	0.002318	21.67	4.06	0.094346	10.76	22.63	4.30	0.06074	26.50	278.5	11.7
CHY17-7.1	1.59	241.06	321.07	1.38	9.23	0.000869	22.44	3.84	0.064672	2.50	22.80	3.88	0.05194	9.56	276.6	10.5
CHY17-8.1	1.69	262.85	231.51	0.91	9.69	0.000925	23.31	3.83	0.065652	4.90	23.71	3.85	0.05210	9.82	266.2	10.0
CHY17-9.1	2.22	150.62	95.55	0.66	5.55	0.001212	23.32	3.81	0.067992	3.26	23.85	3.89	0.05018	14.22	264.7	10.1
CHY17-10.1	1.96	222.34	121.96	0.57	10.04	0.001078	19.03	3.72	0.067333	3.02	19.41	3.75	0.05152	9.42	323.7*	11.9*
CHY17-11.1	3.68	107.59	70.12	0.67	4.14	0.002011	22.31	3.92	0.085921	7.22	23.17	4.04	0.05661	19.41	272.2	10.8
CHY17-12.1	1.37	323.96	285.05	0.91	13.06	0.000753	21.32	3.69	0.061827	2.19	21.61	3.72	0.05077	8.23	291.5	10.6
															CHY-17 Dark green rhyolitic tuff, La Tabla Formation; Concordia U-Pb age = 273.9±3.3 Ma	
Sample CHY-15																
CHY15-1.1	4.24	191.01	101.52	0.55	7.61	0.002322	21.56	3.78	0.084799	2.88	22.52	3.88	0.05071	17.30	279.8	10.6
CHY15-2.1	9.53	52.71	44.29	0.87	2.05	0.005206	22.13	4.85	0.130619	5.45	24.46	5.52	0.05456	45.35	257.8	14.0
CHY15-3.1	8.41	53.29	34.42	0.67	2.22	0.004602	20.65	4.18	0.136515	11.98	22.54	4.80	0.07063	38.60	279.2	13.1
CHY15-4.1	2.85	129.22	78.48	0.63	4.90	0.001559	22.66	3.91	0.074758	3.12	23.32	3.99	0.05190	14.76	270.4	10.6
CHY15-5.1	3.49	145.40	92.40	0.66	5.42	0.001905	23.07	3.82	0.078859	4.56	23.90	3.92	0.05089	17.15	264.0	10.1
CHY15-6.1	4.47	187.72	206.53	1.14	7.17	0.002442	22.51	3.76	0.094346	2.39	23.56	3.89	0.05887	15.83	267.7	10.2
CHY15-7.1	2.97	173.46	226.51	1.35	6.56	0.001622	22.73	3.82	0.074749	3.06	23.43	3.88	0.05095	13.04	269.3	10.2
CHY15-8.1	1.26	946.76	1,299.53	1.42	35.55	0.000688	22.88	3.66	0.061801	1.31	23.17	3.66	0.05171	4.48	272.3	9.8
CHY15-9.1	0.67	560.17	770.55	1.42	21.22	0.000367	22.68	3.64	0.056703	3.16	22.83	3.65	0.05132	5.47	276.3	9.9
CHY15-10.1	2.76	147.19	121.90	0.86	5.81	0.001510	21.77	3.82	0.072750	3.08	22.39	3.89	0.05058	14.28	281.5	10.7
															CHY-15 Dark green, rhyolitic tuff, La Tabla Formation; Concordia U-Pb age = 272.6±3.4 Ma	

appendix 2 continued.

Grain Spot	Common ^{206}Pb %	U ppm	Th ppm	$^{232}Th/^{238}U$	Radiogenic ^{206}Pb ppm	$^{204}Pb/^{206}Pb$	Total $^{238}U/^{206}Pb$	error %	Total $^{207}Pb/^{206}Pb$	error %	Radiogenic $^{238}U/^{206}Pb$	error %	Radiogenic $^{207}Pb/^{206}Pb$	error %	^{204}Pb corrected $^{206}Pb/^{238}U$ Age Ma	error ±1σ
Sample CHY-22																
CHY22-1.1	1.36	89.88	48.59	0.56	3.55	0.000744	21.76	2.86	0.066617	3.56	22.06	2.90	0.05576	8.27	285.7*	8.1*
CHY22-2.1	4.13	137.81	82.60	0.62	6.07	0.002267	19.52	3.51	0.088233	2.60	20.36	3.63	0.05514	15.99	308.8*	11.0*
CHY22-3.1	3.62	65.91	37.85	0.59	2.58	0.001979	21.97	2.90	0.081928	5.60	22.79	3.10	0.05296	20.25	276.5	8.4
CHY22-4.1	1.37	213.45	135.82	0.66	8.23	0.000747	22.29	2.57	0.062097	4.88	22.60	2.61	0.05113	9.18	279.0	7.1
CHY22-5.1	1.92	139.39	88.28	0.65	5.20	0.001049	23.03	2.64	0.066392	3.09	23.48	2.68	0.05099	9.26	268.8	7.0
CHY22-6.1	1.07	119.91	70.52	0.61	4.64	0.000583	22.19	2.67	0.060664	4.02	22.43	2.73	0.05212	10.13	281.1	7.5
CHY22-7.1	1.60	150.06	127.22	0.88	5.59	0.000876	23.06	2.63	0.064212	2.83	23.43	2.68	0.05136	9.15	269.3	7.1
CHY22-8.1	1.20	241.90	206.14	0.88	8.88	0.000655	23.40	2.55	0.061805	2.32	23.69	2.57	0.05221	5.97	266.5	6.7
CHY22-9.1	3.24	104.73	55.33	0.55	3.77	0.001771	23.84	2.81	0.076918	13.42	24.64	2.95	0.05092	26.26	256.3	7.4
CHY22-10.1	2.78	193.86	176.11	0.94	7.05	0.001520	23.64	2.96	0.074004	3.03	24.32	3.02	0.05172	12.08	259.6	7.7
CHY22-11.1	1.31	142.35	138.86	1.01	5.45	0.000718	22.44	2.67	0.064104	3.03	22.74	2.71	0.05360	7.76	277.4	7.4
CHY22-12.1	2.72	118.12	66.84	0.58	4.34	0.001487	23.40	2.75	0.074841	7.49	24.05	2.94	0.05308	19.57	262.4	7.6
															CHY-22 Purple, banded rhyolite, La Tabla Formation; Concordia U-Pb age = 270.4±2.3 Ma	
Sample CHY-25																
CHY25-1.1	0.17	186.74	90.20	0.50	7.09	0.000093	22.64	2.18	0.059000	4.07	22.68	2.20	0.05764	5.76	278.2	6.0
CHY25-2.1	0.48	355.80	184.10	0.53	13.23	0.000265	23.11	2.34	0.056234	1.98	23.22	2.35	0.05235	4.09	271.8	6.3
CHY25-3.1	2.05	105.79	62.69	0.61	4.01	0.001120	22.65	2.97	0.065425	6.07	23.12	3.07	0.04894	16.11	272.8	8.2
CHY25-4.1	1.36	159.81	65.27	0.42	5.86	0.000742	23.45	2.23	0.063856	5.18	23.77	2.25	0.05300	8.08	265.6	5.9
CHY25-5.1	3.26	65.96	34.04	0.53	3.17	0.001795	17.88	2.40	0.080115	3.36	18.48	2.69	0.05387	19.77	339.4*	8.9*
CHY25-6.1	1.35	156.83	58.92	0.39	15.44	0.000769	8.73	2.17	0.083766	2.52	8.85	2.20	0.07279	5.77	689.7*	14.4*
CHY25-7.1	1.62	97.84	62.68	0.66	3.56	0.000887	23.63	2.34	0.063397	3.57	24.02	2.40	0.05037	9.75	262.9	6.2
CHY25-8.1	0.47	438.21	236.21	0.56	16.12	0.000255	23.35	2.24	0.055472	1.81	23.46	2.24	0.05173	2.46	269.1	5.9
CHY25-9.1	1.91	495.71	358.84	0.75	14.38	0.001040	29.62	2.14	0.068363	2.07	30.19	2.20	0.05314	8.96	210.0*	4.5*
CHY25-10.1	0.26	277.76	140.14	0.52	10.34	0.000140	23.07	2.30	0.053833	2.30	23.13	2.30	0.05178	2.92	272.9	6.2
CHY25-11.1	1.29	184.35	134.84	0.76	7.02	0.000708	22.55	2.15	0.061342	4.12	22.84	2.19	0.05095	8.72	276.1	5.9
CHY25-12.1	2.33	181.41	78.98	0.45	6.64	0.001271	23.47	2.58	0.072821	7.09	24.02	2.66	0.05425	14.34	262.8	6.8
															CHY-25 Pinkish gray, dacite, Pantanoso Formation; Concordia U-Pb age = 270.3±2.1 Ma	

appendix 2 continued.

Grain Spot	Common ^{206}Pb %	U ppm	Th ppm	$^{232}Th/^{238}U$	Radiogenic ^{206}Pb ppm	$^{204}Pb/^{206}Pb$	Total $^{238}U/^{206}Pb$	error %	Total $^{207}Pb/^{206}Pb$	error %	Radiogenic $^{238}U/^{206}Pb$	error %	Radiogenic $^{207}Pb/^{206}Pb$	error %	^{204}Pb corrected $^{206}Pb/^{238}U$ Age Ma	error ±1σ
Sample CHY-27																
CHY27-1.1	1.42	280.86	171.51	0.63	19.04	0.000792	12.67	2.40	0.072883	7.95	12.86	2.42	0.06141	10.87	482.6	11.3
CHY27-2.1	2.22	134.69	94.54	0.73	5.08	0.001215	22.78	2.57	0.078842	4.81	23.30	2.76	0.06123	15.12	270.7	7.3
CHY27-3.1	0.79	504.52	585.09	1.20	18.91	0.000434	22.92	2.38	0.059328	1.81	23.10	2.41	0.05298	6.50	273.1	6.4
CHY27-4.1	8.99	168.95	95.25	0.58	6.86	0.004918	21.16	2.47	0.127000	13.08	23.25	3.07	0.05521	45.91	270.8	8.2
CHY27-5.1	0.44	617.70	555.55	0.93	22.85	0.000239	23.22	2.35	0.054702	1.65	23.33	2.36	0.05119	3.00	270.6	6.2
CHY27-6.1	0.81	532.64	470.34	0.91	19.68	0.000440	23.25	2.45	0.058763	2.43	23.44	2.48	0.05231	6.32	269.2	6.5
CHY27-7.1	0.95	406.74	218.24	0.55	14.82	0.000519	23.58	2.43	0.058762	1.98	23.81	2.46	0.05115	6.16	265.2	6.4
CHY27-8.1	0.67	497.01	518.49	1.08	18.08	0.000364	23.62	2.54	0.060990	2.69	23.77	2.55	0.05567	4.83	265.6	6.6
CHY27-9.1	3.42	138.96	91.91	0.68	5.23	0.001869	22.84	2.51	0.081687	7.52	23.64	2.72	0.05438	20.24	266.8	7.1
CHY27-10.1	1.00	407.40	356.53	0.90	15.32	0.000548	22.85	2.38	0.060552	1.97	23.08	2.41	0.05252	6.24	273.4	6.4
CHY27-11.1	1.57	239.07	222.63	0.96	8.81	0.000858	23.31	2.90	0.065562	2.61	23.68	2.96	0.05300	9.69	266.5	7.7
CHY27-12.1	0.26	479.43	50.75	0.11	120.57	0.000162	3.42	2.49	0.106599	0.57	3.42	2.49	0.10438	0.86	1650.8*	36.3*
CHY27-13.1	0.66	523.50	307.71	0.61	89.48	0.000391	5.03	2.56	0.083052	0.72	5.06	2.56	0.07751	1.78	1162.0*	27.2*
CHY27-14.1	0.90	286.87	187.23	0.67	11.73	0.000495	21.01	2.40	0.059984	2.25	21.21	2.45	0.05273	7.95	297.0*	7.1*
CHY27-15.1	1.42	377.15	316.00	0.87	13.85	0.000775	23.40	2.38	0.062873	2.55	23.74	2.41	0.05150	6.97	265.9	6.3
CHY27-16.1	2.42	144.86	155.95	1.11	5.78	0.001325	21.55	2.84	0.071248	2.95	22.08	2.91	0.05183	11.40	285.4	8.1
															CHY-27 Purple rhyolite, Pantanoso Formation; Concordia U-Pb age = 269.9±2.0 Ma	
Sample CHY-26																
CHY26-1.1	0.81	1,238.36	1,539.65	1.28	43.55	0.000443	24.43	2.42	0.057983	1.19	24.63	2.43	0.05149	4.10	256.5	6.1
CHY26-2.1	1.23	428.99	220.13	0.53	16.12	0.000674	22.86	2.39	0.061637	4.66	23.14	2.42	0.05175	8.61	272.6	6.5
CHY26-3.1	2.34	794.46	893.76	1.16	26.71	0.001277	25.55	2.49	0.068765	1.90	26.17	2.53	0.04999	9.24	241.7*	6.0*
CHY26-4.1	0.93	487.37	318.37	0.67	18.53	0.000509	22.59	2.46	0.059089	1.82	22.80	2.47	0.05163	5.45	276.6	6.7
CHY26-5.1	1.07	452.10	205.07	0.47	16.31	0.000583	23.82	2.55	0.061920	3.59	24.07	2.57	0.05339	6.99	262.3	6.6
CHY26-6.1	1.82	289.26	186.98	0.67	10.67	0.000994	23.28	2.58	0.064488	3.08	23.71	2.62	0.04989	9.12	266.2	6.8
CHY26-7.1	0.84	524.38	286.44	0.56	19.09	0.000461	23.60	2.43	0.058119	3.66	23.80	2.45	0.05135	7.34	265.3	6.4
CHY26-8.1	0.30	496.49	233.93	0.49	18.22	0.000163	23.41	2.48	0.055111	2.61	23.48	2.48	0.05273	4.19	268.8	6.5
CHY26-9.1	0.99	497.07	289.31	0.60	18.14	0.000543	23.54	2.50	0.059986	3.07	23.78	2.52	0.05202	6.24	265.5	6.6
CHY26-10.1	0.80	570.35	376.60	0.68	20.56	0.000436	23.83	2.40	0.057905	2.70	24.02	2.41	0.05151	4.49	262.9	6.2
															CHY-26 Purple, rhyolitic ignimbrite, Pantanoso Formation; Concordia U-Pb age = 266.1±2.2 Ma	

appendix 2 continued.

Grain Spot	Common ^{206}Pb %	U ppm	Th ppm	$^{232}Th/^{238}U$	Radiogenic ^{206}Pb ppm	$^{204}Pb/^{206}Pb$	Total $^{238}U/^{206}Pb$	error %	Total $^{207}Pb/^{206}Pb$	error %	Radiogenic $^{238}U/^{206}Pb$	error %	Radiogenic $^{207}Pb/^{206}Pb$	error %	^{204}Pb corrected $^{206}Pb/^{238}U$ Age Ma	error ±1σ
Sample CHY-36																
CHY36-1.1	0.52	904.23	699.08	0.80	32.34	0.000285	24.02	2.00	0.055113	1.41	24.14	2.01	0.05093	3.65	261.6	5.2
CHY36-2.1	0.39	536.04	230.79	0.44	19.85	0.000215	23.20	2.04	0.056110	1.81	23.29	2.05	0.05297	3.95	271.0	5.4
CHY36-3.1	0.59	405.23	250.09	0.64	14.55	0.000323	23.93	2.09	0.056208	2.11	24.08	2.14	0.05147	7.85	262.3	5.5
CHY36-4.1	0.29	701.42	563.28	0.83	24.82	0.000157	24.28	2.01	0.054291	1.61	24.35	2.03	0.05199	4.12	259.5	5.2
CHY36-5.1	0.47	544.82	303.06	0.57	19.35	0.000256	24.19	2.04	0.055220	1.87	24.30	2.05	0.05147	4.40	259.9	5.2
CHY36-6.1	0.68	508.61	556.23	1.13	17.80	0.000372	24.55	2.21	0.056085	2.64	24.72	2.23	0.05062	5.52	255.7	5.6
CHY36-7.1	0.63	528.89	393.06	0.77	19.36	0.000344	23.47	2.04	0.056469	1.81	23.62	2.04	0.05142	2.42	267.3	5.3
CHY36-8.1	0.62	434.19	281.63	0.67	17.98	0.000341	20.74	2.41	0.056825	1.86	20.87	2.41	0.05182	2.74	301.6*	7.1*
CHY36-9.1	0.46	925.51	1101.19	1.23	32.97	0.000253	24.12	2.06	0.055238	1.75	24.23	2.08	0.05153	4.51	260.7	5.3
CHY36-10.1	0.30	832.22	508.18	0.63	29.59	0.000162	24.16	2.07	0.054003	1.62	24.23	2.08	0.05163	3.29	260.7	5.3
CHY36-11.1	0.34	673.10	533.75	0.82	23.70	0.000186	24.40	2.08	0.054271	1.66	24.49	2.08	0.05155	2.94	258.0	5.3
CHY36-12.1	0.29	1,290.46	819.16	0.66	46.94	0.000160	23.62	2.01	0.053566	1.86	23.69	2.01	0.05122	2.77	266.6	5.2
CHY36-13.1	0.34	824.12	615.58	0.77	29.29	0.000188	24.17	2.01	0.054379	1.53	24.26	2.02	0.05162	3.63	260.4	5.1
CHY36-14.1	0.32	803.69	466.09	0.60	28.61	0.000176	24.13	2.01	0.054402	1.49	24.21	2.01	0.05182	3.13	260.9	5.1
CHY36-15.1	0.46	1034.36	718.77	0.72	37.30	0.000252	23.83	2.00	0.055344	1.42	23.94	2.01	0.05164	2.50	263.8	5.2
CHY-36 Dark purple, fluidal rhyolite, La Tabla Formation; Concordia U-Pb age = 262.0±1.4 Ma																
Sample FO-11-27																
FO11-27-1.1	0.33	220.56	113.18	0.53	7.39	0.000179	25.64	4.31	0.057567	3.38	25.72	4.32	0.05496	4.80	245.9	10.4
FO11-27-2.1	1.04	278.11	179.12	0.67	9.74	0.000570	24.52	4.28	0.058036	3.26	24.78	4.28	0.04966	4.51	255.0	10.7
FO11-27-3.1	0.58	697.03	482.98	0.72	25.24	0.000316	23.73	4.39	0.056653	2.22	23.86	4.40	0.05203	4.55	264.6	11.4
FO11-27-4.1	0.35	675.21	594.47	0.91	23.60	0.000190	24.58	4.20	0.054483	1.91	24.67	4.20	0.05169	3.07	256.1	10.6
FO11-27-5.1	0.28	510.14	366.54	0.74	17.75	0.000152	24.70	4.22	0.053670	2.27	24.77	4.22	0.05144	2.54	255.2	10.6
FO11-27-6.1	0.27	513.94	387.35	0.78	18.27	0.000149	24.17	4.22	0.053872	2.26	24.24	4.22	0.05169	3.05	260.6	10.8
FO11-27-7.1	0.43	391.89	310.79	0.82	13.42	0.000237	25.08	4.40	0.054809	2.58	25.19	4.40	0.05133	3.46	251.0	10.8
FO11-27-8.1	0.21	627.08	447.31	0.74	22.63	0.000117	23.81	4.21	0.053034	2.00	23.86	4.21	0.05132	2.57	264.7	10.9
FO11-27-9.1	0.27	663.85	457.23	0.71	23.40	0.000148	24.37	4.22	0.052112	2.01	24.44	4.22	0.04993	2.80	258.5	10.7
FO11-27-10.1	0.55	266.92	123.30	0.48	9.42	0.000300	24.34	4.28	0.056061	3.06	24.47	4.29	0.05167	5.19	258.2	10.9
FO11-27-11.1	0.00	261.67	183.36	0.72	8.68	0.000000	25.91	4.32	0.053556	3.49	25.91	4.32	0.05356	3.49	244.2	10.4
FO11-27-12.1	0.35	263.28	140.00	0.55	9.35	0.000190	24.19	4.28	0.054950	3.10	24.27	4.29	0.05217	5.17	260.3	10.9
FO-11-27 Pink rhyolitic ignimbrite, Cas Formation, Peine Group; Concordia U-Pb age = 255.9±3.1 Ma																

appendix 2 continued.

Grain Spot	Common ^{206}Pb %	U ppm	Th ppm	$^{232}Th/^{238}U$	Radiogenic ^{206}Pb ppm	$^{204}Pb/^{206}Pb$	Total $^{238}U/^{206}Pb$	error %	Total $^{207}Pb/^{206}Pb$	error %	Radiogenic $^{238}U/^{206}Pb$	error %	Radiogenic $^{207}Pb/^{206}Pb$	error %	^{204}Pb corrected $^{206}Pb/^{238}U$ Age Ma	error ±1σ
Sample CHY-56																
CHY56-1.1	0.28	841.19	28.82	0.04	28.96	0.000152	24.96	2.02	0.053824	1.41	25.03	2.03	0.051593	2.63	252.5	5.0
CHY56-2.1	0.15	1,957.98	78.38	0.04	68.27	0.000080	24.64	1.95	0.052579	0.96	24.67	1.95	0.051407	1.48	256.1	4.9
CHY56-3.1	0.52	449.81	22.30	0.05	15.56	0.000285	24.83	2.02	0.056736	1.86	24.96	2.03	0.052567	3.63	253.2	5.0
CHY56-4.1	0.30	456.08	177.40	0.40	20.65	0.000166	18.97	2.00	0.055662	1.67	19.03	2.00	0.053233	3.07	330.1*	6.4*
CHY56-5.1	0.49	520.15	259.24	0.51	22.47	0.000271	19.89	2.06	0.056471	1.58	19.99	2.06	0.052501	2.62	314.7*	6.3*
CHY56-6.1	0.53	474.69	340.95	0.74	21.21	0.000293	19.22	1.99	0.055786	1.66	19.33	2.00	0.051483	3.26	325.1*	6.3*
CHY56-7.1	1.93	311.76	227.29	0.75	13.62	0.001059	19.66	2.11	0.069732	1.80	20.05	2.16	0.054259	8.21	313.6*	6.6*
CHY56-8.1	0.46	253.40	176.39	0.72	8.32	0.000250	26.16	2.07	0.053720	2.87	26.28	2.09	0.050051	5.07	240.8	4.9
CHY56-9.1	0.52	595.95	42.48	0.07	20.58	0.000283	24.88	1.99	0.055668	1.63	25.01	1.99	0.051524	2.84	252.7	4.9
CHY56-10.1	0.20	1,660.55	172.64	0.11	55.69	0.000112	25.62	1.96	0.051563	1.02	25.67	1.96	0.049920	1.63	246.4	4.7
CHY56-11.1	0.25	336.83	170.58	0.52	15.45	0.000137	18.73	2.01	0.056559	1.91	18.78	2.02	0.054556	2.48	334.5*	6.6*
CHY56-12.1	0.78	872.26	49.35	0.06	29.57	0.000423	25.35	1.97	0.059870	1.37	25.54	1.98	0.053677	3.65	247.5	4.8
															CHY-56 Dark greenish, basaltic tuff, La Totora Formation; Concordia U-Pb age = 249.7±1.9 Ma	
Sample FO-11-26																
FO11-26-1.1	0.26	456.09	348.08	0.79	14.88	0.000141	26.33	4.25	0.054280	2.66	26.40	4.26	0.05222	4.24	239.7	10.0
FO11-26-2.1	0.00	354.50	225.72	0.66	11.88	0.000000	25.63	4.25	0.052670	2.76	25.63	4.25	0.05267	2.76	246.8	10.3
FO11-26-3.1	0.87	355.32	260.23	0.76	11.34	0.000474	26.91	4.27	0.055675	2.70	27.15	4.28	0.04870	5.57	233.1	9.8
FO11-26-4.1	0.41	361.48	293.25	0.84	12.05	0.000221	25.77	4.25	0.054140	2.76	25.87	4.26	0.05089	5.22	244.5	10.2
FO11-26-5.1	0.75	407.99	237.91	0.60	13.66	0.000411	25.67	4.39	0.055790	2.49	25.86	4.41	0.04975	6.37	244.5	10.6
FO11-26-6.1	0.58	367.76	225.97	0.63	12.28	0.000316	25.72	4.25	0.052309	2.70	25.87	4.25	0.04765	3.89	244.5	10.2
FO11-26-7.1	0.00	1,100.86	683.98	0.64	36.87	0.000000	25.65	4.18	0.051038	1.56	25.65	4.18	0.05104	1.56	246.6	10.1
FO11-26-8.1	0.43	453.81	259.77	0.59	15.13	0.000233	25.77	4.25	0.053494	2.41	25.88	4.25	0.05008	3.80	244.4	10.2
FO11-26-9.1	0.28	646.04	333.26	0.53	21.79	0.000154	25.48	4.22	0.053635	2.00	25.55	4.22	0.05138	3.28	247.5	10.2
FO11-26-10.1	0.20	445.77	347.78	0.81	14.83	0.000112	25.82	4.23	0.052456	2.46	25.87	4.23	0.05082	3.50	244.5	10.2
FO11-26-11.1	0.20	482.74	438.19	0.94	15.92	0.000111	26.05	4.22	0.055143	2.29	26.10	4.22	0.05352	2.68	242.4	10.0
FO11-26-12.1	0.31	781.84	626.91	0.83	25.36	0.000171	26.48	4.29	0.053293	1.90	26.56	4.29	0.05078	3.98	238.2	10.0
															FO-11-26 Redish rhyolite, Cas Formation, Peine Group; Concordia U-Pb age = 242.7±2.9 Ma	

appendix 2 continued.

Grain Spot	Common ^{206}Pb %	U ppm	Th ppm	$^{232}Th/^{238}U$	Radiogenic ^{206}Pb ppm	$^{204}Pb/^{206}Pb$	Total $^{238}U/^{206}Pb$	error %	Total $^{207}Pb/^{206}Pb$	error %	Radiogenic $^{238}U/^{206}Pb$	error %	Radiogenic $^{207}Pb/^{206}Pb$	error %	^{204}Pb corrected $^{206}Pb/^{238}U$ Age Ma	error ±1σ
Sample CHY-10																
CHY10-1.1	3.32	135.22	70.00	0.53	4.46	0.002409	26.04	3.27	0.083220	4.89	27.24	3.59	0.04772	28.19	232.2	8.2
CHY10-2.1	4.91	165.62	99.01	0.62	5.45	0.003225	26.11	3.21	0.099324	6.80	27.75	3.48	0.05207	27.45	228.0	7.8
CHY10-3.1	2.32	344.80	251.30	0.75	11.24	0.001438	26.35	3.02	0.073604	4.81	27.06	3.10	0.05254	13.71	233.8	7.1
CHY10-4.1	5.26	143.86	76.75	0.55	4.84	0.002892	25.53	3.25	0.095967	5.98	26.96	3.55	0.05366	26.30	234.5	8.2
CHY10-5.1	1.99	350.76	259.02	0.76	11.62	0.001280	25.94	3.32	0.069019	5.09	26.56	3.41	0.05022	15.08	238.1	8.0
CHY10-6.1	3.53	169.93	131.41	0.80	5.66	0.002361	25.77	3.21	0.084973	4.12	26.94	3.42	0.05030	22.28	234.8	7.9
CHY10-7.1	1.39	534.61	465.22	0.90	17.59	0.000994	26.12	2.96	0.066104	2.95	26.60	2.98	0.05153	8.18	237.8	7.0
CHY10-8.1	4.18	217.43	157.93	0.75	7.09	0.002273	26.35	3.12	0.085024	7.69	27.49	3.30	0.05170	22.81	230.1	7.5
CHY10-9.1	3.25	200.78	102.62	0.53	6.38	0.001870	27.02	3.15	0.082031	4.50	27.98	3.29	0.05472	16.53	226.2	7.3
CHY10-10.1	1.06	538.74	450.89	0.86	17.16	0.000613	26.98	3.12	0.062125	2.13	27.28	3.14	0.05316	6.85	232.0	7.2
CHY10-11.1	1.40	310.29	219.98	0.73	9.68	0.001354	27.53	3.04	0.069834	5.41	28.23	3.10	0.04993	13.77	224.3	6.8
CHY-10 Redish brown, banded rhyolite, Los Tilos Sequence, Pastos Blancos Group; Concordia U-Pb age = 232.1±2.3 Ma																
Sample CHY-01																
CHY1-1.1	-0.05	558.61	461.67	0.85	17.32	0.000245	27.70	2.55	0.053401	1.39	27.83	2.56	0.04980	3.52	227.6	5.7
CHY1-2.1	0.32	264.74	186.25	0.73	8.25	0.000431	27.56	2.78	0.057965	1.92	27.78	2.80	0.05165	6.30	228.0	6.3
CHY1-3.1	0.03	396.18	364.90	0.95	12.21	0.000298	27.87	2.48	0.055225	2.09	28.03	2.49	0.05085	3.98	226.0	5.5
CHY1-4.1	0.67	711.31	915.67	1.33	22.74	0.000224	26.88	2.45	0.054378	1.26	26.99	2.46	0.05109	2.54	234.5	5.7
CHY1-5.1	0.22	233.03	183.39	0.81	7.24	0.000463	27.67	2.53	0.058822	1.99	27.90	2.54	0.05204	4.91	226.9	5.7
CHY1-6.1	0.00	351.68	219.36	0.64	10.87	0.000186	27.79	2.51	0.054733	2.37	27.89	2.52	0.05200	4.48	227.1	5.6
CHY1-7.1	0.33	256.72	156.72	0.63	7.63	0.000667	28.90	2.54	0.060712	2.21	29.25	2.57	0.05092	7.40	216.6	5.5
CHY1-8.1	-0.36	423.45	374.17	0.91	12.23	0.000505	29.73	2.53	0.057132	1.73	30.01	2.56	0.04971	5.91	211.3	5.3
CHY1-9.1	1.36	194.56	78.88	0.42	5.92	0.000868	28.25	2.58	0.062567	2.55	28.71	2.63	0.04981	9.77	220.6	5.7
CHY1-10.1	-0.15	382.83	306.86	0.83	11.92	0.000291	27.59	2.63	0.054973	2.57	27.74	2.64	0.05070	4.04	228.3	5.9
CHY1-11.1	-0.14	343.94	263.46	0.79	10.07	0.000439	29.34	2.53	0.057797	1.91	29.58	2.54	0.05135	4.56	214.3	5.4
CHY-01 Redish brown, banded rhyolite, Los Tilos Sequence, Pastos Blancos Group; Concordia U-Pb age = 224.0±1.7 Ma																

appendix 2 continued.

Grain Spot	Common ^{206}Pb %	U ppm	Th ppm	$^{232}Th/^{238}U$	Radiogenic ^{206}Pb ppm	$^{204}Pb/^{206}Pb$	Total $^{238}U/^{206}Pb$	error %	Total $^{207}Pb/^{206}Pb$	error %	Radiogenic $^{238}U/^{206}Pb$	error %	Radiogenic $^{207}Pb/^{206}Pb$	error %	^{204}Pb corrected $^{206}Pb/^{238}U$ Age Ma	error ±1σ
Sample CHY-02																
CHY2-1.1	-0.10	469.83	347.62	0.76	14.03	0.000329	28.77	2.48	0.054718	1.50	28.94	2.49	0.04988	4.42	218.9	5.4
CHY2-2.1	0.10	259.20	218.18	0.87	7.99	0.000249	27.87	2.65	0.055215	2.04	28.00	2.66	0.05157	3.37	226.2	5.9
CHY2-3.1	0.72	169.98	91.57	0.56	5.17	0.000776	28.27	2.63	0.062207	3.97	28.68	2.71	0.05082	11.72	220.9	5.9
CHY2-4.1	-0.26	487.86	358.83	0.76	15.02	0.000309	27.91	2.49	0.055644	1.67	28.07	2.50	0.05111	3.99	225.6	5.6
CHY2-5.1	-0.37	459.86	379.74	0.85	14.04	0.000422	28.15	2.50	0.056974	1.69	28.36	2.51	0.05078	4.60	223.3	5.5
CHY2-6.1	1.71	589.94	507.79	0.89	18.10	0.000945	28.01	2.47	0.067904	2.18	28.50	2.50	0.05410	6.55	222.2	5.5
CHY2-7.1	0.43	318.34	196.08	0.64	9.46	0.000594	28.90	2.53	0.059638	3.23	29.22	2.55	0.05093	6.72	216.9	5.4
CHY2-8.1	-0.05	582.11	556.52	0.99	17.25	0.000291	28.99	2.70	0.055341	2.01	29.14	2.71	0.05107	4.03	217.5	5.8
CHY2-9.1	0.28	324.82	229.28	0.73	9.65	0.000471	28.93	2.53	0.056661	2.28	29.18	2.56	0.04974	7.26	217.2	5.5
CHY2-10.1	-0.03	680.36	773.56	1.17	20.48	0.000352	28.53	2.46	0.055193	1.61	28.72	2.46	0.05002	3.77	220.6	5.3
CHY2-11.1	1.31	167.78	91.38	0.56	5.23	0.000612	27.56	2.63	0.063611	3.00	27.87	2.69	0.05468	8.73	227.2	6.0
															CHY-02 Pink rhyolitic tuff, Los Tilos Sequence, Pastos Blancos Group; Concordia U-Pb age = 221.6±1.7 Ma	
Sample CHY-57																
CHY57-1.1	1.83	271.41	196.96	0.75	8.31	0.000997	28.05	2.14	0.065904	2.51	28.58	2.23	0.05128	10.97	221.6	4.9
CHY57-2.1	1.47	461.64	399.45	0.89	14.09	0.000801	28.14	2.17	0.061775	3.71	28.56	2.22	0.05000	9.17	221.8	4.8
CHY57-3.1	1.56	516.66	463.96	0.93	15.58	0.000848	28.49	2.05	0.066294	3.86	28.95	2.10	0.05389	8.70	218.9	4.5
CHY57-4.1	1.11	567.34	803.17	1.46	17.26	0.000607	28.24	2.06	0.060378	3.07	28.56	2.09	0.05148	6.84	221.8	4.6
CHY57-5.1	1.05	790.78	1162.20	1.52	24.14	0.000572	28.14	2.02	0.059293	2.24	28.44	2.05	0.05090	6.85	222.7	4.5
CHY57-6.1	2.60	330.97	185.33	0.58	10.48	0.001419	27.12	2.11	0.070679	4.22	27.85	2.24	0.04982	14.64	227.3	5.0
CHY57-7.1	3.33	281.07	210.12	0.77	8.33	0.001810	28.99	2.39	0.078392	5.66	29.99	2.57	0.05186	18.21	211.4	5.3
CHY57-8.1	2.89	380.23	471.74	1.28	11.97	0.001575	27.29	2.32	0.073061	2.01	28.10	2.47	0.04992	15.15	225.3	5.5
CHY57-9.1	1.54	625.61	728.15	1.20	18.90	0.000836	28.44	2.24	0.063353	3.25	28.88	2.31	0.05109	9.85	219.3	5.0
CHY57-10.1	1.77	455.81	418.03	0.95	13.66	0.000963	28.67	2.09	0.063743	3.39	29.18	2.20	0.04958	12.18	217.1	4.7
CHY57-11.1	0.72	678.93	932.38	1.42	20.32	0.000391	28.70	2.08	0.058951	2.78	28.90	2.09	0.05324	4.99	219.2	4.5
CHY57-12.1	1.66	598.58	924.60	1.60	18.28	0.000903	28.14	2.04	0.063643	3.39	28.61	2.09	0.05038	9.14	221.4	4.6
CHY57-13.1	4.04	207.92	192.36	0.96	7.12	0.002203	25.08	2.22	0.087375	6.83	26.14	2.79	0.05522	27.88	241.8*	6.6*
CHY57-14.1	1.63	410.34	274.60	0.69	14.81	0.000893	23.80	2.18	0.064030	5.57	24.20	2.24	0.05093	10.97	261.0*	5.7*
CHY57-15.1	2.93	320.48	220.31	0.71	10.09	0.001596	27.29	2.17	0.074017	4.40	28.11	2.34	0.05058	16.62	225.2	5.2
CHY57-16.1	5.24	221.58	292.32	1.36	7.89	0.002859	24.12	2.19	0.093070	8.69	25.45	2.51	0.05112	27.56	248.2*	6.1*
															CHY-57 Dark redish brown, porphyritic basalt, La Totora Formation; Concordia U-Pb age = 221.0±1.3 Ma	

appendix 2 continued.

Grain Spot	Common ^{206}Pb %	U ppm	Th ppm	$^{232}Th/^{238}U$	Radiogenic ^{206}Pb ppm	$^{204}Pb/^{206}Pb$	Total $^{238}U/^{206}Pb$	error %	Total $^{207}Pb/^{206}Pb$	error %	Radiogenic $^{238}U/^{206}Pb$	error %	Radiogenic $^{207}Pb/^{206}Pb$	error %	^{204}Pb corrected $^{206}Pb/^{238}U$ Age Ma	error ±1σ
Sample CHY-08																
CHY8-1.1	7.85	156.08	135.08	0.89	3.51	0.004148	38.19	3.33	0.112271	7.12	41.36	3.92	0.05143	39.51	153.9	6.0
CHY8-3.1	4.38	211.77	214.02	1.04	4.59	0.003315	39.67	3.20	0.099050	6.53	42.25	3.57	0.05036	31.26	150.7	5.3
CHY8-4.1	3.24	277.41	218.89	0.82	5.99	0.002268	39.81	3.12	0.082336	4.96	41.55	3.29	0.04897	20.91	153.2	5.0
CHY8-5.1	0.09	547.40	135.25	0.26	88.01	0.000179	5.34	2.90	0.077940	0.86	5.36	2.90	0.07539	1.25	1102.5*	29.4*
CHY8-6.1	5.81	209.98	188.35	0.93	4.59	0.002738	39.29	3.20	0.091561	10.22	41.38	3.48	0.05140	30.32	153.8	5.3
CHY8-7.1	7.35	163.36	136.28	0.86	3.41	0.004050	41.14	3.39	0.108891	8.58	44.47	3.89	0.04934	40.48	143.2	5.5
CHY8-8.1	4.95	194.96	165.74	0.88	4.35	0.002751	38.52	3.24	0.091338	6.06	40.58	3.52	0.05097	26.43	156.8	5.5
CHY8-9.1	6.27	150.90	112.04	0.77	3.42	0.003681	37.88	3.35	0.103714	5.01	40.64	3.83	0.04960	35.26	156.5	5.9
CHY8-10.1	1.59	436.61	621.44	1.47	9.79	0.001435	38.33	3.04	0.068933	5.58	39.37	3.14	0.04779	16.68	161.6	5.0
CHY-08 Reddish brown, porphyritic andesite, Picudo Formation; Concordia U-Pb age = 154.3±1.9 Ma																
Sample CHY-05																
CHY5-1.1	1.06	166.83	110.31	0.68	7.30	0.000829	19.62	2.61	0.064518	3.49	19.92	2.65	0.05238	8.92	315.6	8.2
CHY5-2.1	1.45	131.50	84.89	0.67	5.63	0.000661	20.08	2.83	0.063700	2.94	20.32	2.90	0.05404	10.08	309.6	8.8
CHY5-2.2	0.49	228.01	109.03	0.49	9.75	0.000539	20.08	2.56	0.060811	2.30	20.28	2.58	0.05293	6.04	310.2	7.8
CHY5-3.1	0.35	253.95	95.40	0.39	10.90	0.000473	20.02	2.54	0.058288	2.23	20.20	2.56	0.05135	5.34	311.5	7.8
CHY5-4.1	0.64	214.81	149.16	0.72	9.51	0.000323	19.41	2.60	0.058235	3.39	19.52	2.61	0.05352	5.33	322.0	8.2
CHY5-5.1	0.85	231.16	144.16	0.64	9.68	0.000508	20.52	2.58	0.059791	3.06	20.71	2.61	0.05234	6.57	303.9	7.7
CHY5-6.1	-0.52	310.84	259.81	0.86	13.41	0.000368	19.92	2.64	0.058509	2.99	20.05	2.65	0.05312	3.91	313.7	8.1
CHY5-7.1	-0.09	266.21	183.94	0.71	11.75	0.000537	19.47	2.54	0.059207	2.18	19.66	2.56	0.05133	5.72	319.7	8.0
CHY5-8.1	0.37	385.73	182.52	0.49	16.73	0.000327	19.81	2.52	0.061382	3.46	19.93	2.53	0.05661	4.96	315.6	7.8
CHY5-9.1	0.54	293.61	138.11	0.49	13.12	0.000637	19.23	2.52	0.058728	2.09	19.45	2.54	0.04936	6.28	323.1	8.0
CHY5-10.1	1.20	139.39	90.62	0.67	6.01	0.000835	19.91	2.66	0.065420	2.78	20.22	2.71	0.05320	9.09	311.0	8.2
CHY5-11.1	0.19	658.03	333.23	0.52	29.54	0.000201	19.14	2.48	0.056337	1.57	19.21	2.49	0.05339	2.60	327.1	7.9
CHY-05 Light gray, coarse-grained, biotite monzogranite; Guachicay pluton; Concordia U-Pb age = 315.7±2.3 Ma																

appendix 2 continued.

Grain Spot	Common ^{206}Pb %	U ppm	Th ppm	$^{232}Th/^{238}U$	Radiogenic ^{206}Pb ppm	$^{204}Pb/^{206}Pb$	Total $^{238}U/^{206}Pb$	error %	Total $^{207}Pb/^{206}Pb$	error %	Radiogenic $^{238}U/^{206}Pb$	error %	Radiogenic $^{207}Pb/^{206}Pb$	error %	^{204}Pb corrected $^{206}Pb/^{238}U$ Age Ma	error ±1σ
Sample CHY-09																
CHY9-1.1	1.77	299.74	166.30	0.57	12.87	0.001421	20.01	3.00	0.074889	2.23	20.55	3.08	0.05412	11.93	306.2	9.2
CHY9-2.1	5.77	91.83	64.63	0.73	4.24	0.003223	18.60	3.38	0.099852	6.44	19.76	3.77	0.05265	31.07	317.7	11.7
CHY9-3.1	0.76	366.96	151.83	0.43	15.77	0.000537	19.99	3.15	0.060614	2.37	20.19	3.18	0.05274	6.79	311.6	9.7
CHY9-4.1	0.32	783.55	478.60	0.63	34.67	0.000297	19.42	2.90	0.057828	1.55	19.52	2.91	0.05348	3.40	322.0	9.1
CHY9-5.1	0.89	325.92	169.47	0.54	13.94	0.000713	20.09	3.00	0.064486	3.42	20.36	3.02	0.05406	7.49	309.0	9.1
CHY9-6.1	1.15	299.00	231.53	0.80	12.86	0.000838	19.98	3.01	0.064691	2.61	20.29	3.04	0.05242	8.04	310.1	9.2
CHY9-7.1	2.69	168.43	53.19	0.33	7.20	0.001194	20.09	3.17	0.073225	7.08	20.53	3.26	0.05582	14.98	306.4	9.8
CHY9-8.1	1.04	417.74	188.98	0.47	18.09	0.001025	19.83	3.10	0.064925	3.13	20.21	3.14	0.04987	9.50	311.2	9.5
CHY9-9.1	0.17	547.35	329.80	0.62	23.77	0.000580	19.79	2.93	0.062516	1.75	20.00	2.94	0.05404	4.86	314.5	9.0
CHY9-10.1	1.97	280.89	180.74	0.66	12.06	0.001027	20.00	3.19	0.070230	4.74	20.39	3.24	0.05524	10.32	308.6	9.8
CHY-09 Pink, coarse-grained, biotite syenogranite; Guanta pluton; Concordia U-Pb age = 311.9±3.0 Ma																
Sample CHY-06																
CHY6-1.1	0.39	229.70	124.76	0.56	9.38	0.000370	21.05	2.55	0.059576	3.28	21.19	2.57	0.05417	5.60	297.2	7.5
CHY6-2.1	-0.03	1,363.90	164.64	0.12	67.12	0.000026	17.46	2.58	0.053162	1.42	17.47	2.58	0.05278	1.54	358.9*	9.0*
CHY6-3.1	-0.24	357.42	171.50	0.50	59.70	0.000154	5.14	2.47	0.074754	0.84	5.16	2.48	0.07256	1.21	1142.2*	25.9*
CHY6-4.1	-0.07	902.07	360.40	0.41	38.14	0.000099	20.32	2.44	0.054067	1.41	20.36	2.45	0.05262	2.05	309.1	7.4
CHY6-5.1	0.68	168.66	105.44	0.65	7.04	0.000696	20.58	3.09	0.065034	4.04	20.85	3.13	0.05487	8.42	301.9	9.2
CHY6-6.1	-0.16	2,324.88	1,094.68	0.49	99.32	0.000029	20.11	2.41	0.052486	0.86	20.12	2.42	0.05207	1.17	312.7	7.4
CHY6-7.1	0.04	653.08	257.52	0.41	27.72	0.000268	20.24	2.46	0.055611	1.58	20.34	2.47	0.05168	3.06	309.3	7.5
CHY6-8.1	-0.44	567.72	349.40	0.64	37.02	0.000255	13.18	2.46	0.059168	2.51	13.24	2.46	0.05544	3.33	469.4*	11.2*
CHY6-8.2	0.03	410.94	206.10	0.52	17.22	0.000326	20.50	2.50	0.056570	2.11	20.62	2.51	0.05179	4.07	305.2	7.5
CHY6-9.1	-0.23	1,209.40	542.66	0.46	51.71	0.000087	20.09	2.43	0.053297	1.18	20.12	2.43	0.05202	1.56	312.6	7.4
CHY6-10.1	-0.06	148.40	68.61	0.48	23.94	0.000329	5.33	2.65	0.079568	1.52	5.35	2.66	0.07488	2.70	1103.1*	27.0*
CHY6-11.1	0.91	168.78	115.74	0.71	7.17	0.000587	20.22	2.61	0.062762	3.69	20.44	2.65	0.05417	8.70	307.9	8.0
CHY6-12.1	-0.10	997.49	373.40	0.39	41.49	0.000184	20.65	2.44	0.054981	1.27	20.72	2.44	0.05228	2.40	303.8	7.2
CHY6-13.1	0.61	238.93	189.29	0.82	9.40	0.000884	21.85	2.88	0.064261	2.33	22.21	2.91	0.05129	8.26	283.8*	8.1*
CHY6-7.2	0.75	179.38	146.98	0.85	7.74	0.000935	19.90	2.91	0.064616	3.26	20.25	2.98	0.05089	11.44	310.7	9.0
CHY-06 Coarse-grained, foliated, biotite-hornblende tonalite; Guanta pluton; Concordia U-Pb age = 307.1±2.4 Ma																

appendix 2 continued.

Grain Spot	Common ^{206}Pb %	U ppm	Th ppm	$^{232}Th/^{238}U$	Radiogenic ^{206}Pb ppm	$^{204}Pb/^{206}Pb$	Total $^{238}U/^{206}Pb$	error %	Total $^{207}Pb/^{206}Pb$	error %	Radiogenic $^{238}U/^{206}Pb$	error %	Radiogenic $^{207}Pb/^{206}Pb$	error %	^{204}Pb corrected $^{206}Pb/^{238}U$ Age Ma	error ±1σ
Sample CHY-24																
CHY24-1.1	2.63	142.29	81.70	0.59	5.76	0.001440	21.20	2.71	0.072813	5.26	21.78	2.80	0.05170	14.42	289.2	7.9
CHY24-2.1	0.28	505.20	310.78	0.64	19.66	0.000155	22.08	2.47	0.054418	2.31	22.14	2.48	0.05215	3.06	284.7	6.9
CHY24-3.1	0.86	305.97	304.78	1.03	12.36	0.000473	21.27	2.53	0.060241	3.44	21.45	2.55	0.05332	6.14	293.6	7.3
CHY24-4.1	1.13	203.39	213.25	1.08	8.10	0.000620	21.56	2.61	0.062243	2.66	21.81	2.64	0.05317	7.78	288.9	7.5
CHY24-5.1	1.31	163.23	125.37	0.79	6.42	0.000720	21.84	2.66	0.064821	5.57	22.13	2.71	0.05431	9.99	284.9	7.5
CHY24-6.1	0.87	411.54	404.48	1.02	16.43	0.000478	21.52	2.49	0.060051	1.89	21.71	2.51	0.05306	5.21	290.2	7.1
CHY24-7.1	1.02	138.11	139.82	1.05	5.66	0.000560	20.95	2.70	0.069512	3.45	21.17	2.74	0.06141	7.38	297.5	8.0
CHY24-8.1	0.88	277.83	178.07	0.66	11.15	0.000481	21.41	2.55	0.060680	2.29	21.60	2.57	0.05364	5.26	291.7	7.3
CHY24-9.1	0.80	449.80	220.09	0.51	17.65	0.000436	21.90	2.48	0.058297	1.86	22.07	2.50	0.05191	4.37	285.6	7.0
CHY24-10.1	2.49	196.73	125.44	0.66	7.57	0.001363	22.33	3.09	0.071788	4.26	22.90	3.16	0.05181	12.35	275.4	8.5
CHY24-11.1	1.13	322.09	336.66	1.08	12.52	0.000618	22.11	2.54	0.062610	2.22	22.36	2.57	0.05356	6.66	281.9	7.1
CHY24-12.1	1.87	173.23	117.62	0.70	6.57	0.001023	22.67	2.68	0.066082	2.95	23.10	2.74	0.05107	10.33	273.1	7.3
CHY-24 Coarse-grained, hornblende-biotite quartz monzodiorite; Pedernales Batholith; Concordia U-Pb age = 287.0±2.1 Ma																
Sample CHY-07																
CHY7-1.1	0.16	1,247.44	52.98	0.04	49.92	0.000346	21.47	2.88	0.056650	1.29	21.60	2.88	0.05157	3.13	291.7	8.2
CHY7-2.1	2.63	208.31	72.66	0.36	8.33	0.001595	21.48	3.08	0.074898	6.24	22.12	3.16	0.05150	15.60	284.8	8.8
CHY7-3.1	0.36	1,175.42	92.83	0.08	46.67	0.000303	21.64	2.88	0.055825	1.33	21.76	2.88	0.05138	2.94	289.6	8.2
CHY7-4.1	-0.09	339.97	362.83	1.10	13.02	0.001030	22.43	3.23	0.065816	3.76	22.86	3.26	0.05070	9.51	275.9	8.8
CHY7-5.1	0.39	602.35	213.43	0.37	38.70	0.000243	13.37	2.91	0.060541	1.94	13.43	2.91	0.05700	2.76	462.9*	13.0*
CHY7-6.1	0.41	1,590.96	82.23	0.05	63.68	0.000295	21.46	2.87	0.056280	1.12	21.58	2.87	0.05196	2.32	292.0	8.2
CHY7-7.1	1.89	273.78	262.22	0.99	10.84	0.000815	21.70	3.03	0.064295	5.31	22.03	3.08	0.05235	10.86	286.1	8.6
CHY7-8.1	-0.07	1,754.39	92.43	0.05	67.64	0.000240	22.28	2.87	0.055475	1.09	22.38	2.87	0.05196	2.08	281.8	7.9
CHY7-9.1	0.06	1,211.96	630.25	0.54	52.44	0.000280	19.85	3.02	0.056857	1.32	19.96	3.03	0.05275	2.61	315.2	9.3
CHY7-10.1	0.25	766.96	538.80	0.73	37.12	0.000413	17.75	2.90	0.059809	2.70	17.89	2.91	0.05377	4.49	350.6*	9.9*
CHY-07 Light gray, coarse-grained, muscovite-biotite granite; Burro Muerto pluton; Cochiguaz Unit; Concordia U-Pb age = 286.3±3.1 Ma																

appendix 2 continued.

Grain Spot	Common ^{206}Pb %	U ppm	Th ppm	$^{232}Th/^{238}U$	Radiogenic ^{206}Pb ppm	$^{204}Pb/^{206}Pb$	Total $^{238}U/^{206}Pb$	error %	Total $^{207}Pb/^{206}Pb$	error %	Radiogenic $^{238}U/^{206}Pb$	error %	Radiogenic $^{207}Pb/^{206}Pb$	error %	^{204}Pb corrected $^{206}Pb/^{238}U$ Age Ma	error ±1σ
Sample CHY-19a																
CHY19A-1.1	0.47	276.45	215.44	0.81	11.16	0.000259	21.28	4.75	0.056364	2.34	21.38	4.75	0.05257	3.36	294.7	13.7
CHY19A-2.1	2.02	244.59	54.50	0.23	9.97	0.001109	21.08	4.27	0.072065	6.10	21.51	4.37	0.05589	16.09	292.8	12.5
CHY19A-3.1	0.09	1,461.19	21.54	0.02	55.01	0.000049	22.82	4.75	0.051257	1.19	22.84	4.75	0.05053	1.23	276.2	12.9
CHY19A-4.1	0.44	604.21	42.02	0.07	23.33	0.000243	22.25	8.34	0.053948	1.73	22.35	8.34	0.05037	2.78	282.1	23.0
CHY19A-5.1	-0.02	538.56	628.46	1.21	21.87	-0.000009	21.16	4.22	0.052540	1.77	21.15	4.22	0.05267	1.78	297.7	12.3
CHY19A-6.1	0.01	459.58	258.62	0.58	17.78	0.000005	22.21	4.44	0.054340	1.84	22.21	4.44	0.05426	2.26	283.9	12.3
CHY19A-7.1	0.11	1,230.06	315.62	0.27	49.14	0.000061	21.50	4.29	0.053051	1.16	21.53	4.29	0.05216	1.43	292.7	12.3
CHY19A-8.1	0.35	364.00	300.98	0.85	14.58	0.000190	21.44	4.23	0.055675	2.78	21.52	4.23	0.05289	3.34	292.8	12.1
CHY19A-9.1	0.55	256.71	128.25	0.52	9.94	0.000301	22.19	4.26	0.056154	2.40	22.31	4.28	0.05173	6.90	282.6	11.8
CHY19A-10.1	-0.03	2,520.25	451.11	0.18	98.89	-0.000019	21.89	4.19	0.052062	0.80	21.89	4.19	0.05233	0.80	288.0	11.8
CHY19A-11.1	0.44	398.18	244.23	0.63	16.04	0.000241	21.33	4.24	0.055656	2.15	21.43	4.24	0.05212	3.75	294.0	12.2
CHY19A-12.1	0.07	981.44	31.23	0.03	37.02	0.000041	22.78	4.19	0.052207	1.59	22.79	4.19	0.05161	1.68	276.8	11.3
CHY19A-13.1	0.20	801.68	27.43	0.04	30.28	0.000110	22.74	4.20	0.053643	1.41	22.79	4.20	0.05202	2.08	276.8	11.4
CHY19A-14.1	2.25	278.91	185.59	0.69	10.46	0.001228	22.90	5.27	0.069662	2.09	23.43	5.34	0.05165	13.87	269.3	14.1
CHY-19a Foliated, dark green, biotite-hornblende tonalite; Sierra Castillo batholith; Concordia U-Pb age = 285.3±3.2 Ma																
Sample CHY-23																
CHY23-1.1	0.39	268.30	102.02	0.39	41.82	0.000231	5.51	2.55	0.077804	1.08	5.53	2.55	0.07451	1.93	1070.5*	25.2*
CHY23-2.1	1.01	343.99	173.60	0.52	13.63	0.000555	21.69	2.51	0.059725	3.41	21.91	2.53	0.05159	7.47	287.6	7.1
CHY23-3.1	0.27	613.93	258.82	0.44	23.40	0.000150	22.54	2.52	0.053481	1.65	22.60	2.52	0.05128	3.08	279.1	6.9
CHY23-4.1	1.85	197.11	238.41	1.25	7.46	0.001013	22.70	2.62	0.066795	2.79	23.13	2.67	0.05194	9.72	272.7	7.1
CHY23-5.1	1.88	208.52	108.62	0.54	7.61	0.001029	23.54	2.58	0.065961	4.32	23.99	2.63	0.05086	10.52	263.1*	6.8*
CHY23-6.1	0.78	272.63	78.72	0.30	10.70	0.000425	21.89	2.75	0.058061	4.13	22.06	2.77	0.05184	7.21	285.7	7.7
CHY23-7.1	4.59	85.57	56.88	0.69	3.61	0.002517	20.37	2.98	0.089490	6.36	21.36	3.24	0.05263	24.26	294.7	9.3
CHY23-8.1	0.26	1,060.99	146.91	0.14	41.85	0.000144	21.78	2.42	0.054039	1.27	21.84	2.42	0.05193	2.00	288.6	6.8
CHY23-9.1	0.39	127.40	43.78	0.36	36.00	0.000251	3.04	2.56	0.139095	0.93	3.05	2.56	0.13579	1.26	1825.7*	40.8*
CHY23-9.2	0.51	693.65	174.79	0.26	26.46	0.000277	22.52	2.71	0.056944	2.80	22.63	2.71	0.05289	3.85	278.7	7.4
CHY23-10.1	0.44	753.28	134.02	0.18	28.00	0.000241	23.11	2.56	0.055499	1.49	23.21	2.56	0.05196	2.52	271.9	6.8
CHY23-11.1	0.17	258.43	251.68	1.01	74.44	0.000112	2.98	2.48	0.112030	0.70	2.99	2.48	0.11052	0.85	1860.5*	40.0*

appendix 2 continued.

Grain Spot	Common ^{206}Pb %	U ppm	Th ppm	$^{232}Th/^{238}U$	Radiogenic ^{206}Pb ppm	$^{204}Pb/^{206}Pb$	Total $^{238}U/^{206}Pb$	error %	Total $^{207}Pb/^{206}Pb$	error %	Radiogenic $^{238}U/^{206}Pb$	error %	Radiogenic $^{207}Pb/^{206}Pb$	error %	^{204}Pb corrected $^{206}Pb/^{238}U$ Age Ma	error ±1σ
CHY23-12.1	1.81	194.91	166.53	0.88	7.71	0.000990	21.73	2.64	0.067738	2.72	22.13	2.69	0.05326	9.28	284.8	7.5
CHY23-13.1	0.35	654.08	328.95	0.52	25.34	0.000190	22.18	2.46	0.055393	1.68	22.26	2.46	0.05261	2.68	283.3	6.8
CHY23-14.1	1.22	401.79	80.09	0.21	14.97	0.000668	23.06	2.57	0.062463	2.15	23.35	2.59	0.05269	6.20	270.3	6.9
CHY23-15.1	1.57	343.81	214.30	0.64	13.35	0.000860	22.12	2.52	0.064385	3.14	22.47	2.59	0.05177	10.34	280.6	7.1
CHY-23 Pink medium-grained, biotite monzogranite; Pedernales batholith; Concordia U-Pb age = 280.6±2.1 Ma																
Sample CHY-48																
CHY48-1.1	0.08	470.95	56.00	0.12	17.98	0.000042	22.50	2.07	0.053348	1.75	22.52	2.07	0.05274	2.18	280.1	5.7
CHY48-2.1	2.93	587.90	938.36	1.65	18.95	0.001595	26.66	2.01	0.074668	1.56	27.46	2.08	0.05127	10.66	230.5*	4.7*
CHY48-3.1	1.32	290.28	64.03	0.23	11.03	0.000721	22.61	2.10	0.062279	2.22	22.91	2.14	0.05170	7.94	275.4	5.8
CHY48-4.1	0.38	210.88	106.44	0.52	12.52	0.000210	14.47	2.06	0.063587	1.90	14.52	2.08	0.06055	4.39	429.2*	8.6*
CHY48-5.1	0.55	280.87	57.08	0.21	10.60	0.000303	22.77	2.04	0.056360	2.45	22.89	2.07	0.05191	6.39	275.6	5.6
CHY48-6.1	0.99	302.85	53.52	0.18	10.82	0.000540	24.05	2.06	0.058056	3.08	24.29	2.08	0.05013	6.28	260.0	5.3
CHY48-7.1	0.00	313.72	64.39	0.21	11.87	0.000000	22.71	2.02	0.051840	2.09	22.71	2.02	0.05184	2.09	277.8	5.5
CHY48-8.1	0.55	321.91	34.44	0.11	12.11	0.000302	22.83	2.03	0.055904	2.16	22.96	2.03	0.05147	3.05	274.8	5.5
CHY48-9.1	0.58	314.13	49.46	0.16	11.82	0.000319	22.84	2.19	0.055879	2.22	22.97	2.23	0.05120	6.65	274.7	6.0
CHY48-10.1	0.58	168.02	57.22	0.35	6.52	0.000320	22.13	2.29	0.056526	4.58	22.26	2.45	0.05183	14.28	283.2	6.8
CHY48-11.1	0.38	320.52	150.23	0.48	11.97	0.000209	23.01	2.03	0.055098	2.77	23.10	2.04	0.05204	3.64	273.2	5.4
CHY48-12.1	0.19	523.88	297.74	0.59	28.13	0.000104	16.00	2.07	0.056540	1.43	16.03	2.08	0.05502	2.29	390.1*	7.9*
CHY48-13.1	0.65	146.88	68.32	0.48	15.07	0.000369	8.37	2.08	0.073856	1.99	8.43	2.09	0.06856	3.24	722.6*	14.3*
CHY48-14.1	3.29	192.87	126.32	0.68	7.72	0.001800	21.47	2.28	0.079521	2.55	22.20	2.60	0.05318	20.16	283.8	7.2
CHY48-15.1	0.29	411.69	29.79	0.07	15.32	0.000156	23.09	2.02	0.053623	2.08	23.16	2.02	0.05133	2.62	272.5	5.4
CHY-48 Light pink, coarse-grained, biotite, monzogranite; Pan de Azúcar pluton; Concordia U-Pb age = 276.6±1.8 Ma																
Sample CHY-47																
CHY47-1.1	0.81	287.47	37.21	0.13	19.22	0.000451	12.85	2.39	0.063730	1.76	12.95	2.40	0.05716	3.90	479.2*	11.1*
CHY47-1.2	0.96	406.52	46.15	0.12	14.89	0.000525	23.46	2.53	0.059604	5.26	23.69	2.55	0.05192	8.14	266.5	6.7
CHY47-2.1	0.62	1953.02	42.85	0.02	76.38	0.000342	21.97	2.56	0.056471	1.19	22.11	2.56	0.05146	3.08	285.2	7.1
CHY47-3.1	1.51	399.78	157.54	0.41	14.32	0.000827	23.98	2.45	0.062857	2.77	24.34	2.50	0.05072	9.42	259.4	6.4
CHY47-4.1	0.19	817.23	203.76	0.26	112.30	0.000110	6.25	2.34	0.074380	1.35	6.26	2.34	0.07282	1.60	954.7*	20.8*

appendix 2 continued.

Grain Spot	Common ^{206}Pb %	U ppm	Th ppm	$^{232}Th/^{238}U$	Radiogenic ^{206}Pb ppm	$^{204}Pb/^{206}Pb$	Total $^{238}U/^{206}Pb$	error %	Total $^{207}Pb/^{206}Pb$	error %	Radiogenic $^{238}U/^{206}Pb$	error %	Radiogenic $^{207}Pb/^{206}Pb$	error %	^{204}Pb corrected $^{206}Pb/^{238}U$ Age Ma	error ±1σ
CHY47-5.1	1.16	565.85	99.39	0.18	23.25	0.000638	20.91	2.37	0.063974	1.85	21.16	2.38	0.05465	4.30	297.6*	6.9*
CHY47-6.1	0.87	603.40	133.19	0.23	21.65	0.000476	23.94	2.37	0.058550	3.67	24.15	2.38	0.05158	6.30	261.5	6.1
CHY47-7.1	2.11	291.08	35.52	0.13	11.10	0.001152	22.52	2.44	0.063359	7.43	23.01	2.58	0.04635	18.52	274.2	6.9
CHY47-8.1	0.88	650.32	88.74	0.14	23.65	0.000479	23.62	2.37	0.059079	1.99	23.83	2.41	0.05206	6.71	264.9	6.2
CHY47-9.1	0.40	1,620.80	38.52	0.02	61.29	0.000220	22.72	2.38	0.055960	1.13	22.81	2.39	0.05274	2.92	276.5	6.5
CHY47-10.1	0.44	186.15	233.63	1.30	31.43	0.000261	5.09	2.42	0.081307	1.54	5.11	2.42	0.07760	2.15	1151.6*	25.5*
CHY47-10.2	0.33	494.57	52.25	0.11	18.43	0.000179	23.05	2.37	0.053781	1.97	23.13	2.37	0.05116	2.48	272.9	6.3
CHY47-11.1	0.72	199.46	116.79	0.61	18.54	0.000409	9.24	2.41	0.070145	2.63	9.31	2.42	0.06424	3.97	657.4*	15.1*
CHY47-11.2	0.30	1,019.09	49.74	0.05	37.95	0.000167	23.07	2.34	0.054068	2.14	23.14	2.35	0.05162	3.12	272.7	6.3
CHY47-12.1	3.00	204.38	23.35	0.12	7.62	0.001638	23.04	2.49	0.072670	3.89	23.75	2.66	0.04857	17.95	265.7	6.9
CHY47-13.1	5.31	166.94	43.35	0.27	6.48	0.002905	22.12	2.68	0.078760	8.92	23.36	3.00	0.03529	40.99	269.9	7.9
CHY-47 Pink, coarse-grained, leucocratic granite; Pan de Azúcar pluton; Concordia U-Pb age = 269.5±2.0 Ma																
Sample CHY-35																
CHY35-1.1	0.76	307.95	186.00	0.62	11.35	0.000415	23.30	2.25	0.057901	1.97	23.48	2.25	0.05182	2.83	268.8	5.9
CHY35-2.1	0.64	333.56	130.49	0.40	12.42	0.000351	23.08	2.41	0.056809	2.98	23.23	2.43	0.05166	6.25	271.7	6.5
CHY35-3.1	0.99	302.27	198.17	0.68	10.88	0.000543	23.86	2.11	0.060806	2.59	24.10	2.14	0.05285	6.04	262.0	5.5
CHY35-4.1	0.68	226.21	117.53	0.54	8.51	0.000371	22.83	2.15	0.061643	2.31	22.98	2.15	0.05623	3.26	274.5	5.8
CHY35-5.1	0.92	359.90	190.59	0.55	13.56	0.000506	22.81	2.14	0.061138	3.03	23.02	2.16	0.05374	5.91	274.0	5.8
CHY35-6.1	0.64	361.18	139.34	0.40	13.67	0.000351	22.70	2.20	0.056674	3.29	22.85	2.21	0.05152	5.44	276.1	6.0
CHY35-7.1	0.67	691.76	322.83	0.48	28.17	0.000370	21.10	2.08	0.059201	1.90	21.24	2.10	0.05380	5.22	296.5*	6.1*
CHY35-8.1	1.80	244.21	150.71	0.64	8.97	0.000981	23.40	2.16	0.065968	2.90	23.83	2.24	0.05158	10.49	264.9	5.8
CHY35-9.1	1.04	269.79	185.81	0.71	9.77	0.000568	23.73	2.13	0.062330	3.28	23.97	2.15	0.05403	5.96	263.4	5.5
CHY35-10.1	0.65	319.21	178.54	0.58	11.81	0.000358	23.21	2.18	0.056364	2.05	23.37	2.20	0.05111	5.35	270.1	5.8
CHY35-11.1	1.22	258.58	180.06	0.72	9.36	0.000668	23.74	2.14	0.062363	5.28	24.04	2.19	0.05258	9.78	262.7	5.6
CHY35-12.1	0.53	628.80	412.00	0.68	25.15	0.000288	21.48	2.21	0.056466	2.69	21.59	2.22	0.05224	4.72	291.8*	6.3*
CHY-35 Pink, coarse-grained, biotite monzogranite; El Hielo batholith; Concordia U-Pb age = 267.9±1.9 Ma																

appendix 2 continued.

Grain Spot	Common ^{206}Pb %	U ppm	Th ppm	$^{232}Th/^{238}U$	Radiogenic ^{206}Pb ppm	$^{204}Pb/^{206}Pb$	Total $^{238}U/^{206}Pb$	error %	Total $^{207}Pb/^{206}Pb$	error %	Radiogenic $^{238}U/^{206}Pb$	error %	Radiogenic $^{207}Pb/^{206}Pb$	error %	^{204}Pb corrected $^{206}Pb/^{238}U$ Age Ma	error ±1σ
Sample CHY-12																
CHY12-1.1	5.66	98.87	60.63	0.63	3.80	0.003094	22.34	3.96	0.095167	6.77	23.68	4.21	0.04969	29.32	266.3	11.0
CHY12-2.1	8.63	471.36	968.90	2.12	7.75	0.004655	52.22	3.75	0.118905	3.95	57.15	4.05	0.05055	32.25	111.7*	4.5*
CHY12-3.1	3.51	217.42	127.08	0.60	8.02	0.001917	23.30	3.77	0.075467	6.11	24.15	3.87	0.04720	19.77	261.4	9.9
CHY12-4.1	3.16	170.61	90.65	0.55	6.57	0.001728	22.32	3.81	0.077812	7.06	23.05	3.90	0.05251	17.83	273.6	10.5
CHY12-5.1	4.83	116.98	99.01	0.87	4.37	0.002640	23.01	4.47	0.090116	5.51	24.18	4.65	0.05139	24.74	260.9	11.9
CHY12-6.1	6.20	73.86	48.31	0.68	2.73	0.003385	23.21	4.07	0.108344	6.56	24.74	4.41	0.05917	28.38	255.1	11.0
CHY12-7.1	2.38	199.48	151.28	0.78	7.59	0.001299	22.58	3.91	0.070235	2.78	23.13	3.97	0.05117	12.43	272.7	10.6
CHY12-8.1	2.02	279.43	180.69	0.67	10.37	0.001107	23.15	3.72	0.069220	4.10	23.62	3.75	0.05302	10.10	267.1	9.8
CHY12-9.1	4.70	311.26	163.96	0.54	10.39	0.002562	25.75	3.87	0.093255	2.18	27.02	3.99	0.05589	16.65	234.1	9.2
CHY12-10.1	3.48	170.36	123.40	0.75	6.26	0.001901	23.39	3.82	0.070762	5.73	24.23	3.93	0.04258	21.86	260.5	10.0
CHY12-11.1	1.43	236.83	163.11	0.71	8.58	0.000784	23.72	3.73	0.066821	4.56	24.07	3.76	0.05538	9.13	262.3	9.7
CHY12-12.1	8.74	351.17	541.79	1.59	16.64	0.004796	18.13	3.73	0.129700	2.02	19.87	3.96	0.06012	24.38	315.8*	12.2*
CHY-12 Pink, coarse-grained, biotite-hornblende monzogranite; Pedernales batholith; Concordia U-Pb age = 264.9±3.5 Ma																
Sample CHY-16																
CHY16-1.1	2.70	176.78	169.25	0.99	6.61	0.001476	22.98	3.97	0.071719	7.93	23.62	4.04	0.05003	17.49	267.1	10.6
CHY16-2.1	1.72	285.36	384.41	1.39	10.58	0.000938	23.18	3.71	0.065167	3.44	23.58	3.75	0.05141	10.20	267.6	9.8
CHY16-3.1	9.11	48.55	51.66	1.10	1.98	0.004984	21.06	4.28	0.132968	6.45	23.17	4.99	0.06072	40.55	271.7	13.3
CHY16-4.1	6.62	78.68	88.74	1.17	3.03	0.003618	22.29	4.02	0.107767	7.89	23.87	4.41	0.05493	33.75	264.1	11.4
CHY16-5.1	6.32	112.05	134.58	1.24	4.26	0.003452	22.58	3.91	0.103026	5.82	24.10	4.24	0.05247	30.84	261.7	10.9
CHY16-6.1	8.48	139.84	168.07	1.24	5.47	0.004635	21.96	3.84	0.125606	7.63	24.00	4.16	0.05821	32.55	262.7	10.7
CHY16-7.1	4.22	202.34	120.39	0.61	7.59	0.002306	22.89	3.77	0.081467	4.87	23.90	3.97	0.04748	24.96	264.0	10.3
CHY16-8.1	3.93	140.06	93.29	0.69	5.22	0.002148	23.05	3.85	0.083298	4.95	23.99	4.05	0.05180	22.40	263.0	10.4
CHY16-9.1	2.40	447.76	434.81	1.00	16.78	0.001313	22.92	3.71	0.069653	2.50	23.48	3.76	0.05037	10.70	268.7	9.9
CHY16-10.1	2.07	242.16	247.85	1.06	8.78	0.001132	23.70	3.75	0.069031	3.25	24.20	3.79	0.05245	10.63	260.9	9.7
CHY-16 Andesite dike that crosscut La Tabla Formation; Concordia U-Pb age = 264.6±3.5 Ma																

appendix 2 continued.

Grain Spot	Common ^{206}Pb %	U ppm	Th ppm	$^{232}Th/^{238}U$	Radiogenic ^{206}Pb ppm	$^{204}Pb/^{206}Pb$	Total $^{238}U/^{206}Pb$	error %	Total $^{207}Pb/^{206}Pb$	error %	Radiogenic $^{238}U/^{206}Pb$	error %	Radiogenic $^{207}Pb/^{206}Pb$	error %	^{204}Pb corrected $^{206}Pb/^{238}U$ Age Ma	error ±1σ
Sample CHY-38																
CHY38-1.1	3.94	239.34	183.87	0.79	8.91	0.002152	23.07	2.17	0.082216	4.09	24.02	2.42	0.05062	20.19	262.7	6.2
CHY38-2.1	5.26	160.56	154.61	1.00	6.13	0.002876	22.50	2.26	0.091692	2.57	23.75	3.26	0.04940	40.23	265.6	8.5
CHY38-3.1	5.04	122.78	160.40	1.35	4.69	0.002753	22.49	2.37	0.089883	4.07	23.69	3.01	0.04940	32.95	266.3	7.8
CHY38-4.1	7.64	111.75	149.42	1.38	4.32	0.004174	22.24	3.04	0.115722	10.81	24.08	3.75	0.05476	43.13	261.8	9.6
CHY38-5.1	3.60	184.77	103.55	0.58	6.92	0.001967	22.92	2.46	0.083042	9.00	23.78	2.93	0.05429	28.22	265.3	7.6
CHY38-6.1	1.93	552.85	436.38	0.82	20.69	0.001053	22.96	2.10	0.066204	2.50	23.41	2.16	0.05075	9.45	269.5	5.7
CHY38-7.1	1.86	387.08	292.07	0.78	14.13	0.001014	23.53	2.10	0.067482	3.96	23.98	2.18	0.05263	10.84	263.3	5.6
CHY38-8.1	6.91	125.04	155.49	1.28	4.79	0.003778	22.43	2.37	0.105745	7.90	24.10	3.12	0.05026	39.82	261.7	8.0
CHY38-9.1	2.09	369.35	272.77	0.76	13.60	0.001144	23.33	2.10	0.068340	5.85	23.83	2.26	0.05157	15.90	264.9	5.9
CHY38-10.1	5.38	164.68	271.07	1.70	6.23	0.002943	22.69	2.28	0.094728	10.11	23.98	2.79	0.05158	33.65	263.0	7.2
CHY38-11.1	0.20	476.65	324.22	0.70	16.91	0.000110	24.21	2.18	0.054797	2.22	24.26	2.21	0.05319	5.42	260.4	5.6
CHY38-12.1	0.77	342.86	126.88	0.38	12.34	0.000420	23.87	2.08	0.057883	2.20	24.06	2.09	0.05172	3.62	262.5	5.4
CHY38-13.1	2.59	95.33	106.29	1.15	3.50	0.001415	23.41	2.77	0.074786	3.71	24.03	2.92	0.05411	15.54	262.7	7.5
CHY38-14.1	1.73	130.18	140.41	1.11	4.66	0.000943	24.01	2.33	0.067585	3.49	24.44	2.52	0.05380	15.45	258.5	6.4
CHY38-15.1	5.27	356.38	234.25	0.68	13.51	0.002881	22.66	2.08	0.093388	8.16	23.92	2.49	0.05111	28.69	263.7	6.4
															CHY-38 Pink, medium-grained, biotite granite; Caballo Muerto pluton; Concordia U-Pb age = 263.5±1.7 Ma	
Sample CHY-58																
CHY58-1.1	2.16	130.07	74.05	0.59	4.79	0.001180	23.31	2.21	0.074855	5.05	23.83	2.36	0.05769	13.87	264.9	6.1
CHY58-2.1	0.22	779.02	106.01	0.14	33.20	0.000120	20.16	2.21	0.053701	1.26	20.20	2.21	0.05195	2.57	311.4*	6.7*
chy58-3.1	0.13	697.30	34.39	0.05	26.48	0.000073	22.62	2.27	0.053472	1.43	22.65	2.28	0.05241	2.90	278.4*	6.2*
CHY58-4.1	0.28	1,231.81	50.62	0.04	42.62	0.000155	24.83	2.21	0.053835	1.54	24.90	2.21	0.05157	2.09	253.8	5.5
CHY58-5.1	0.08	821.81	29.12	0.04	120.10	0.000044	5.88	2.08	0.074071	0.58	5.88	2.08	0.07344	0.69	1,011.9*	19.5*
CHY58-5.2	0.53	734.20	24.10	0.03	26.54	0.000288	23.77	2.11	0.055709	3.24	23.89	2.11	0.05149	4.52	264.3	5.5
CHY58-6.1	0.28	1,187.61	251.67	0.22	52.72	0.000156	19.35	2.32	0.055732	0.96	19.41	2.32	0.05345	1.69	323.9*	7.3*
CHY58-7.1	0.20	1,683.06	35.08	0.02	58.38	0.000108	24.77	2.16	0.053922	1.02	24.81	2.16	0.05235	2.12	254.7	5.4
CHY58-8.1	0.33	638.16	236.89	0.38	25.97	0.000178	21.11	2.18	0.056066	1.91	21.18	2.19	0.05346	2.91	297.4*	6.4*

appendix 2 continued.

Grain Spot	Common ^{206}Pb %	U ppm	Th ppm	$^{232}Th/^{238}U$	Radiogenic ^{206}Pb ppm	$^{204}Pb/^{206}Pb$	Total $^{238}U/^{206}Pb$	error %	Total $^{207}Pb/^{206}Pb$	error %	Radiogenic $^{238}U/^{206}Pb$	error %	Radiogenic $^{207}Pb/^{206}Pb$	error %	^{204}Pb corrected $^{206}Pb/^{238}U$ Age Ma	error ±1σ
CHY58-9.1	0.19	871.98	97.01	0.11	32.79	0.000105	22.85	2.09	0.053602	1.66	22.89	2.09	0.05206	1.94	275.6*	5.6*
CHY58-10.1	1.16	553.56	145.45	0.27	52.63	0.000659	9.04	2.07	0.074967	0.85	9.14	2.13	0.06547	6.55	668.6*	13.5*
CHY58-10.2	0.55	664.46	25.27	0.04	23.42	0.000302	24.38	2.08	0.056386	1.63	24.51	2.08	0.05196	2.70	257.8	5.3
CHY-58 Quebrada Pintado Tonalite mylonitized; Concordia U-Pb age = 258.9±2.5 Ma																
Sample CHY-46																
CHY46-1.1	1.58	412.25	78.81	0.20	14.34	0.000865	24.70	2.38	0.063618	3.93	25.10	2.45	0.05092	10.78	251.8	6.1
CHY46-2.1	0.93	628.87	102.85	0.17	20.88	0.000506	25.87	2.42	0.058748	1.91	26.12	2.43	0.05133	5.49	242.2	5.8
CHY46-3.1	1.64	331.73	69.56	0.22	11.03	0.000897	25.83	2.49	0.065919	6.06	26.26	2.60	0.05279	14.03	240.8	6.1
CHY46-4.1	1.03	357.65	88.83	0.26	20.74	0.000569	14.81	2.75	0.064095	2.30	14.97	2.76	0.05580	4.60	416.8*	11.1*
CHY46-5.1	0.72	603.30	65.64	0.11	21.13	0.000394	24.53	2.37	0.056315	2.08	24.71	2.37	0.05053	3.85	255.7	5.9
CHY46-6.1	0.79	874.44	155.67	0.18	28.78	0.000429	26.10	3.31	0.057885	2.92	26.31	3.32	0.05160	4.97	240.4	7.8
CHY46-7.1	2.17	449.02	77.48	0.18	15.55	0.001182	24.81	2.38	0.060920	5.64	25.36	2.45	0.04341	14.24	249.2	6.0
CHY46-8.1	0.14	1,114.63	1,033.46	0.96	220.13	0.000087	4.35	2.32	0.090999	0.50	4.36	2.32	0.08979	0.64	1,331.9*	27.9*
CHY46-9.1	1.13	522.39	102.66	0.20	17.55	0.000618	25.56	2.38	0.060461	3.37	25.86	2.41	0.05140	7.46	244.5	5.8
CHY46-10.1	1.78	405.32	49.81	0.13	13.56	0.000974	25.67	2.38	0.067357	5.76	26.14	2.48	0.05311	12.98	242.0	5.9
CHY46-11.1	0.50	965.85	661.44	0.71	32.93	0.000275	25.20	2.35	0.055139	1.62	25.33	2.36	0.05110	3.89	249.6	5.8
CHY-46 Leucocratic, coarse-grained granite; Cerros del Vetado pluton; Concordia U-Pb age = 246.5±2.0 Ma																
Sample CHY-60																
CHY60-1.1	0.60	272.71	179.40	0.68	9.22	0.000328	25.41	2.05	0.056160	3.97	25.56	2.09	0.05135	7.41	247.3	5.1
CHY60-2.1	0.28	485.26	363.60	0.77	16.28	0.000154	25.60	2.05	0.053358	2.28	25.67	2.05	0.05110	2.88	246.3	5.0
CHY60-3.1	-0.12	779.68	587.88	0.78	26.12	-0.000068	25.64	2.05	0.050493	5.39	25.61	2.06	0.05149	5.44	246.9	5.0
CHY60-4.1	2.03	118.95	129.61	1.13	4.04	0.001107	25.29	2.26	0.068183	3.33	25.82	2.52	0.05195	17.94	244.9	6.1
CHY60-5.1	0.77	564.07	930.23	1.70	18.32	0.000422	26.46	2.03	0.056619	1.71	26.66	2.05	0.05042	5.21	237.3	4.8
CHY60-6.1	2.04	168.93	157.52	0.96	5.80	0.001115	25.04	2.16	0.068887	4.60	25.56	2.30	0.05255	14.16	247.3	5.6
CHY60-7.1	1.71	179.53	220.97	1.27	6.29	0.000936	24.54	3.30	0.065350	4.36	24.97	3.42	0.05162	15.39	253.1	8.5
CHY60-8.1	1.59	357.77	389.73	1.13	11.74	0.000869	26.18	2.28	0.063107	4.34	26.60	2.35	0.05035	11.53	237.8	5.5
CHY60-9.1	4.03	165.77	204.00	1.27	5.64	0.002200	25.26	2.20	0.087269	6.92	26.32	2.52	0.05515	22.51	240.2	5.9
CHY60-10.1	1.29	327.50	209.76	0.66	11.02	0.000706	25.54	2.09	0.063132	3.64	25.88	2.18	0.05279	10.56	244.4	5.2

appendix 2 continued.

Grain Spot	Common ^{206}Pb %	U ppm	Th ppm	$^{232}Th/^{238}U$	Radiogenic ^{206}Pb ppm	$^{204}Pb/^{206}Pb$	Total $^{238}U/^{206}Pb$	error %	Total $^{207}Pb/^{206}Pb$	error %	Radiogenic $^{238}U/^{206}Pb$	error %	Radiogenic $^{207}Pb/^{206}Pb$	error %	^{204}Pb corrected $^{206}Pb/^{238}U$ Age Ma	error ±1σ
CHY60-11.1	2.49	196.63	168.35	0.88	6.74	0.001360	25.08	2.18	0.071249	2.59	25.72	2.42	0.05129	17.54	245.8	5.8
CHY60-12.1	2.16	225.68	188.55	0.86	7.71	0.001180	25.15	2.14	0.069409	5.01	25.71	2.28	0.05211	14.55	245.9	5.5
CHY60-13.1	1.20	486.21	355.60	0.76	16.32	0.000657	25.60	2.04	0.059532	2.68	25.91	2.10	0.04988	8.93	244.0	5.0
CHY60-14.1	0.74	633.75	266.91	0.44	27.72	0.000407	19.64	2.28	0.059278	3.21	19.79	2.29	0.05333	4.82	317.8*	7.1*
CHY60-15.1	0.76	946.20	1,793.87	1.96	31.24	0.000417	26.02	2.00	0.057384	2.81	26.22	2.02	0.05127	5.85	241.2	4.8
CHY-60 Pink, coarse-grained, biotite monzogranite; Chollay batholith; Concordia U-Pb age = 244.0±1.4 Ma																
Sample CHY-45																
CHY45-1.1	-0.12	355.48	39.27	0.11	21.97	-0.000069	13.90	2.22	0.056452	1.77	13.88	2.22	0.05746	2.18	448.4*	9.6*
CHY45-2.1	1.46	319.05	105.55	0.34	10.38	0.000794	26.42	2.33	0.066727	5.17	26.81	2.42	0.05514	11.78	236.0	5.6
CHY45-3.1	0.71	684.53	53.06	0.08	22.73	0.000388	25.88	2.09	0.056120	1.62	26.06	2.10	0.05043	4.06	242.7	5.0
CHY45-4.1	0.48	354.79	81.79	0.24	32.39	0.000271	9.41	2.19	0.073684	2.09	9.46	2.19	0.06979	2.61	647.9*	13.5*
CHY45-5.1	0.70	597.10	222.11	0.38	19.24	0.000382	26.66	2.09	0.056956	1.76	26.85	2.10	0.05135	3.88	235.7	4.9
CHY45-6.1	-0.06	540.44	120.97	0.23	59.98	-0.000036	7.74	2.08	0.076165	1.00	7.74	2.08	0.07667	1.00	783.8*	15.3*
CHY45-7.1	0.85	492.09	272.27	0.57	15.78	0.000461	26.79	2.30	0.057555	3.93	27.02	2.31	0.05079	5.48	234.2	5.3
CHY45-8.1	0.47	663.50	282.38	0.44	21.32	0.000257	26.74	2.58	0.056006	3.46	26.86	2.59	0.05224	5.11	235.6	6.0
CHY45-9.1	1.58	406.14	154.25	0.39	13.32	0.000859	26.19	2.12	0.066092	5.55	26.61	2.23	0.05353	12.76	237.8	5.2
CHY45-10.1	0.63	1,014.67	588.24	0.60	32.74	0.000341	26.63	2.21	0.055175	3.10	26.80	2.26	0.05017	8.45	236.2	5.2
CHY45-11.1	0.17	1,076.33	163.52	0.16	60.88	0.000097	15.19	2.62	0.056929	1.04	15.22	2.62	0.05552	1.54	410.3*	10.4*
CHY45-12.1	0.43	741.27	365.92	0.51	47.22	0.000242	13.49	2.07	0.060337	1.82	13.54	2.08	0.05681	3.04	459.1*	9.2*
CHY45-13.1	2.62	442.99	99.00	0.23	12.04	0.001422	31.60	2.14	0.071201	4.44	32.45	2.26	0.05031	14.08	195.6*	4.4*
CHY-45 Coarse-grained, biotite monzogranite; Cerros del Vetado pluton; Concordia U-Pb age = 237.0±2.0 Ma																

appendix 2 continued.

Grain Spot	Common ^{206}Pb %	U ppm	Th ppm	$^{232}Th/^{238}U$	Radiogenic ^{206}Pb ppm	$^{204}Pb/^{206}Pb$	Total $^{238}U/^{206}Pb$	error %	Total $^{207}Pb/^{206}Pb$	error %	Radiogenic $^{238}U/^{206}Pb$	error %	Radiogenic $^{207}Pb/^{206}Pb$	error %	^{204}Pb corrected $^{206}Pb/^{238}U$ Age Ma	error ±1σ
Sample CHY-03																
CHY3-1.1	High U, Th and commom Pb															
CHY3-2.1	2.99	89.20	61.93	0.72	2.92	0.001840	26.24	2.82	0.076956	4.69	27.16	3.01	0.04991	20.02	232.9	6.9
CHY3-3.1	0.85	246.61	257.36	1.08	7.91	0.000746	26.80	2.67	0.061409	3.57	27.17	2.75	0.05046	11.69	232.9	6.3
CHY3-4.1	0.23	186.92	160.56	0.89	5.83	0.000662	27.56	2.60	0.061199	4.94	27.90	2.66	0.05148	10.44	226.9	5.9
CHY3-5.1	0.91	210.32	173.48	0.85	6.77	0.000836	26.67	2.58	0.061703	4.61	27.09	2.69	0.04941	13.90	233.6	6.2
CHY3-6.1	1.17	247.78	266.93	1.11	7.59	0.000652	28.06	2.56	0.060095	3.72	28.40	2.59	0.05053	7.77	223.1	5.7
CHY3-7.1	1.39	204.91	132.88	0.67	6.49	0.001045	27.12	3.21	0.065674	3.20	27.65	3.27	0.05032	11.56	228.9	7.4
CHY3-8.1	0.55	326.10	225.48	0.71	12.64	0.000432	22.16	2.61	0.058505	2.50	22.34	2.62	0.05217	5.07	282.2*	7.2*
CHY3-9.1	High U, Th and commom Pb															
CHY-03 Brick-red, fine-grained, syenogranite; La Coneja pluton; Colorado Unit; Concordia U-Pb age = 229.6±2.6 Ma																

Notes: (**1**) ^{204}Pb corrected ages; (**2**) Uncertainties are given at the one σ level for individual spot analyses and calculated concordia ages; (**3**) ***** indicate excluded spot analyses from age calculation.